The Dissertation Committee for Wenjuan Ru Certifies that this is the approved version of the following dissertation:

GLIA-MEDIATED MECHANISMS OF HIV-1-GP120-INDUCED SYNAPTIC DEGENERATION

Committee:

Yogesh Wairkar, Ph.D., Chair

Shao-Jun Tang, Ph.D.

Thomas A. Green, Ph.D.

Fernanda Laezza, MD., Ph.D.

Italo Mocchetti, Ph.D.

Dean, Graduate School

GLIA-MEDIATED MECHANISMS OF HIV-1-GP120-INDUCED SYNAPTIC DEGENERATION

by

Wenjuan Ru, M.S.

Dissertation

Presented to the Faculty of the Graduate School of

The University of Texas Medical Branch

in Partial Fulfillment

of the Requirements

for the Degree of

Doctor of Philosophy

The University of Texas Medical Branch

October 2018

Dedication

This work is dedicated to my parents, my cousin and my friends who have always given me support and encouragement. Thank you all for your love and care.

Acknowledgements

This dissertation would not have been possible without the assistance, guidance and support from the following special people. First and foremost, I would like to thank my mentor, Dr. Shao-Jun Tang for the opportunity to work and learn in his laboratory as well as for his support, guidance, advice, and patience throughout my training. He gave me the freedom to explore on my own but also provided the guidance to complete my dissertation.

Additional thanks go to my dissertation committee members: Drs. Yogesh Wairkar, Fernanda Laezza, Italo Mocchetti, and Thomas A. Green for their invaluable inputs and suggestions towards the completion of my dissertation.

Special thanks to all Dr. Tang's lab members, both past and present. it is a tough road to do science, and it becomes easier with their help. Dr. Yuqiang Shi for innumerable discussions and suggestions. Drs. Xin Liu and Chilman Bae for technical assistance and collaboration. Drs. Junying Zheng and Subo Yuan for the continuous support. Deep gratitude to Dr. Paul Boakye for comments on my dissertation. Thanks to the former laboratory member Mati De Cabo for the friendship and insights of confocal imaging.

Profound gratitude goes to Dr. Yuejin Liang for flow cytometry analysis, Lorenzo Ochoa and Paula Villarreal for confocal images processing and analysis.

I would also give my sincere thanks to Dr. Owen Hamill, Ms. Aurora Galvan and Ms. Debra L. Moncrief in the Neuroscience Graduate Program for all their help and support.

I am also hugely appreciative to my friends, soul mates and companions: Alice, Claudia, Emanuele, Guorui, Guang, Huanle, Hui, Ju, Jie, Lorenzo, Mauro, Paula, Salvo, Tizianna, Xianxiu, Yaohua and Yuejin.

Finally, but by no means least, thanks go to my parents and my cousin for their never-ending love, and unbelievable support. They are the most important people in my world and I could not complete this project without their support.

This work would not be possible without the financial support of the UTMB McLaughlin Fellowship (to W. Ru) and the NIH grants (R01NS079166, R01DA036165 to S-J. Tang).

GLIA-MEDIATED MECHANISMS OF HIV-1-GP120-INDUCED SYNAPTIC DEGENERATION

Publication No._____

Wenjuan Ru, Ph.D.

The University of Texas Medical Branch, 2018

Supervisor: Shao-Jun Tang

HIV-1 infection of the nervous system causes various neurologic diseases. Synaptic degeneration is a critical underlying neurological pathology. However, the mechanism by which HIV-1 causes synaptic degeneration is unclear. In this dissertation, we tested the role of HIV- envelope protein gp120 in pathogenesis of degeneration both in the spinal cord and the cortex.

In the spinal cord, gp120 exposure caused synaptic degeneration. Because gp120 induced microglial activation, we further tested the hypothesis that microglia contribute to gp120-induced synaptic degeneration. We found that blockage of microglial activation abolished the synapse loss induced by gp120. Fractalkine (FKN; a.k.a.CX3C ligand-1 or CX3CL1), a microglia-activation chemokine that is specifically expressed in neurons, was up-regulated in response to gp120 stimulation. Knockout (KO) of the FKN receptor CX3CR1, which is specifically expressed on microglia, protected synapses from gp120-induced degeneration. These results indicate that the neuron-to-microglia intercellular

FKN/CX3CR1 signaling is critical for gp120-induced synaptic degeneration. To elucidate the molecular mechanism that controls this intercellular signaling, we tested the role of the Wnt3a/β-catenin pathway in regulating FKN expression. We found that inhibition of this pathway blocked both the gp120-induced FKN up-regulation and the synaptic degeneration. We also found that gp120 stimulates FKN expression, which is mediated by Wnt3a/β-catenin signaling, via NMDA receptor activation. These findings collectively suggest that HIV-1 gp120 induces synapse degeneration via microglial activation regulated by the Wnt3a/β-catenin/ FKN pathway.

Significant synaptic degeneration was observed in the cortex of gp120 transgenic (Tg) mice. Our data suggest that glial phagocytosis greatly contributed to gp120-induced synaptic loss. Interestingly, microglia predominately engulf and eliminate pre-synaptic structures, while reactive astrocytes act predominantly at the postsynaptic compartment. Ablation of microglia protected pre-synaptic elements from gp120-induced elimination. Furthermore, the MerTk signal pathway contributed to gp120- induced microglial phagocytosis of pre-synaptic terminal but was not involved in astrocytic phagocytosis of post-synaptic terminal. Our studies reveal critical roles microglial and astrocytic phagocytosis in HIV-associated synaptic degeneration.

Table of Contents

List of Tables

`List of Figures

List of Abbreviations

AAAS	American Association for the Advancement of Science
ACSF	Artificial cerebrospinal fluid
AIDS	Acquired immunodeficiency syndrome
ANI	Asymptomatic neurocognitive impairment
ANOVA	Analysis of variance
BL	Burzenski LM
CNS	Central nervous system
DIV	Days in vitro
DT	Diphtheria toxin
FKN	fractalkine
GFAP	Glial fibrillary acidic protein
GFP	Green fluorescent protein
HAART	Highly active antiretroviral therapy
HAD	HIV-associated dementia
HAND	HIV-associated neurocognitive disorder
HBSS	Hank's balanced salt solution
HIVE	HIV- associated encephalitis
HS	Henriksen SJ
LCM	Laser capture microdissection
LRP	Lipoprotein receptor-related protein
MND	Mild neurocognitive disorder
MS	Mass spectrometry
NMDAR	NMDA receptor
NRTI	Nucleoside reverse transcriptase inhibitors
OCT	Optimal cutting temperature
PBL	Peripheral blood leukocytes
PDL	Poly-D-lysine
PWT	Paw withdrawal thresholds
RGC	Retinal ganglion cell
RL	Ryan LA
SCID	Severe combined immunodeficiency deficient
SDH	Spinal dorsal horn
SHIV	Simian-human immunodeficiency virus

SIV	Simian immunodeficiency virus
TBI	Traumatic brain injury
UTMB	University of Texas Medical Branch
VM	Vacuolar myelopathy

MAJOR SECTION

Chapter 1 Introduction[1]

There are almost 36.7 million HIV-infected people worldwide, with over 1 million in U.S by the end of 2016 (https://www.hiv.gov/hiv-basics/overview/data-and-trends/global-statistics). HIV-1 attacks the immune system, specifically the CD4 cells (T cells), leading to acquired immunodeficiency syndrome (AIDS). No cure is currently available. Highly active antiretroviral therapy (HAART) is the current standard treatment for HIV infection. It is a customized combination of different classes of antiretroviral agents, including nucleoside reverse transcriptase inhibitors (NRTIs), non-nucleoside reverse transcriptase inhibitors, protease inhibitors, integrase inhibitors and entry inhibitors. With the proper HAART treatment, the lifespan of people infected with HIV is dramatically prolonged.

HIV is a lentivirus, a subtype of retrovirus. There are two genetically distinct types of the HIV virus: HIV-1 and HIV-2. HIV-1 is the predominant and most common type, being responsible for 95% of all infections worldwide **(**http://i-base.info/qa/36). HIV-2, a less prevalent, lower transmission efficiency and less pathogenic (fewer deaths) type, found primarily in western Africa. HIV viral particle is spherical in shape with a diameter of about 100 nm enveloped by a lipoprotein membrane. Below the envelope, there is protein matrix, whose core region consists of a conical capsid containing two copies of the positive sense single-stranded RNA (ssRNA) genome, the reverse transcriptase, integrase

[1] Portions of this Chapter were previously published. Ru, W and Tang, S-J. HIV-associated synaptic degeneration. *Molecular Brain.* 2017**.** 10:4**0**

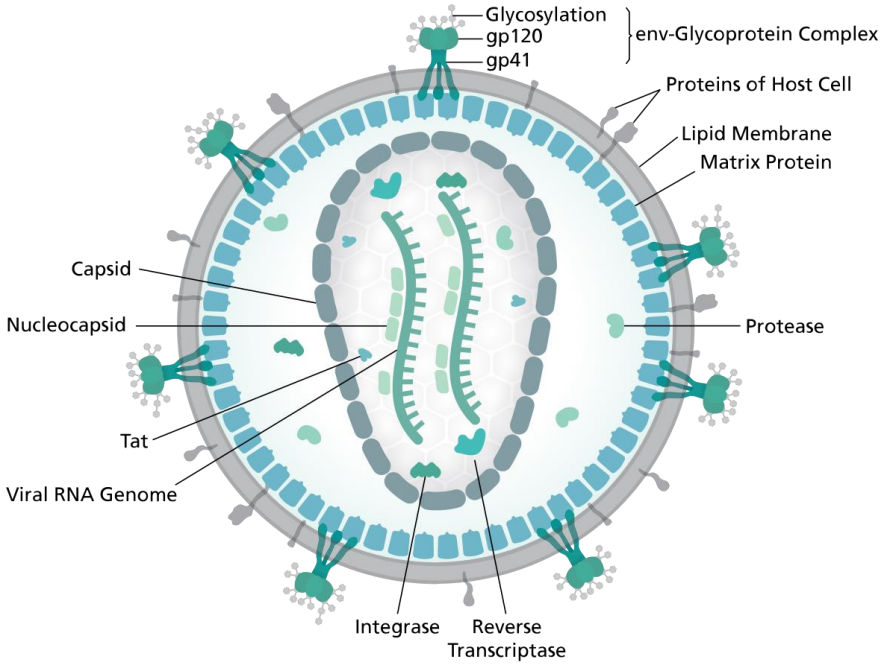

Fig 1. 1 The structure of matured HIV viral particle. HIV is a spherical virus with a diameter of 100 nm (source: http://www.onlinebiologynotes.com/structure-genome-proteins-hiv/).

and protease enzymes (Fig.1.1). The genome of HIV-1 consists of 3 structural genes: *gag* (group specific antigen), *pol* (polymerase)：the viral enzymes and *env* (envelope), and 6 regulatory genes: *tat*, rev, *nef*, *vif*, *vpr* and *vpu*. The organization of HIV-1 genome and the main function of each gene are shown in Fig. 1.2.

HIV primarily infects $CD4^+$ T cells and cells of the monocytes-macrophage lineage (such as monocytes, macrophages, skin dendritic cells and brain microglial cells). In order to enter to host cells and replicate, HIV firstly binds, via its surface glycoprotein gp120, to CD4 receptor and co-receptor CCR5 (macrophage) or CXCR4 (T-cell) on the surface of host cells. Once HIV attatches to the host cell, glycoprotein gp41 undergoes conformational change and triggers the fusion of HIV envelope and the cell plasma membrane, leadinig to viral genome and protein entering to the cell. Inside the host cell, retrovrial reversed transcriptase converts HIV RNA to DNA, and the HIV DNA is then transfered to the nucleus and integrates into the host genome (facilitated by integrase). The integrated viral genome (provirus) can synthesize new HIV RNAs using the host

trascription machinery, to make viral protein and the genome for assembling of new viral particles that are bud from the plasma memberane (Fig. 1.3).

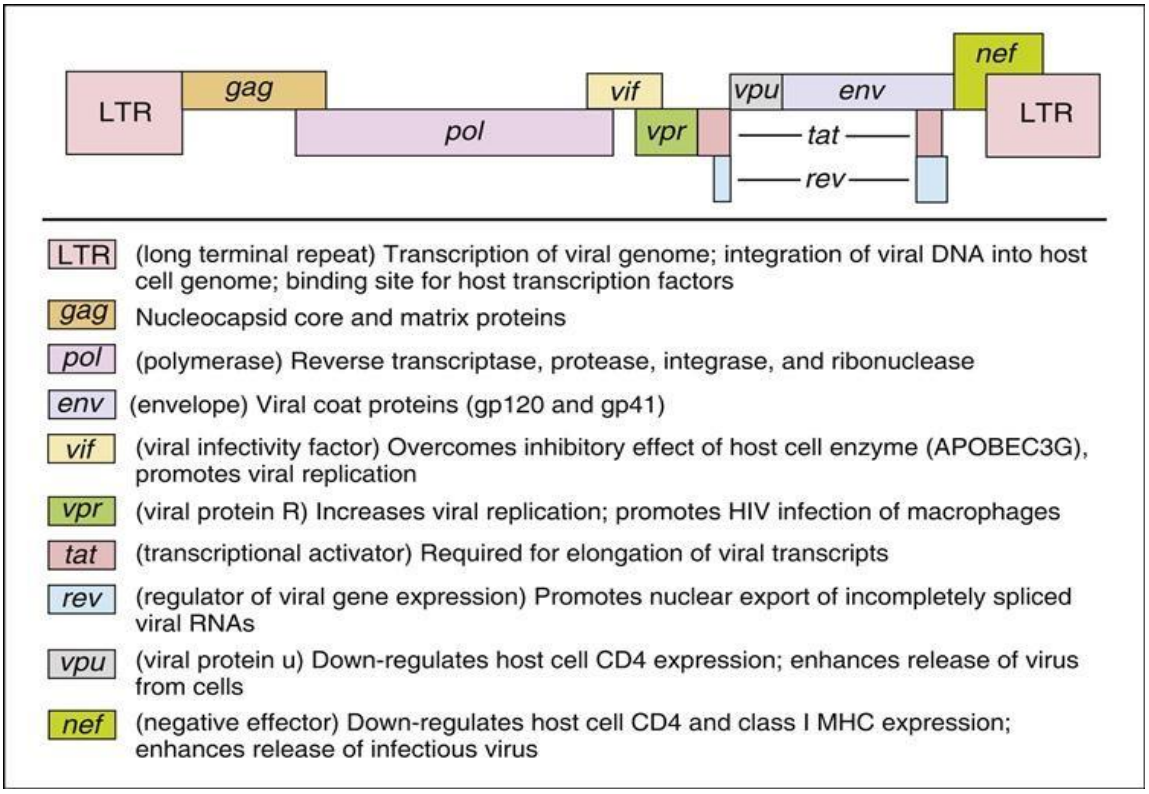

Fig 1. 2 An overview of the organization of genome of HIV-1 and a summary of the functions of its genes (source: https://clinicalgate.com/acquired-immune-deficiency-syndrome/).

1.1 HIV-ASSOCIATED NEUROLOGICAL DISORDERS

Soon after the infection, HIV enters the central nervous system (CNS) and causes neurological dysfunction. Even with the effective anti-retroviral therapy that suppresses viral replication and transmission, about 70% of HIV patients still develop neurological complications (Sacktor, 2002). Multiple neurological disorders are manifested in HIV patients.

HIV-associated neurocognitive disorder (HAND) is a common primary neurological disorder associated with HIV infection of the CNS. Patients with HAND often

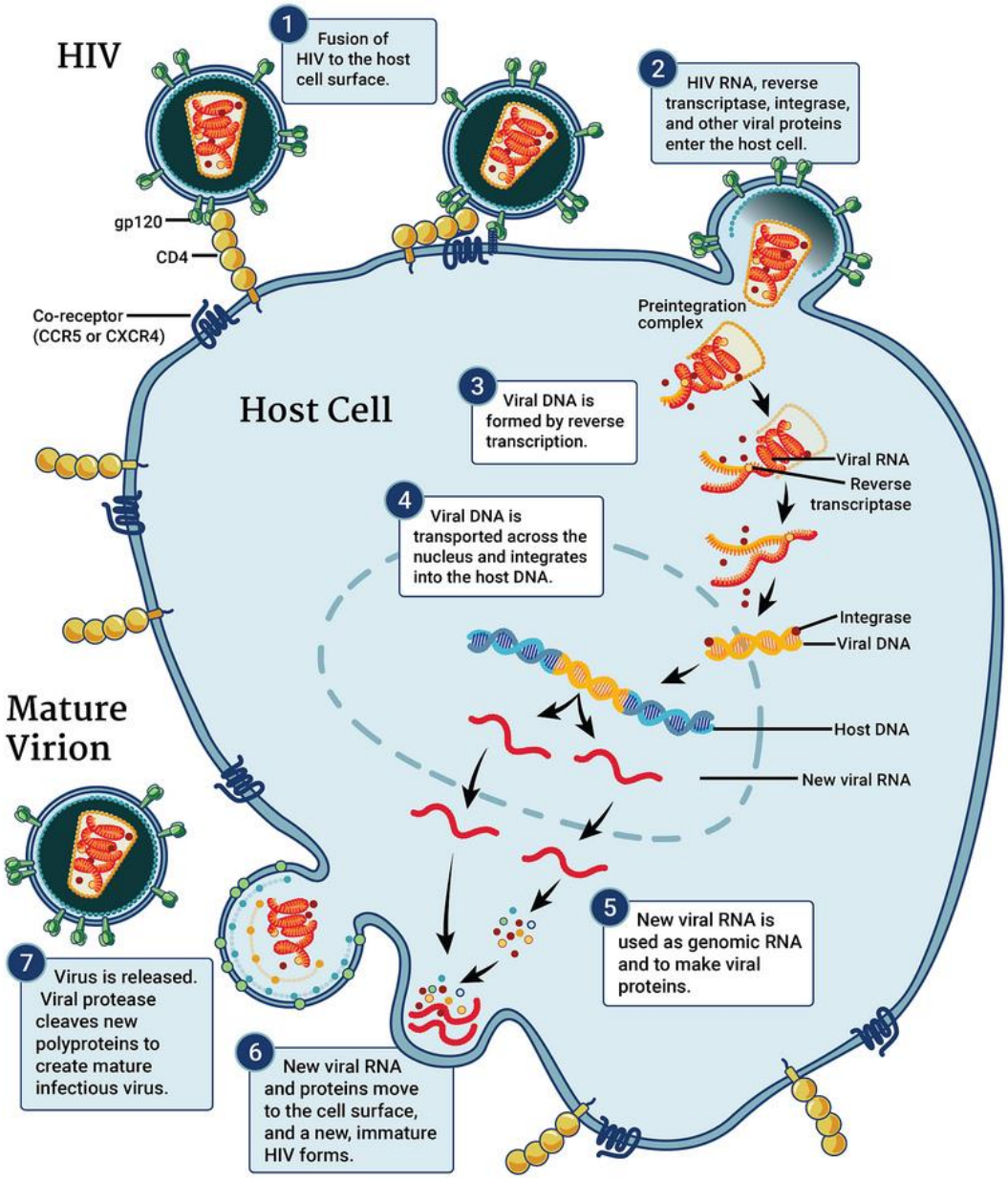

Fig 1. 3 Schematic overview of HIV-1 entry to the host cells and replication cycles. (adapted from: https://www.niaid.nih.gov/diseases-conditions/hiv-replication-cycle)

develop cognitive impairment, motor dysfunction and speech problems. Clinical severity of HAND ranges from asymptomatic neurocognitive impairment (ANI) and mild neurocognitive disorder (MND) to HIV-associated dementia (HAD) (Antinori et al., 2007). Due to the success of HAART, HAD has declined, with a prevalence of less than 5% of

HIV patient who are on the treatment (Saylor et al., 2016). However, the mild forms of HAND are still common and significantly affect patients' quality of life (Fig. 1. 4).

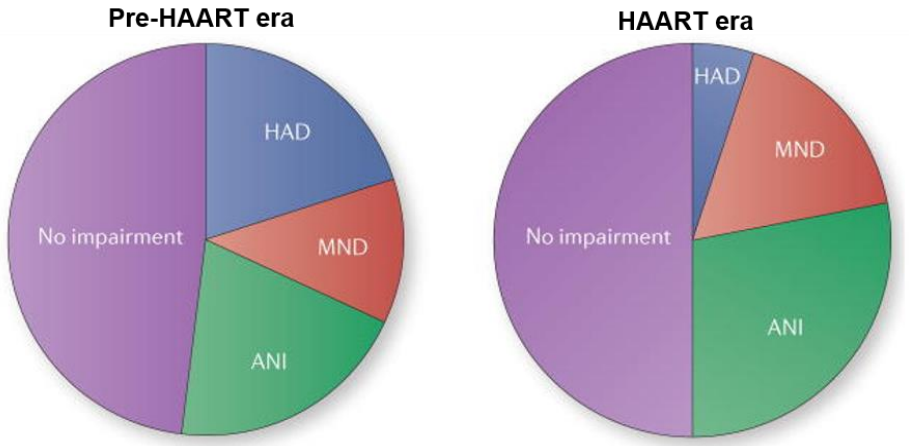

Fig 1. 4 Comparison of the prevalence of HANDs between pre-HAART era and the era of widespread HAART usage. The prevalence of severe form of HAND, HAD, has declined significantly, but milder forms of HAND are still common. (modified from *Deanna Saylor et al., Nat Rev Neurol. 2016 Apr; 12(4): 234–248.)*

Neuropathy of the peripheral nerves often develops in HIV patients. With an improved survival of HIV patients on HAART, the prevalence of HIV-associated neuropathy has increased, with about 42% of HIV patients showing neuropathy symptoms (Smyth et al., 2007). The clinical symptoms include unusual sensation, numbness and severe pain. However, pathological analysis of autopsies indicate that almost all patients with AIDS develop peripheral neuropathy, including those who did not show clinical symptoms (Cornblath and McArthur, 1988).

HIV-associated vacuolar myelopathy (VM) is commonly associated with late stages of HIV infection. Of AIDS patients, 20%-55% exhibit symptoms of VM (Di Rocco and Simpson, 1998). Vacuolization in dorsal and lateral tracts in the thoracic spinal cord is a common pathological characteristic. Patients with VM manifest progressive weakness of legs and sensory abnormalities, and VM may ultimately lead to paralysis of lower limbs (Di Rocco and Simpson, 1998).

In addition to HIV infection, anti-retroviral therapy may also contribute to neurological disorders. For example, patients treated with NRTIs are prone to develop neuropathy and/or myopathy in a dose-dependent manner (Dalakas et al., 1990; Bozzette et al., 1991; Jay et al., 1994). A major side effect of protease inhibitors on the CNS is lipodystrophy syndrome, which is characterized by peripheral fat wasting and central adiposity (Carr et al., 1998). NRTIs have also been linked to lipodystrophy (Carr et al., 2000). HAART was also reported to increase the incidence of encephalitis (Langford et al., 2003) and induce neuropathy (Maschke et al., 2000).

1.2 NEUROPATHOLOGICAL ALTERATION IN CNS

1.2.1 Early stages.

Although 70% of people with HIV have neuropathological abnormalities in the era of HAART (Sacktor, 2002), only a few studies have reported neuropathology in HIV-infected individuals before the onset of AIDS due to the limited availability of postmortem brains. Most HIV-1 patients remain neurologically unimpaired during early pre-AIDS stages. It generally takes 3 to 6 weeks to become seropositive after HIV infection, and this period is known as seroconversion. During seroconversion, 50-70% of HIV-infected people experience transient “acute HIV syndrome”, such as symptomatic meningitis (Ho et al., 1985), encephalopathy (Carne et al., 1985; Nzwalo et al., 2012) or myelopathy (Denning et al., 1987). Some clinicopathological studies revealed that the CNS entry of HIV-1 might also induce demyelination in the white matter during seroconversion (Jones et al., 1988; Gray et al., 1991a).

1.2.2 Asymptomatic period.

After the seroconversion period, HIV infection enters a latency phase called the asymptomatic period, which usually lasts for 8-10 years. Neurological pathologies are noted during this stage, especially in the white matter, although the pathological changes are not consistent. Vascular inflammation is frequently observed in the white matter and basal ganglia, and microglial activation, astrocytosis and myelin pallor are observed in the white matter during this stage (Gray et al., 1992; An et al., 1996; Gray et al., 1996). Although microglial activation is observed in the cerebral cortex (Sinclair et al., 1994), neuronal loss and astrocyte proliferation are rarely seen there (Gray et al., 1996).

1.2.3 AIDS stage.

Autopsies found that 80%-100% of AIDS patients had neuropathological changes in the CNS (Anders et al., 1986; Navia et al., 1986; Kanzer, 1990; Gray et al., 1991b). HIV-associated encephalitis (HIVE) was also observed in some patients at this stage. The neuropathological characteristics of HIVE include microglial nodules, multinucleated giant cells, reactive astrocytosis, microglial proliferation, myelin pallor, and infiltration of peripheral monocytes (Budka, 1986, 1991; Gelman, 1993; Tauber et al., 2016). In contrast to the pre-AIDS stages, when neuronal loss is not seen, neuronal death is frequently observed in AIDS patients (Adle-Biassette et al., 1995). Significant neuronal loss has been reported in the frontal cortex (Ketzler et al., 1990; Weis et al., 1993; Adle-Biassette et al., 1995). Neuronal death via apoptosis occurs in AIDS patients (Shi et al., 1996; Garden et al., 2002). Non-apoptotic neuronal injuries, including retraction of dendritic spines, dendritic pruning or aberrant sprouting, axonal disruption and synaptic degeneration, were also observed. Immunostaining analysis of postmortem brain tissues using synaptic and dendritic markers revealed dendritic beading, synaptic degeneration and dendritic spine loss in the brain of HIV patients (Masliah et al., 1997; Everall et al., 1999; Gisslén et al.,

2005). Axonal injury indicated by elevated neurofilament protein in CSF is also detected in HIV patients (Hagberg et al., 2000; Norgren et al., 2003; Gisslén et al., 2005). Loss of synaptodendritic structures in HIV patients is correlated with reduced volume of neuropil and white matter (Grant et al., 1987; Norgren et al., 2003).

1.3 SYNAPTIC DEGENERATION

Among all the neuropathological changes observed in HIV-infected CNS, synaptic degeneration is particularly interesting. Synapses mediate communication and interaction between neurons. A typical chemical synapse consists of a presynaptic ending that contains neurotransmitters, a synaptic cleft between pre- and post-synaptic terminal and postsynaptic terminal that contains receptor sites for neurotransmitters. The arrival of electrical impulse at the pre-synaptic terminal causes the movement of vesicles containing neurotransmitters towards presynaptic membrane (Fig 1.5). The synaptic vesicle then fuses with the presynaptic membrane and triggers the release of neurotransmitters into the synaptic cleft. The diffused transmitters bind to receptor on the postsynaptic membrane to either excite or inhibit post-synaptic neurons. Synaptic degeneration likely results in aberrant communication between neurons.

Both HIV encephalitis and neuronal loss are observed in the brain after HIV infection, and they appear to associate with severe dementia. However, they do not correlate well with milder forms of cognitive impairment (Adle-Biassette et al., 1999). HIV encephalitis occurs in some but not all HIV-infected individuals. Its presence and severity do not correspond to the degree of cognitive deficits (Brew et al., 1995; Wiley and Achim, 1995; Cherner et al., 2002). In addition, different from other neurocognitive conditions such as Alzheimer's or Parkinson's diseases, the early dementing process in HIV patients is not associated with substantial neuronal apoptosis. Weis et al. reported that AIDS

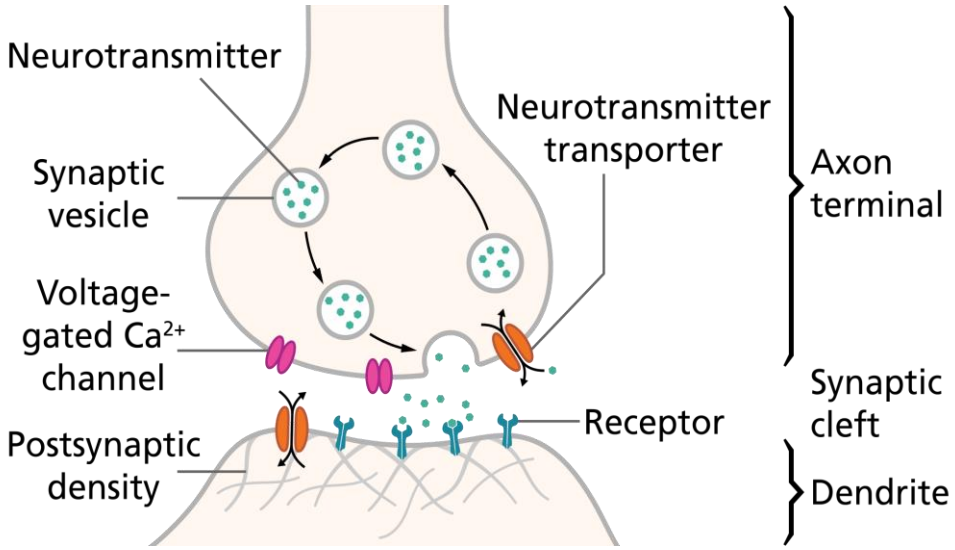

Fig 1. 5 Structure of a typical chemical synapse. It consists of a presynaptic ending containing neurotransmitters, a synaptic cleft and postsynaptic ending that contains neurotransmitter receptor. (adapted from https://en.wikipedia.org/wiki/Synapse).

patients with clinical signs of progressive dementia showed no significant difference in neuronal densities compared to patients without dementia, indicating that neuronal loss was not causally linked to the development of dementia (Weis et al., 1993). But synaptic alteration and degeneration in the brains of HIV patients appear to correlate well with the presence and severity of cognitive impairment (Everall et al., 1999; Sá et al., 2004; Ellis et al., 2007).

Consistent with this notion, our earlier study found significant reductions of synaptic proteins: PSD95, NMDA receptor subunit 1 (NR1) and Synapsin I (Syn I) in the spinal dorsal horn (SDH) of HIV patients who develop pathological pain (‘pain-positive patients) but not in the patients who do not develop the pain syndrome (‘pain-negative’ patients), indicating the synaptic degeneration in SDH of pain-positive HIV patients (Yuan et al., 2014). These findings suggest that synaptic degeneration in the pain neural circuitry contribute to the pathogenesis of HIV pain syndromes.

Identification of the pathogenic role of synaptic degeneration in neurological dysfunction significantly improve our understanding of HIV-associated neurological

disorders. Inhibition of synaptic degeneration may provide an attractive therapeutic target to prevent the pathogenesis of HIV-associated dementia and pain.

1.4 ANIMAL AND IN VITRO MODELS

To investigate the underling mechanism of HIV-infection- caused synaptic alteration observed in human patients, relevant animal models are essential. The following animal models are currently used to study the HIV- associated neurological disorders.

1.4.1 Non-human primate models.

The simian immunodeficiency virus (SIV)-infected macaque is an established relevant model for studying the neuropathogenesis of HIV-associated disorders. In monkeys, SIV can enter the brain shortly after infection and causes brain abnormalities. SIV infection recapitulates the main features of immune response of HIV infection (Roberts et al., 2003; Roberts et al., 2004; Roberts et al., 2006; Marcondes et al., 2007; Fox, 2008). Additionally, HIV-associated neuropathologies in the brains of HIV patients are also developed in the SIV-infected macaque. For example, pre-synaptic damage was reported in SIV-infected macaques, as indicated by elevated levels of neuronal damage marker 14-3-3 protein in the CSF (Sharer et al., 1988; Helke et al., 2013). SIV-infected macaques developed various types of behavioral impairments, similar to those observed in HIV patients, as shown by a number of behavioral and neurophysiological testing modalities (Gold et al., 1998; Horn et al., 1998; Weed et al., 2003; Weed et al., 2004; Marcondes et al., 2009). This model is particularly useful to study the pathogenesis of HIV-associated disorders in the era of HAART, because the infected macaque can be treated with HAART regimens to mimic the clinical settings (Zink et al., 2010). It is also very

helpful for the investigation of the synergized effects of drug abuse and HIV infection during neuropathogenesis (Marcondes et al., 2010; Bokhari et al., 2011; Hollenbach et al., 2014; Marcario et al., 2016). In addition, because of the multi-time accessibility of CSF, plasma and CNS samples during the progression of infection, this model allows to investigate the development of HIV-associated disorders through the progressive stages.

Although studies with SIV-infected macaques provide valuable insights into the pathogenesis of HIV infection, it is important to keep in mind that SIV and HIV are not the same. For example, CCR5-preferred HIV can gain the ability to use CXCR4 to enter into monocyte-derived macrophages (Gorry et al., 2001; Gray et al., 2009), while CCR5-preferred SIV uses other co-receptors such as CXCR6, GPR15 and GPR but not CXCR4 to enter host cells (Riddick et al., 2010). To address these limitations, simian-human immunodeficiency virus (SHIV) was constructed, in which the env gene of SIV was replaced by HIV-1 env. Therefore, the hybrid viruses are biologically more similar to HIV than SIV. Macaques infected with SHIV89.6P (CXCR4/CCR5 virus) developed encephalitis characterized by multinucleated giant cells, astrogliosis, microglial nodules, activated macrophages and astrocytes, and perivascular cuffing with mononuclear cells in the white matter (Buch et al., 2000). CCR5 (R5)-tropic SHIVSF162P3N virus caused giant cell SIV encephalitis in approximately 30% of infected rhesus macaques that developed AIDS (Harbison et al., 2014). Giant cell SIV encephalitis lesions included white matter damage, necrosis, and astrocytic and microglial activation (Harbison et al., 2014). SHIVKU, a CXCR4 virus, also could productively replicate in the CNS of rhesus macaques and caused pathological changes (Raghavan et al., 1997; Buch et al., 2002; Li et al., 2015). Despite the significant contributions of non-human primate models to understanding HIV-1-associated neuropathogenesis, these models are limited by their availability and high cost of maintenance.

1.4.2 Rodent models.

For reasons that are not completely defined, rodents cannot be productively infected by HIV-1. To circumvent this drawback, transgenic mice are generated to express HIV-1 proteins such as the envelope protein gp120 and the transactivator of transcription (Tat), both of which are neurotoxic. In a gp120 transgenic mouse (gp120 Tg) model, the gp120 transgene is controlled by the glial fibrillary acidic protein (GFAP) promoter, and thus gp120 is restricted to astrocytes (Toggas et al., 1994). The release of astrocytically expressed gp120 protein can affect nearby neurons. Confocal imaging of brain sections labeled with dendritic and synaptic markers revealed the dendritic vacuolization, loss of dendritic spines and presynaptic termini in the neocortex and the hippocampus (Toggas et al., 1994). This gp120 Tg mouse also showed activation of glial cells (Toggas et al., 1994) and impaired proliferation and differentiation of neuronal progenitor cells (Okamoto et al., 2007; Lee et al., 2011). Additionally, aging (12 months) gp120 Tg mice develop deficits in motor and cognitive performance (Toggas et al., 1994; D'hooge et al., 1999).

In another transgenic mouse model, the Tat transgene is expressed in astrocytes in a Dox-regulated manner (Kim et al., 2003). The inducible expression of Tat provides the ability to study the temporal effect of Tat released from astrocytes. This transgenic mouse displays degeneration of neuronal dendrites, neuron death, astrocytosis and enhanced infiltration of activated monocytes and T lymphocytes, and these alterations are largely observed in the cerebellum and cortex (Kim et al., 2003). Other studies described subtler neuronal injuries such as spine loss and synaptic degeneration in hippocampal pyramidal CA1 neurons and striatal neurons (Bruce-Keller et al., 2008; Fitting et al., 2010; Fitting et al., 2013). The Tat transgenic mice develop impairments in spatial memory and novel object recognition memory (Kim et al., 2003; Carey et al., 2012; Fitting et al., 2013).

Transgenic mice with full-length (Thomas et al., 1994; Wang et al., 2003a) or *gag-pol*-deleted HIV-1 genomic DNA (Santoro et al., 1994) have been reported. The integrated

HIV-1 genome in the transgenic mouse somewhat resembles HIV-1 provirus. In addition, the transgenic HIV-1 genome has the potential to express multiple HIV-1 proteins. These strengths of this transgenic strategy, however, also complicate the result interpretation for determining the causal relationship between specific HIV-1 proteins and observed phenotypes. Despite low levels of viral protein expression, the full-length transgenic mouse model shows impaired nerve conduction, axonal degeneration and decreased nerve fiber density in the peripheral nervous system. They are also impaired in motor function (Thomas et al., 1994), and show hyper-reactivation of microglia and astrocytes (Wang et al., 2003a; Sun et al., 2008).

The HIV-1 transgenic rat has been studied by multiple groups as a model of HIV-associated neurological diseases. It contains a *gag-pol*-deleted HIV-1 genome that is controlled by the viral promoter. Since without *gag* and *pol* genes that are responsible for viral replication, it cannot produce infectious virions (Reid et al., 2001). This rat model expresses multiple viral proteins. In particular, the expression of Tat, gp120, Nef and Vif RNAs show age-dependent profiles, shifting from peripheral immune organs to the CNS at 10-11 months of age. These features of HIV-1 gene expression indicate that the HIV-1 transgenic rats can model specific aspects of HIV-1-infected individuals on HAART (Peng et al., 2010). The 7-to-9-month-old animals show up-regulated expression of neuroinflammation markers such as interleukin-1β (IL-1β), tumor necrosis factor α (TNF-α) and microglial/macrophage marker CD11b (Rao et al., 2011), which may contribute to the observed synapto-dendritic injury (Rao et al., 2011). The transgenic rats develop spatial learning deficits (Vigorito et al., 2007; Lashomb et al., 2009) and are impaired in motor performance (Reid et al., 2016).

The HIV-1 transgenic rodent models described above provide useful tools to study the contribution of viral proteins to the pathogenesis of HIV-associated disorders. However, they have significant limitations. Foremost, they do not acquire HIV-1 infection and thus cannot faithfully model the initial infection stages or the AIDS progression, which

are key events associating with the development of neurological disorders. Understandably, efforts continue to create additional rodent models to mimic HIV infection. One strategy is to introduce human HIV-1 receptors and co-receptors in transgenic rodents (Seay et al., 2013). However, it appears that HIV-1 replication was defective in CD4 or CCR5 transgenic rodents (Goffinet et al., 2007; Tervo et al., 2008).

Potash et al. designed a creative approach to generate a novel mouse model of HIV-1 infection. They constructed a chimeric HIV-1 virus by replacing the HIV-gp120 coding region with the gp80 envelope gene from the ecotropic murine leukemia virus. This chimeric virus, called EcoHIV, can enter to the host cells by binding to cationic amino acid transpoter-1 (mCAT) (Potash et al., 2005). Despite the widespread expression of mCAT in the mouse tissues, persistent infection seems to be restricted to splenic lymphocytes, peritoneal macrophages and brain (Potash et al., 2005; Hadas et al., 2013). EcoHIV infection by stereotactic inoculation into the mouse basal ganglia caused pre-clinical brain pathology such as microglia and astrocyte activation (Potash et al., 2005; Kelschenbach et al., 2012). However, the lack of gp120 in the chimeric virus presents specific limitations in this model. First, it is unclear to what degree the chimeric virus mimics the HIV-1 infection. For example, it may not target the same populations of cells as HIV-1. In addition, because gp120 is a major HIV-1 neurotoxic protein, this model may not recapitulate some of the neuropathological phenotypes related to HIV infection.

HIV-infected humanized mice are the exciting new rodent models. One strategy is to generate humanized mice with CNS HIV infection by direct injection of infected human cells. HIV-infected human monocyte-derived macrophages or HIV-infected human microglia cells are injected into the brain of severe combined immunodeficiency deficient (SCID) mice (Persidsky et al., 1996; Persidsky et al., 1997) or reconstituted SCID mice with human peripheral blood leukocytes (PBLs) (huPBL/SCID) (Poluektova et al., 2002; Poluektova et al., 2004). SCID and huPBL/SCID mice with the infected human cells recapitulate the several neurological pathologies observed in HIV patients with HIVE,

including multinucleated giant cells, astrogliosis, microglial activation and neuronal damage (Persidsky et al., 1996; Persidsky et al., 1997; Poluektova et al., 2002; Poluektova et al., 2004). The SCID-HIVE mouse model also develops cognitive deficits. Morris water maze tests revealed their learning and memory impairments, regardless of HAART treatment (Cook-Easterwood et al., 2007). Using these models, isolate-specific cognitive deficits and neuropathology were reported. Intracranial injection of macrophages infected with a clade B HIV-1 isolate (HIV-1(ADA)) into SCID mice caused worse performance in cognitive tests and more severe pathological changes than a clade C HIV-1 isolate (HIV-1(Indie-C1)) (Rao et al., 2008).

Another strategy to generate humanized mice is systemic transplantation of human hematopoietic stem cells ($CD34^+$ cells) or adult human peripheral blood mononuclear cells into various immunodeficient mice so that the mice host the human target cells for HIV-1 infection (Mosier et al., 1988; Ito et al., 2002; Traggiai et al., 2004; Shultz et al., 2005; Melkus et al., 2006; Hatziioannou and Evans, 2012). Various neuropathologies were reported in HIV-infected humanized mouse models. For example, NOD/SCID-IL-2Rγ_c^{nul} (NSG) mice with engrafted human $CD34^+$ stem cells (NSG-h$CD34^+$) developed a functional human immune system containing T lymphocytes, monocytes and macrophages could be efficiently infected with HIV (Gorantla et al., 2010; Dash et al., 2011; Boska et al., 2014; Marsden and Zack, 2015). Neuronal and synaptic damage were detected by immunohistochemical staining of various neuronal and synaptic markers such as microtubule associated protein-2, neurofilament and synaptophysin. The neuropathologies appeared to correlate with glial cell activation (Dash et al., 2011; Boska et al., 2014). The animals also showed memory deficits and persistent anxiety (Dash et al., 2011; Boska et al., 2014). Although less used for CNS infection, other humanized mouse models (e.g. humanized bone marrow/liver/thymus mouse models) have been used for studies on HIV pathogenesis, transmission, replication and prevention.

To understand the underlying mechanism especially in the spinal pain circuit level of HIV- caused pain. Watkins and Tang et al generated a model by perispinal (intrathecal, i.t.) injection of gp120. Thermal hyperalgesia and mechanical allodynia were produced in mice with gp120 i.t. application (Milligan et al., 2000; Milligan et al., 2001; Yuan et al., 2014). Meanwhile, astrocytes and microglial activation, elevated proinflammatory cytokines such as interleukin-1β (IL-1β) and tumor necrosis factor-α (TNF-α) and down-regulated synaptic markers were observed in the SDH of gp120 i.t. mice (Milligan et al., 2000; Milligan et al., 2001; Yuan et al., 2014).

1.4.3 In vitro models.

Primary neuron cultures are useful for studying the neurotoxicity of HIV-1 proteins such as gp120 and Tat. Confocal imaging of cultured rat hippocampal neurons revealed that gp120 application caused a dramatic decrease in the number of synapses (Kim et al., 2011). Similarly, Tat treatment also induced synaptic loss (Kim et al., 2008; Shin et al., 2012; Shin and Thayer, 2013). In addition, gp120 was shown to cause dendritic damage in human primary neurons (Iskander et al., 2004; Kim et al., 2011). Mixed primary cultures that have neurons and glia cells provide an in vitro experimental setting for investigating the interaction between neurons and other cell types (e.g. microglia and astrocytes) during the HIV-induced neuropathogenesis.

1.5 MECHANISMS OF SYNAPTIC DEGENERATION INDUCED BY HIV-1 INFECTION

As HIV-1 cannot infect neurons, HIV-associated synaptic degeneration is likely a bystander effect of the infected cells, including perivascular macrophages, microglia and astrocytes. The infected cells may elicit neurodegenerative responses by releasing viral

proteins and other toxic factors such as chemokines and cytokines. The neurotoxins may induce arrays of cellular and molecular cascades that eventually lead to synaptic loss, including Ca^{2+} overload, energy hemostasis disturbance, neurotransmitter (e.g. glutamate) metabolism perturbation, oxidative stresses and excitatory toxicity. In the following sections, we discuss potential mechanisms regulating HIV-induced synaptic degeneration (Fig. 1.6).

1.5.1 Neurotoxicity of viral proteins.

Viral proteins, particularly gp120 and Tat, are released from infected microglia/macrophages and astrocytes. Gp120 is thought to induce synaptic degeneration via multiple mechanisms. One suggested pathway is glutamate receptor activation-mediated excitotoxicity such as the hyperactivation of N-methyl-D-aspartate receptor (NMDAR) and its associated excessive Ca^{2+} influx (Choi, 1992). Gp120 can activate NMDARs by binding to their glycine binding sites (Fontana et al., 1997). Gp120 may also enhance synaptic activity by potentiating the phosphorylation and synaptic trafficking of NMDARs (Xu et al., 2011). In addition to stimulating NMDARs, gp120 can bind to its chemokine co-receptor CXCR4 or CCR5 on the neurons to mediate neuronal damage (Lavi et al., 1997; Rottman et al., 1997). M-tropic HIV-1 strains preferably bind to CCR5 (Alkhatib et al., 1996; Choe et al., 1996; Dragic et al., 1996), and T-tropic strains use CXCR4 to gain entry into the cells (Feng et al., 1996). After binding to its co-receptor,

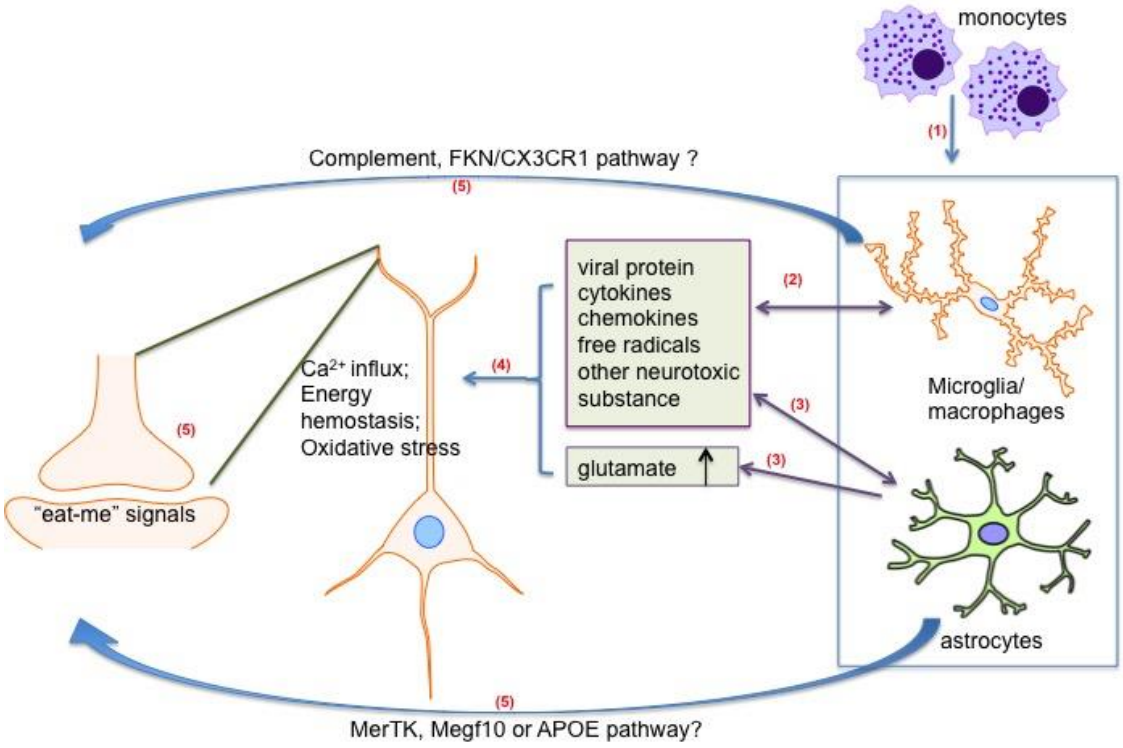

Fig 1. 6 Potential mechanisms of HIV-induced synaptic degeneration. (1) HIV-1 infection of the CNS initiates from transmigration of HIV-1-infected peripheral blood monocytic cells/macrophages across the blood-brain barrier (BBB). Subsequently, microglia and astrocytes become infected and reactivated. (2) The immune-activated and HIV-1-infected microglia/macrophages release viral proteins (e.g. gp120, Tat, Vpr), cytokines (e.g. IL-1β, IL-6, TNF-α), chemokines (CXCL12, MCP1) and other neurotoxic factors. (3) Infected/reactivated astrocytes can also release neurotoxic substances and pathogenically enhance synaptic activity with increased transmitter release and impaired glutamate re-uptake. (4) The released neurotoxins and extracellular glutamate can cause excessive Ca^{2+} influx, disturbance of energy metabolism and production of reactive oxidative species, which then lead to the disruption of normal neuronal function. On the other hand, the released viral proteins, cytokines, chemokines and free radicals can activate more glial cells and macrophages. (5) These damaged neurons may mark the abnormal synapses with some kind of "eat-me" signals, which can be recognized and eliminated by microglia and/or astrocytes through phagocytotic pathways such as the complementary and FKN/CX3CR1 pathways in microglia or the MerTK, Megf10 and APOE pathway in astrocytes.

gp120 may facilitate NMDAR activation and intracellular Ca^{2+} increase to induce neuronal damage (Catani et al., 2000; Kaul et al., 2001; Nicolai et al., 2010; Marchionni et al., 2012; Maung et al., 2014; Ru and Tang, 2016) and/or activate signaling cascacades (e.g. ERK and p38 MAPK signaling pathways) that are asssociated with cell damage and death

(Lazarini et al., 2000; Garden et al., 2004; Medders et al., 2010). Alternatively, gp120 might cause neurotoxicity via indirect mechanisms. Gp120 can potentiate NMDAR activity by inducing release of proinflammatory cytokines from glial cells (Brabers and Nottet, 2006; Viviani et al., 2006). For instance, after binding to the interleukin-1 receptor, IL-1β can stimulate the phosphorylation of NR2B at tyrosine 1472 to potentiate NMDAR activation (Viviani et al., 2006). In addition, gp120 may cause glial dysfunction and impair extracellular glutamate reuptake. Accumulated extracellular glutamate and NMDAR hyperactivation will induce synaptic damage (Dreyer and Lipton, 1995; Potter et al., 2013; Vázquez-Santiago et al., 2014; Melendez et al., 2015). Furthermore, the neurotoxicity of gp120 may be mediated by down-regulating release of neurotrophic factors (such as BDNF) from activated glia cells (Kaul and Lipton, 1999; Viviani et al., 2001; Bachis et al., 2003; Nosheny et al., 2004; Mocchetti et al., 2007).

By binding to the low-density lipoprotein receptor-related protein (LRP), Tat protein can cause NMDAR activation, excessive Ca^{2+} influx (Haughey et al., 1999; Self et al., 2004; Li et al., 2008; Shin et al., 2012) and mitochondrial dysfunction (Rappaport et al., 1999; Perry et al., 2005). These Tat effects trigger downstream events that contribute to synaptic loss, including the activation of the ubiquitin–proteasome pathway (Kim et al., 2008; Shin and Thayer, 2013), the disturbance of energy metabolism (Liu et al., 2000) and the production of reactive oxidative species (Aksenov et al., 2001; Perry et al., 2005). Tat also stimulates glial cells and macrophages to release cytokines, chemokines and other neurotoxic factors that cause neuronal injury (Nath et al., 1999; Bokhari et al., 2009; Jin et al., 2012).

1.5.2 Neuroinflammation.

HIV-1 enter the CNS soon after peripheral infection of blood monocytes and circulating T cells, mainly through a “Trojan horse” mechanism (Haase, 1986) as well as other routes such as “transcytosis” or infection of BBB endothelial cells (Mankowski et al., 1994; Bomsel, 1997; Liu et al., 2002; Argyris et al., 2003; Bobardt et al., 2004). The viral proteins, inflammatory cytokines and chemokines released from infected and/or activated cells can lead to disruption of BBB integrity and hence exacerbation of the entry of infected cells (Strazza et al., 2011). As a key component in the BBB structure, astrocytes that become infected can directly cause the increase of BBB permeability (Eugenin et al., 2011).

Microglia and perivascular macrophages are CNS-resident immunocompetent cells that can be productively infected by HIV-1. After HIV infection, substantial pro-inflammatory cytokines (e.g. TNF-α, IL-6 and IL-1β) are released from infected/reactivated microglial cells/macrophages (Saha and Pahan, 2003; Brabers and Nottet, 2006; Viviani et al., 2006; Shah et al., 2011b). Cytokines in peripheral circulation may also traffic to the CNS (Orandle et al., 2002; Cinque et al., 2007; Ellis et al., 2009). The cytokines are elevated in the CSF of HIV patients with cognitive impairments (Bandaru et al., 2007; Yuan et al., 2013). They may contribute to the pathogenesis of synaptic degeneration via multiple pathways, including NMDAR hyperactivation. For instance, TNF-α and IL-1β can stimulate L-cysteine release from macrophages, which then activates NMDARs to cause neuronal damage (Yeh et al., 2000). In addition, cytokines may also induce synaptic abnormalities by aberrantly activating cytokine receptors (Kaul et al., 2005; Khairova et al., 2009; Kovalevich and Langford, 2012). After binding to its receptors on neurons, TNF-α activates multiple pathways that are implicated in neuronal damage, including the nuclear factor-kappa B (NF-κB), ERK, p38 MAPK, the c-Jun N-terminal kinase, and caspase pathways (Kaul et al., 2001; Olmos and Lladó, 2014).

HIV-infected microglia and macrophages may also release chemokines, which can stimulate neurons via chemokine receptors to induce synaptic degeneration. For example, CXCL12/SDF-1α is elevated in the brain and CSF of HIV patients with HAD (Rostasy et

al., 2003; Peng et al., 2006). By binding to its receptors, CXCL12 can function as either neuroprotective or neurotoxic mediator (Kaul and Lipton, 1999; Zheng et al., 1999; Khan et al., 2008). When CXCL12 is cleaved, it switches its preferred receptor from CXCR4 to CXCR3, leading to enhanced neurotoxic effects (Vergote et al., 2006). Another chemokine, CXCL10, promotes neuron injury by stimulating Ca^{2+} flux (Sui et al., 2004; Sui et al., 2005; Sui et al., 2006). Chemokines may also cause neuronal damage by inducing monocyte infiltration. For instance, monocyte chemoattractant protein-1 (MCP1, a.k.a. CCL2) increases in the CSF of HIV patients with cognitive impairment (Kelder et al., 1998), and the MCP-1 increase is implicated in neuronal injury by promoting migration and infiltration of monocytes/macrophages (Sevigny et al., 2004; Ragin et al., 2006; Sevigny et al., 2007; Deshmane et al., 2009). The neuron-released chemokine fractalkine (FKN; a.k.a. CX3CL1), which is also up-regulated in HIV patients (Tong et al., 2000; Foussat et al., 2001; Sporer et al., 2003; Letendre et al., 2011) and has been implicated in HIV-associated dementia (Pereira et al., 2001; Cotter et al., 2002; Erichsen et al., 2003), may also modulate monocyte migration and neuron damage (Tong et al., 2000; Limatola et al., 2005; Noda et al., 2011; Suzuki et al., 2011).

Besides cytokines and chemokines, reactive microglia can also release other neurotoxic substances such as excitatory amino acids, platelet-activating factor and free radicals (Giulian et al., 1990; Perry et al., 1998; Turchan et al., 2003; Sacktor et al., 2004; Tian et al., 2012). These neurotoxins may cause NMDAR-mediated excitotoxicity by excessive Ca^{2+} influx and oxidative stress.

Reactive microglia assume diverse phenotypes, which are roughly categorized into the "classical" activation (M1) and "alternative" activation (M2) phenotypes. M1 microglia secrete pro-inflammatory cytokines (e.g. TNF-α, IL-1β, interleukin-6 (IL-6)) and reactive oxygen species (Edwards et al., 2006; Colton, 2009; Boche et al., 2013), which are implicated in synaptic damage. On the other hand, M2 microglia play a role in repairing neuronal injuries and clearing debris, and they produce anti-inflammatory cytokines and

substances such as IL-10, arginase-1 (Arg-1), chitinase 3-like 3 (Chi3l3) and transforming growth factor-β (TGF-β) to facilitate the repair processes (Edwards et al., 2006; Colton, 2009; Boche et al., 2013). Therefore, M1-M2 polarization may play a crucial role in determining the potential neurotoxic or neuroprotective activity of microglia in neurodegeneration disorders (Tang and Le, 2016). It is currently unknown if dysregulation of M1/M2 polarization of microglia is involved in the pathogenesis of HIV-associated synaptic degeneration.

Although only a small population of astrocytes can be infected by HIV (Conant et al., 1994; Tornatore et al., 1994; Gorry et al., 2003; Churchill et al., 2006), the infected astroglia play a critical role in the HIV-associated synaptic injury (Gorry et al., 2003; Ton and Xiong, 2013). Astrocytes are a potentially important reservoir for HIV persistence. In autopsy brain tissues of HIV patients, up to 20% of astrocytes contain integrated HIV-1 (Churchill et al., 2006). The infected astrocytes produce and secrete viral protein such as gp120, Tat, Vpr, Rev and Nef, although viral replication is restricted (Ranki et al., 1995; Gorry et al., 1998; Nath, 2002; Chompre et al., 2013; Saylor et al., 2016). Tat and gp120 can activate astrocytes to produce proinflammatory cytokines such as TNF-α, IL-6 and IL-1β (Nottet et al., 1995; Shah et al., 2011b), the chemokine CCL5 (Shah et al., 2011a), and neurotoxic nitric oxide (NO) (Reddy et al., 2012), which, as described above, can cause synaptic damage. More recent studies showed that HIV-infected astrocytes could spread the toxic signals to neighboring neurons or un-infected glial cells through gap junctions (Eugenin and Berman, 2007). The infected astrocytes also increase secretion of CCL2 and glutamate, which may contribute to the dysregulation of the integrity of the BBB as well as defects in monocyte recruitment and immune responses in the CNS (Eugenin and Berman, 2007; Eugenin et al., 2011). In addition, HIV-infected and/or reactivated astrocytes are probably impaired for glutamate re-uptake, resulting in increased extracellular glutamate and excitotoxicity-induced synaptic degeneration (Patton et al., 2000; Wang et al., 2003b; Zhou et al., 2004).

1.5.2 A role of glia-mediated phagocytosis of synapses?

The discovery of microglial phagocytosis in developmental synaptic pruning (Schafer et al., 2012; Brown and Neher, 2014; Xavier et al., 2014) presents an intriguing possibility of similar mechanisms in synaptic degeneration induced by HIV-1 infection. Microglial phagocytosis is mediated by the classical complement system (Stevens et al., 2007b; Schafer et al., 2012). More recent work indicates that this microglia-based mechanism is implicated in synaptic loss in Alzheimer's disease (Schafer et al., 2012; Hong et al., 2016b) and West Nile virus-induced synaptic loss (Vasek et al., 2016a). Although a role of the complement system was suggested in the immune defense for HIV infection (Yu et al., 2010; Liu et al., 2014), little is known about its involvement in HIV-associated neurodegeneration in the CNS. Complement proteins C1q and C3 are significantly increased in the brains and CSF of HIV patients, and the increase is associated with the up-regulation of the neuronal injury marker neurofilament protein in the CSF and with cognitive impairments (McGuire et al., 2016). It will be interesting to investigate if complement-mediated microglial phagocytosis contributes to HIV-associated synaptic degeneration. Moreover, the FKN/CX3CR1 pathway also regulates the microglial phagocytosis (Fuhrmann et al., 2010; Blomster et al., 2011; Zabel et al., 2016), but its potential contribution to HIV-induced synaptic degeneration has not been tested.

Astrocytes have numerous processes that intimately interact with synapses and monitor synaptic activity. Recent studies indicate that astrocytes can eliminate synapses by phagocytosis (Chung et al., 2013; Chung et al., 2015a; Chung et al., 2015b; Allen and Eroglu, 2017). Astrocytes express critical regulators of phagocytotic pathways, including

Megf10 and MerTK, which play important roles during elimination of synapses in the developing and adult brain (Chung et al., 2013). In addtion, the synaptic phagocytic capacity of astrocytes is highly controlled by an APOE isoform in Alzheimer's disease brains. APOE2 enhances the phagocytic activity of astrocytes; whereas APO4 decreases the rate of synaptic phagocytosis by astrocytes (Chung et al., 2016). It is intriguing to conceive that astrocyte dysfunction might contribute to pathogenic synaptic degeneration in CNS in respond to HIV infection.

1.6 PROJECT OVERVIEW

It is clear that HIV-associated synaptic degeneration is a result of cascades of neuropathogenic processes initiated by HIV-1 infection (and often in combination with related comorbidities). The progression of the pathogenesis is determined by the interaction between HIV-1 and the host. The high prevalence of dementia and pain in patients with HAART, which successfully suppresses HIV-1 replication, indicates that intact virions are probably not the major pathogenic agent. Instead, individual HIV-1 toxic proteins such as gp120 and Tat released from infected cells in the CNS may play a major role in inducing the synaptic degeneration. This view posits an interesting and relevant possibility that infected cells that do not productively assemble infective virions, thanks to HAART, may still synthesize pathogenic HIV-1 proteins. The scenario of replication-independent production of HIV-1 protein is superficially counterintuitive, and the underlying mechanism is still poorly understood. Mounting evidence document the neurotoxic effects of individual HIV-1 proteins. Published studies have mainly focused on specific HIV-1

proteins such as gp120 and Tat in different experimental systems, and they have found that more than one HIV-1 protein may elicit complicated molecular pathways that potentially contribute to synaptic degeneration. When these proteins are co-released from the infected cells in the CNS, they likely act in conjunction to cause synaptotoxicity. The conceived interaction of multiple HIV-1 proteins would dramatically increase the complexity of the pathogenic cascades. At the cellular level, in addition to the excitotoxicity from direct stimulation of neurons, reactive microglia and astrocytes likely also attack the neurons at synaptic regions to contribute to the concerted processes of synaptic degeneration.

The long-term goal of this study is to develop new adjunctive therapy to fight against HIV-associated neurological disorders. The objective of this study is to elucidate the mechanism(s) by which gp120 causes synaptic degeneration. Previous work has focused on potential intrinsic mechanisms in neurons. However, we still do not know if glial cells participate in gp120-induced synapse loss through intracellular interaction. Emerging evidence suggests critical roles of microglial and astrocytic phagocytosis in synapse pruning during development and in disease conditions. CX3CR1 and complement receptor 3 (CR3) are two microglial-specific receptors that regulate early postnatal synapse pruning by recognizing the signals from neurons (Chung et al., 2015b). Interestingly, the only known CX3CR1 ligand, fractalkine (FKN; a.k.a. CX3C ligand-1 or CX3CL1), is up-regulated in HIV patients (Tong et al., 2000; Sporer et al., 2003; Letendre et al., 2011), especially in patients with HIV-associated dementia (Pereira et al., 2001; Cotter et al., 2002; Erichsen et al., 2003). On the other hand, recent work found that astrocytes were involved in synapse phagocytosis and elimination through MERTK and MEGF10 pathways (Chung et al., 2013). My preliminary data revealed that gp120 exposure caused

dramatic activation of microglia and astrocytes that was concomitant with synaptic degeneration. Based on these prior and preliminary findings. We hypothesized that HIV-1-gp120 exposure leads to synapse damage and glial cells (especially microglia and astrocytes) activation in the CNS. The activated microglia and astrocytes then mediate synaptic degeneration by cooperatively engulfing and eliminating gp120-damaged synapses. To test this hypothesis, we used interdisciplinary approaches of molecular biology, imaging, electrophysiology and behavioral testing to analyze the synapse loss, glial cells activation and function. The analysis addressed three specific aims:

Specific Aim 1. To determine the role of microglia in gp120-induced synapse degeneration in the spinal cord. A significant decrease of synaptic protein was detected in the spinal dorsal horn (SDH) of the HIV-1 patients who developed pain (Yuan et al., 2014), suggesting a potential role of synaptic degeneration during the pathogenesis of HIV-associated pathological pain. We first examined the alteration of spinal synapses after gp120 stimulation in primary cortical cultures and gp120-treated mice models. We also accessed the gp120 -induced functional changes of synapse in the pain circuit by patch clamp recording and pain behavioral analysis. To determine the role of microglia, we determined the effects of microglia ablation (by either pharmacological or genetic approaches) on gp120 induced alterations of spinal synapses. In addition, we determined the role of the FKN/CX3CR1 signaling in gp120-induced synapse loss and identified the up-stream regulator of FKN/CX3CR1 signaling. The study demonstrates that HIV-1 gp120 induces synapse degeneration via microglial activation that is controlled by the Wnt/β-catenin-regulated KFN expression in neurons.

Specific Aim 2. To determine the role of microglial phagocytosis in gp120-induced cortical synapse elimination. Synapse loss is closely related with the presence and severity of HAND (Sá et al., 2004). Understanding the mechanism of synaptic degeneration after HIV infection would be helpful to discover potential therapeutic targets for HAND treatment. In this specific aim, we validated synapse degeneration in the frontal cortex of gp120 Tg mice using western blotting and double-labeled immunofluorescence staining. We postulate that microglia mediate gp120-induced synaptic degeneration via engulfing and eliminating the damaged synapses. The microglia-mediated phagocytosis of synapses in wildtype (WT) and gp120 Tg mice was carefully compared by immunofluorescence staining of specific pre- or post-synaptic markers. To confirm the role of microglial phagocytosis in synapses removal, we determined the effects of microglial ablation on synapse elimination in gp120 Tg mice. We further determine the regulatory role of the FKN/CX3CR1 signaling and MerTK signaling in gp120 induced-microglial activation and synapse phagocytosis. The results suggest that microglial phagocytosis plays a critical role in gp120-induced synapses elimination, especially at the pre-synaptic compartments. Furthermore, my data reveal that the MerTK signaling pathway and that FKN/CX3CR1 signaling are important in regulating this process.

Specific Aim 3. To determine the role of astrocytic phagocytosis in gp120 -induced synaptic degeneration. Recent studies reveal astrocytic phagocytosis in synapse pruning during development (Chung et al., 2013; Chung et al., 2015a; Chung et al., 2015b; Allen and Eroglu, 2017). In this specific aim, we compared astrocytic alterations between WT and gp120 Tg mice cortices. We found the astrocytes were dramatically activated in gp120 Tg mice. In addition, to determine how astrocytes might participate in gp120-induced

synapse loss, we assessed the role of astrocytic phagocytosis in synapse elimination by immunofluorescent staining the cortical sections with antibodies against specific pre-, post-synaptic markers. We observed that astrocytes predominately engulf and eliminate post-synaptic terminal in the gp120 Tg mice. We also determined the regulatory role of the MerTk pathway in astrocytic phagocytosis of synapses in gp120 Tg mice and found that MerTk knockout did not affect gp120-induced post-synapse elimination.

Chapter 2 Materials and methods

2.1 ANIMALS.

CX3CR1 knockout mice (00582. B6.129P-Cx3cr1tm1Litt/J) were obtained from The Jackson Laboratory. In these mice, the CX3CR1 gene was replaced by a green fluorescent protein (GFP) reporter gene (Jung et al., 2000b). CD11b-DTR mice were from Jackson Laboratory [006000; B6. FVB-Tg (ITGAM-DTR/EGFP)34Lan/J]. The diphtheria toxin receptor is expressed under the control of the human ITGAM (integrin alpha M) promoter (CD11b), and administration of diphtheria toxin (DT) leads to transient depletion of microglia/macrophages in the transgenic mice (Duffield et al., 2005). Gp120 transgenic (Tg) mice (from Dr. Marcus Kaul, Sanford-Burnham Medical Research Institute) express HIV-1 LAV gp120 under the control of the glial fibrillary acidic protein (GFAP) promoter (Toggas et al., 1994). The β-catenin^{flox} mouse (004152. B6.129-Ctnnb1tm2Kem/KnwJ), Thy1-YFP [003709. B6. Cg-Tg (Thy1-YFP)16Jrs/J], MerTK knockout mic (011122. B6;129-Mertktm1Grl/J) and the nestin-Cre mouse (003771. B6. Cg-Tg (Nes-cre)1Kln/J) were from The Jackson Laboratory. For electrophysiological recording, 6-to-8-week-old GAD67-GFP male mice [003718. FVB-Tg (GadGFP)45704Swn/J, Jackson Laboratory] were used. These mice express GFP exclusively in GABAergic neurons (GABAn) (Yowtak et al., 2011; Cadwell et al., 2016).

Thy1-YFP/gp120 double transgenic mice was generated in the lab by crossbreeding Thy-1 mice with gp120 Tg mice. Gp120 Tg/CX3CR1$^{+/-}$ and gp120Tg/CX3CR1$^{-/-}$ mice were generated by crossbreeding gp120 Tg mice and CX3CR1 knockout mice. Gp120 Tg/MerTK$^{-/-}$ mice were generated by crossbreeding gp120Tg mice and MerTK knockout mice.

All animal procedures followed protocols that were approved by the Institutional Animal Care and Use Committee at the University of Texas Medical Branch. Mice were housed in a constant temperature environment (23 ± 3 °C) with standard bedding, free access to food and water, and under a 12/12 hrs light/dark cycle. Both male and female mice were used in cellular and molecular analysis. Only males were used for behavioral testing.

2.2 REAGENTS.

Maraviroc (Cat# 11580) and HIV-1 gp120Bal recombinant protein (Cat # 4961) were obtained from the NIH AIDS Reagent Program. D-APV (cat# 165304) was purchased from Calbiochem, and Minocycline hydrochloride (Cat#M9511) and diphtheria toxin (DT) (Cat# D0564) were from Sigma. The use of DT was approved by the Institutional Chemical Safety Committee. To deplete microglia in CD11b-DTR mice, DT was i.t. injected daily for 3 days (20 ng/injection). HIV-1 gp120Bal in PBS was aliquoted and stored at -80°C until use.

2.3 PRIMARY CORTICAL CULTURES.

Primary cortical cultures were prepared from mouse embryos as described previously (Ru et al., 2012). The newborn C57BL/6J pups (both male and female) were euthanized at postnatal day 0-1. Cortices were dissected and placed in iced Hank's balanced salt solution (HBSS; Invitrogen). Cells were dissociated with trypsin in HBSS with gentle trituration and resuspended in DMEM medium (Invitrogen) containing 10% FBS (Gibco). Dissociated cells were then plated on poly-D-lysine (PDL)- coated dishes (30,000-70,000; Sigma) at a density of 1.5×10^5 cells/cm^2 for western blotting and at 4 ×

10^4 cells/cm^2 onto PDL-coated glass coverslips (Cat#354085; BD Biocoat) for immunofluorescence staining. Cells were grown in a humidified atmosphere of 5% CO_2 and 95% air at 37 °C. Three hours after plating, the media were replaced with Neurobasal Medium (Invitrogen) supplemented with 2% B27 (Invitrogen) and 0.5 mM L-glutamine (Invitrogen). Half of the media was replenished every 5 days until 14 days in vitro (DIV). Only morphologically healthy cultures were used for the further experiments.

2.4 TRANSCUTANEOUS INTRATHECAL INJECTION (I.T).

Mice were anesthetized under 2% isoflurane., A 30.5-gauge stainless steel needle attached to a 10 μl Hamilton syringe (Hamilton, Reno, NV) was used for i.t. injections. 5 μl gp120Bal (500 ng; every other day) in PBS or 5 μl DT (20 ng; daily) in PBS was intrathecally (i.t) injected into the subarachnoid space between the L5 and L6 vertebrae. A correct intrathecal placement of the needle tip was judged by a tail twitch. Mice injected with vehicle were used as controls.

2.5 WESTERN BLOTTING ANALYSIS.

Mice were euthanized with excess anesthesia (isoflurane), and the L4-L5 lumbar spinal cord segments or cortices of mice were collected and homogenized in RIPA lysis buffer (50 mM Tris-HCl, pH 7.4, 150 mM NaCl, 0.1% SDS, 1% Nonidet P-40, 10% glycerol, 1 mM EDTA, pH 8.0) containing PMSF and protease inhibitor mixture (cat# P8340; Sigma-Aldrich)). Protein concentration in the homogenates was determined using a BCA protein assay kit (product 23227; Pierce). Protein concentration was titrated to 2 μg/μl for immunoblotting analysis. For cortical cultures, the cells in 12-well plates (14 DIV) were rinsed with cold PBS and lysed immediately with 150 μl of 2× SDS-PAGE

sample buffer (125 mM Tris, pH 6.8, 4% SDS, 10% 2-mercaptoethanol, 20% glycerol, and 0.0025% bromophenol blue) for 30 min. Equal amounts of protein (30 μg/lane) were loaded and separated on SDS-PAGE, followed by transferring to polyvinylidene difluoride (PVDF) membranes (Millipore). Immunoblots were blocked by 5% non-fat milk in Tris-buffered saline Tween-20 (TBST; 20 mM Tris–HCl, 150 mM NaCl, pH 7.5, 0.1% Tween-20) for 2 hrs at room temperature. The blots were then sequentially incubated with primary and secondary antibodies. Protein bands were visualized using the Enhanced Chemiluminescence kit from Pierce. β-actin was blotted as a loading control. The intensity of bands was quantified by densitometry analysis with NIH ImageJ.

Table. 1 Primary antibodies for western blotting analysis.

Antibody	Species	Source	Cat. No.	Dilution
PSD95	Rabbit	CST	3450	1:1,000
PSD95	Rabbit	Millipore	04-1066	1:1,000
Synaptotagmin-1	Rabbit	CST	14558	1:1,000
Synapsin I	Rabbit	Millipore	AB1543	1:2,000
cleaved caspase-3	Rabbit	CST	9661	1:1,000
total-caspase-3	Rabbit	CST	9662	1:2,000
IBa1	Rabbit	Wako	016-20001	1:1,000
IBa1	Rabbit	Abcam	ab178847	1:1,000
GFAP	Mouse	Millipore	MAB360	1:5,000
CD11b	Rabbit	Abcam	ab133357	1:2,000
β-catenin	Mouse	BD Biosciences	610153	1:5,000
Wnt3a	Rat	R&D	MAB1324	1:1,000
FKN	Rabbit	Abcam	ab25088	1:1,000
vGluT1	Mouse	Millipore	MAB5502	1:2,000

Megf10	Rabbit	Millipore	ABC10	1:1,000
MerTK	Goat	R&D	AF591	1:1,000
p-MerTK (Y749 + Y753 + Y754)	Rabbit	Abcam	ab14921	1:1000
CCR5	Mouse	NIH AIDS Reagent Program	4088	1:1,000
CXCR4	Rabbit		11236	1:1,000
β-actin	Rabbit	Santa Cruz	sc-1616-R	1:2,000

2.6 IMMUNOFLUORESCENT STAINING AND QUANTIFICATION.

For cultured cells, immunofluorescent staining was conducted as previously described (Ru and Tang, 2016). Briefly, the cultured cells were fixed in 4% paraformaldehyde (PFA) for 20 min and then incubated in blocking buffer (5% BSA and 0.3% Triton X-100 in 0.1 M PBS) for 1 hr at room temperature. After blocking, the cells were incubated with anti-PSD95 and anti-Syn I antibodies at 4 °C overnight, followed by incubating with FITC and cy3 -conjugated secondary antibodies (1:200, Jackson ImmunoResearch Laboratories) for 1 hr at room temperature. Images were captured using a confocal microscope (Nikon A1). NIH ImageJ software and NeuronJ plugin were used to trace the neuronal processes and determine the regions of interest (ROIs). For each channel, "Subtract Background" was applied to remove the background and threshold (50-225) were set to remove the outliers, puncta analyzer then was used to count the number of $PSD95^+$, $SynI^+$ puncta and colocalized puncta within ROIs. At least 3 cultured coverslips were included for each condition, and 4 neurons from each coverslip were randomly picked for synaptic puncta analysis.

For tissue immunofluorescent staining, mice were anesthetized with isoflurane and perfused transcardially with cold PBS. The lumbar spinal segments were removed from

gp120 or vehicle i.t. treated mice, the frontal cortices were removed from WT or gp120 Tg mice. Collected tissues were immediately placed in 4% PFA in PBS at 4 °C overnight and then cryoprotected in 30% sucrose solution in PBS for at least 24 hours at 4 °C. Tissues were embedded in optimal cutting temperature (OCT) compound (Sakura Finetek, Torrance, CA). Transverse sections (35 μm) were prepared on a cryostat (Leica CM 1900). The sections were kept in Hito floating section storage solution (Hitobiotec Corp) at -20°C until they were stained for immunocytochemistry. For immunostaining, sections were rinsed with PBS 2 times to remove storage solution and blocked with 5% BSA and 0.3% Triton X-100 in PBS for 2 hrs at room temperature. This was followed by 48 hrs incubation with primary antibodies in Table 2. After five washes with PBS, the sections were incubated with fluorophore-conjugated secondary antibodies (Table. 3) before mounting. Confocal Z-stacks images were captured within the spinal cord dorsal horn or within the layer I-II of cortex by using a confocal microscope (Nikon A1). For each mouse, at least 3 fixed-frozen sections were included for each experiment, and at least 3 z-stacks images at 20 x, 40 x or 60 x magnification were taken. 30-50 consecutive optical sections with 0.5 μm interval thickness at 60 x magnification or 1 μm interval thickness at 20 x and 40 x magnification were captured for each z-stacks image.

Table. 2 Primary antibodies for immunofluorescent staining.

Antibody	**Species**	**Source**	**Cat. No.**	**Dilution**
PSD95 (UCT80)	Rabbit	Dr. Randall Walikonis University of Connecticut	N/A	1:200
Synapsin I	Mouse	Synaptic Systems	106001	1:200
vGluT1	Guinea pig	Millipore	AB5905	1:500
IBa1	Goat	Abcam	ab6076	1:500

IBa1	Rabbit	Abcam	ab178847	1:500
GFAP	Chicken	Abcam	ab4674	1:1000
GFAP	Mouse	Millipore	MAB360	1:500
Bassoon	Guinea pig	Synaptic Systems	141004	1:300
NR1	Mouse	Millipore	MAB363	1:200
TMEM119	Rabbit	Abcam	ab209064	1:200
galectin-3	Rat	Cedarlane	CLCR2A00	1:1000
STAT3	Rabbit	Abcam	ab68153	1:200

Table. 3 Secondary antibodies for immunofluorescent staining.

Antibody	**Species**	**Source**	**Cat. No.**	**Dilution**
Alexa Fluor® 488 AffiniPureAnti-Goat IgG	Donkey	Jackson ImmunoRe-search Laboratories	705-545-147	1:200
Alexa Fluor® 594 AffiniPure Anti-Goat IgG	Donkey		705-585-147	1:500
Alexa Fluor® 488 AffiniPure Anti-Rat IgG	Donkey		712-545-150	1:500
Alexa Fluor® 594 AffiniPure Anti-Rat IgG	Donkey		712-585-150	1:500
Alexa Fluor® 488 AffiniPure Anti-Rabbit IgG	Donkey		711-545-152	1:1000
Alexa Fluor® 488 AffiniPure Anti-mouse IgG	Donkey		715-545-150	1:1000

Alexa Fluor® 594 AffiniPure Anti-Chicken IgY (IgG)	Donkey	Jackson ImmunoRe-search Laboratories	703-585-155	1:500
Alexa Fluor® 594 AffiniPure Anti-Guinea Pig IgG	Donkey		706-585-148	1:300
FITC AffiniPure Anti-Guinea Pig IgG	Donkey		706-095-148	1:200
FITC AffiniPure Anti-Chicken IgY (IgG)	Donkey		703-095-155	1:200
Alexa Fluor 594 Conjugated Anti-Rabbit IgG	Donkey	Invitrogen	A-21207	1:500
Alexa Fluor 594 Conjugated Anti-Mouse IgG	Donkey		A-21203	1:500
Alexa Fluor® 405 Conjugated Anti-Mouse IgG	Donkey	Abcam	ab175658	1:500
Alexa Fluor® 405 Conjugated Anti-Rabbit IgG	Donkey		ab175651	1:500
Alexa Fluor® 405 Conjugated Anti-chicken IgG	Goat		ab175674	1:500

2.7 THREE- DIMENSIONAL (3-D) IMAGES RECONSTRUCTION AND QUANTIFICATION OF SYNAPSE ENGULFMENT.

Confocal z-stack images were taken at 60 x magnification, 30-50 consecutive optical sections with 0.5 μm interval thickness were transformed into 3-D reconstruction images using NIS-Elements Confocal Software or Imaris software. To process images analysis, “Subtract Background” (50 pixels) was applied to remove the background and threshold (50-225) were set to remove the outliers. The colocalization analysis were

perform by using Imaris or Fiji software. The Syn I^+ or $vGluT1^+$ puncta were counted as pre-synaptic termini, $PSD95^+$ or $NR1^+$ puncta were counted as post-synaptic termini. Syn I^+ or $vGluT1^+$ puncta colocalized with $IBa1^+$ cells were considered as the pre-synaptic structures engulfed by microglia, while $PSD95^+$ or $NR1^+$ puncta colocalized the $GFAP^+$ cells as the post-synaptic structures engulfed by astrocytes.

2.8 Measurement of mechanical sensitivity.

Paw withdrawal thresholds (PWT) of hind paws were measured by von Frey testing as described (Callahan et al., 2008). Briefly, the testing was performed at least 6 hrs before treatment and 24 hrs after each gp120Bal or vehicle i.t. injection. After mice habituated to the surrounding environment, a set of calibrated von Frey filaments (Stoelting, Wood Dale, IL) were applied to the plantar surface of each hind paw. The PWT were determined by using the Dixon up/down method. Testing was conducted by an experimenter who did not have information about the treatments.

2.9 Spinal cord slice preparation and whole cell patch recording.

After gp120Bal or vehicle i.t. administration, six-to-eight-week-old male mice were deeply anesthetized with 3% isoflurane. Following decapitation, the lumbar spinal cord was removed and placed into pre-oxygenated, cold (0-4 °C) NMDG (N-methyl-D-glucamine) solution containing: 93 mM NMDG, 2.5 mM KCl, 1.2 mM NaH_2PO_4, 30 mM $NaHCO_3$, 20 mM HEPES, 25 mM glucose, 5 mM sodium ascorbate, 2 mM thiourea, 3 mM sodium pyruvate, 10 mM $MgSO_4$ and 0.5 mM $CaCl_2$ (pH 7.4) saturated with 95% O_2 and 5% CO_2. The spinal cord was then sliced transversely at a thickness of 350 μm using a

Vibratome (Leica VT1200S, Buffalo Grove, IL). Following incubation for 30 min in the NMDG solution at 33°C, the spinal cord slices were transferred to artificial cerebrospinal fluid (ACSF) containing: 124 mM NaCl, 2.5 mM KCl, 1.2 mM NaH_2PO_4, 24 mM $NaHCO_3$, 5 mM HEPES, 12.5 mM glucose, 2 mM $MgSO_4$, and 2 mM $CaCl_2$ (pH 7.4), for 30 min at 33°C. Then, the slices were placed in a recording chamber perfused with 95% O_2 and 5% CO_2 saturated ACSF at a rate of 2 ml/min. Patch clamp recordings were performed 1 day after the last gp120 injection. The patch pipettes (4-8 MΩ) were filled with internal solution containing: 120 mM K-gluconate, 10 mM KCl, 2 mM Mg-ATP, 0.5 mM Na-GTP, 0.5 mM EGTA, 20 mM HEPES, and 10 mM phosphocreatine (pH 7.3). Whole-cell recordings of GFP expressing GABAergic neurons (GABAn) were made using Multiclamp 700B amplifier (Molecular Devices, Sunnyvale, CA), DigiDATA (Molecular Devices) and pClamp software (version 10.6. Molecular Device) with a 10 kHz sampling rate and 2 kHz filtering rate. After making the whole cell recording configuration, we routinely waited for 3 min until the baseline became stable, and then miniature excitatory postsynaptic currents (mEPSC) were recorded for 100 seconds at a -70 mV holding potential with 10 mM lidocaine (Sigma-Aldrich, St. Louis, MO).

2.10 Microglial depletion

Adult mice administrated with PLX5622, a specific colony-stimulating factor 1 receptor (CSF1R) inhibitor, can lead to near-complete microglial elimination from the CNS (Dagher et al., 2015). Six-month old gp120 Tg and WT mice will be treated with PLX5622 (formulated at 1200 mg/kg of chow) or control chow for 3 weeks and then microglial

depletion was confirmed by immunostaining cortical sections with anti- IBa1 and anti-TEME119 antibodies as described in 2.6.

2.11 Dissociation of mouse cortical tissue followed by flow cytometry analysis.

Dissociation of cortical tissue was performed according to the Worthington Biochemical Corp.'s dissociation protocol using the Papain Dissociation system (Cat# LK003150) with minor modifications. Briefly, 6-month-old WT and gp120Tg mice were anesthetized with isoflurane and perfused with cold HBSS. The cortex was immediately dissected and minced into small pieces followed by digestion with 20 U/ml papain and 0,005% DNase in EBSS buffer, for 1 hr at 37 °C. The tissue then was dissociated by careful trituration and centrifuge to collect cell pellet. After resuspending the cell pellet in the dilute DNase/albumin-inhibitor solution, dissociated cell passed through a 40 µm nylon cell strainer (Falcon, Cat# 352340) and followed by centrifugation at 300 g for 5 min to collect cells. The cell pellet was resuspended in 30% Percoll/HBSS solution and slowly laid over the 70% Percoll/HBSS (Sigma-Aldrich). Cells enrich in the 70%-30% junction were collected for flow cytometry analysis.

After wash with FACS buffer (PBS with 5% FBS and 2 mM EDTA), cells were stained with specific makers and flow cytometric analysis was carried out with a LSRII FACSFortessa (Becton Dickinson, San Jose, CA). In brief, cells were blocked with Fc blocker (anti-CD16/32) and stained with fixable viability dye, followed by surface staining with an APC-Cy7-conjugated anti-mouse CD11b (BD Biosciences) antibody for 30 min at 4 °C. After fixation and permeabilization by using the buffers from eBioscience, the cells were stained for intracellular molecular with PE-conjugated anti-GFAP (Miltenyi Biotec),

Alexa 488-conjugated anti-PSD95 (Abcam) and Alexa 647-conjugated anti-Synaptotagmin-1 (Abcam) antibodies. Data were analyzed with FlowJo software (TreeStar, Ashland, OR, USA).

3.12 STATISTICAL ANALYSIS

All data analysis was done using Prism 5 software (Graph-Pad) statistical Analysis. Result summaries were expressed as means ± SEM. Analyses were performed with Student's t-test for comparing two samples with 95% confidence. One-way analysis of variance (ANOVA) with a Tukey post-hoc test was used for comparisons among multiple groups, and two-way ANOVA with a Bonferroni post-hoc test to analyze two categorical explanatory variables. $P < 0.05$ was used to claim statistical significance.

Chapter 3 Wnt3a/β-catenin-regulated neuron-to microglia fractalkine signaling mediates gp120-induced synaptic degeneration in spinal pain neuronal circuits

3.1 INTRODUCTION

HIV-1 enters the central nervous system (CNS) soon after patients are infected (Resnick et al., 1988) and causes a range of neurological and cognitive complications (NeuroAIDS) (Gendelman, 2012). Synaptic degeneration correlates closely with the presence and severity of HIV-associated cognitive impairment (Everall et al., 1999; Sá et al., 2004; Letendre et al., 2011). In support of this notion, HIV-associated pain is associated with a significant decrease of synaptic markers such as synapsin I (Syn I), PSD95 and NMDA receptor subunit 1 (NR1) in the SDH of "pain-positive" HIV-1 patients but not in "pain-negative" patients (Yuan et al., 2014). Similarly, synaptic degeneration is also observed in the HIV pain mouse model that is generated by intrathecal (i.t.) injection of gp120 (Yuan et al., 2014). These prior observations suggest that synaptic degeneration in the spinal cord contributes to the development of HIV-associated pain. However, the mechanism by which HIV-1 causes the synaptic degeneration is unclear.

Microglia are the primary target for HIV infection in the CNS (Lee et al., 1993; Cenker et al., 2017). Microglia can remove excess and dysfunctional synapses by phagocytosis during neural circuit formation and in some disease conditions (Stevens et al., 2007b; Kettenmann et al., 2013; Brown and Neher, 2014; Xavier et al., 2014; Hong et al., 2016b; Vasek et al., 2016a). However, the potential role of microglia in synaptic

degeneration that is induced by HIV-1 infection has not been determined. During HIV infection, neuronal damage is likely a bystander effect of infected cells since neurons are not infected. Reactive microglia due to HIV-1 infection may also release neurotoxic factors, including proinflammatory cytokines (Tyor et al., 1992; Saha and Pahan, 2003; Viviani et al., 2006; Shah et al., 2011b), chemokines (e.g. CXCL12, CXCL10 and CCL2) (Kelder et al., 1998; Langford et al., 2002; Sui et al., 2004; Peng et al., 2006; Sui et al., 2006), excitatory amino acids, platelet-activating factor and free radicals (Giulian et al., 1990; Perry et al., 1998; Turchan et al., 2003; Sacktor et al., 2004; Tian et al., 2012) to induce synaptic degeneration (Ru and Tang, 2017).

Microglial phagocytosis of synapses is elicited by signals that regulate microglia-neuron interactions. These intercellular signals include the complement and fractalkine (FKN) pathways. To remove the "unwanted" synapses, complement components C1q and C3 sequentially translocate to the synapses to act as "eat-me" signals (Schafer et al., 2012), which bind to the microglial receptor CR3 to stimulate synapse elimination (Stevens et al., 2007b; Schafer et al., 2012; Hong et al., 2016b; Vasek et al., 2016a). FKN is primarily expressed by neurons and regulates synapse phagocytosis by stimulating its sole receptor, CX3CR1, on microglia (Harrison et al., 1998; Paolicelli et al., 2011; Zhan et al., 2014). FKN is up-regulated in HIV patients, and this up-regulation is thought to relate to the development of HIV-associated dementia (Pereira et al., 2001; Cotter et al., 2002; Erichsen et al., 2003).

Because HIV infection is associated with FKN up-regulation (Tong et al., 2000; Foussat et al., 2001; Pereira et al., 2001; Sporer et al., 2003; Letendre et al., 2011), we hypothesize that FKN signaling-mediated neuron-microglia cross-talk plays a critical role

in HIV-infection-induced synaptic degeneration. We tested this hypothesis using both in vitro (primary cortical cultures) and in vivo (spinal cord) models of HIV-1 gp120-induced synaptic degeneration. Our results revealed an important role of micrioglia in gp120-induced synaptic degeneration. We also showed that microglia-mediated synapse degeneration depended on CX3CR1 signalling. We further elucidated that activity-dependent Wnt3a/β-catenin signaling controls gp120-induced FKN up-regulation. These findings collectively suggest a critical role of the Wnt3a-FKN-CX3CR1 intercellular signaling from neurons to microglia in regulating gp120-induced synaptic degeneration.

3.2 RESULTS

3.2.1 Gp120 induces synaptic degeneration in vitro and in vivo.

To test the effect of gp120 on synapses, we treated primary cortical neuron-glia co-cultures with gp120 and then measured the levels of synaptic markers, including the pre-synaptic markers Syn I and Syt-1 and post-synaptic marker PSD95. We found that both pre- and post-synaptic proteins decreased in a time-dependent manner after exposure to gp120 (200 pM). A significant decrease of PSD95 was observed from 6 hr to 24 hrs after gp120 treatment (Fig. 3.1 A). The decrease of Syn I occurred between 12 h and 24 h (Fig. 3.1 B), and similarly decreased profiles of Syt-1 were observed (Fig. 3.1 C). Heat-inactivated gp120 control could not lead to the reduction of PSD95 and Syn I (Fig. 3.1 D, 3.1 E). To exclude the possibility of the decrease of synaptic markers that was caused by cell death, we tested if the experiment induced apoptosis in the cultures. We found that treatment with gp120 did not alter the protein level of cleaved caspase-3 (Fig. 3.1 F). Thus,

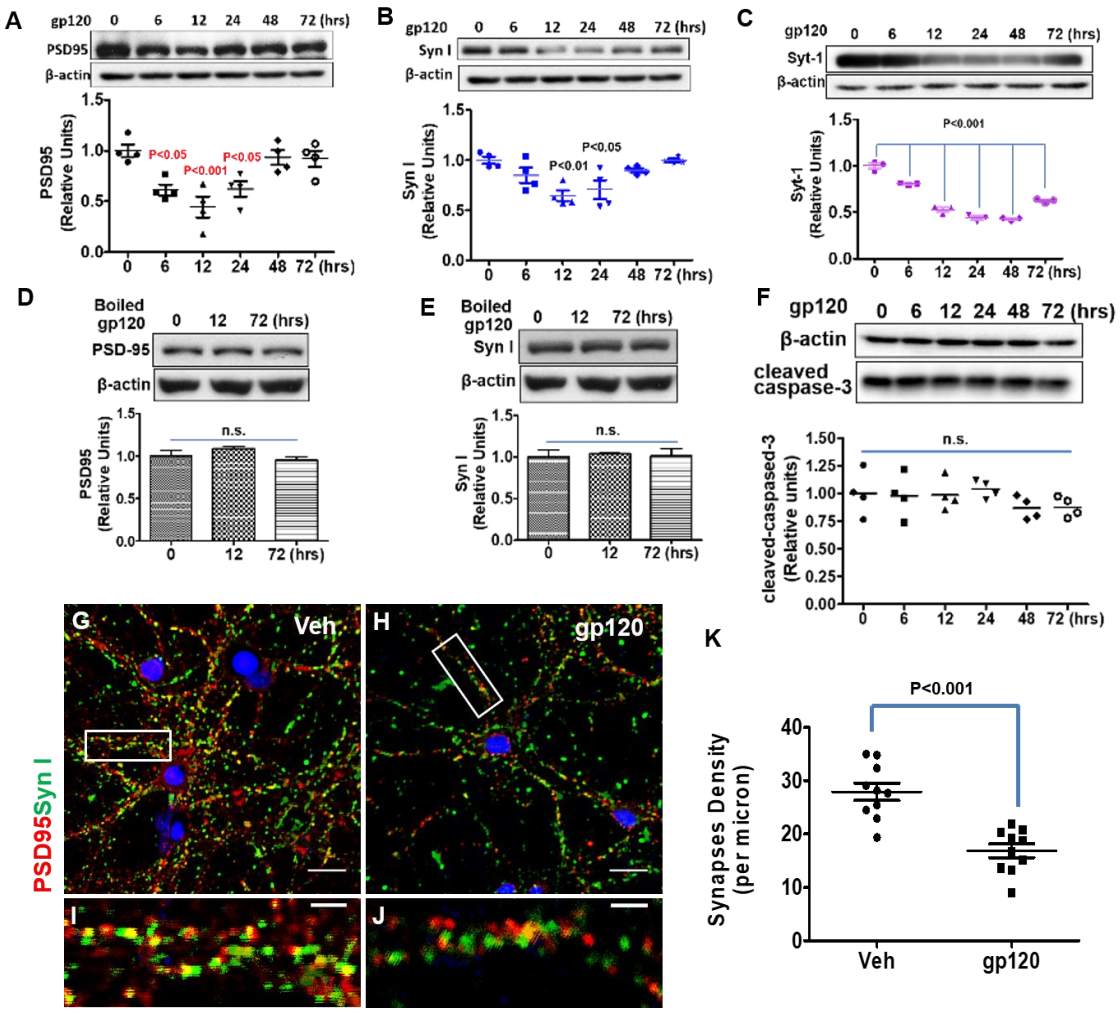

Fig 3. 1 HIV-1 gp120 induces synapse loss in a time-dependent manner in primary cortical cultures. A-C. Time course of gp120-induced decreases of synaptic proteins. Cortical neuron-glia co-cultures (14 DIV) were incubated with 200 pM gp120 for the indicated time. Cell lysates were analyzed by immunoblotting using antibodies against PSD95 (A), Syn I (B) or Syt-1 (C). For A and B, N=4; for C, N=3 cultures per condition. D, E. Heat-inactivated gp120 did not affect PSD95 (D) and Syn I (E) in cultures, N=3. F. Western blot of cleaved caspase-3 from gp120-treated cell lysates, N=4. G-J. Representative immunofluorescent images showing PSD95 and Syn I after 12 hrs vehicle (Veh) or gp120 treatment (PSD95 is red, Syn I is green, and co-localized region is yellow). Higher magnifications of boxed region (I, J). Scale bar for G, H, 20 μm; I, J, 5 μm. K. Bar graph summarizes the effects of gp120 on synapse density. N=12 neurons from 3 cultured coverslips per condition (mean ± SEM).

gp120-induced synaptic protein decreases were not due to apoptosis. To further confirm that the decrease of synaptic markers was associated with a decrease of synapse density, we performed immunostaining of synapses in cultured neurons and quantified the intact

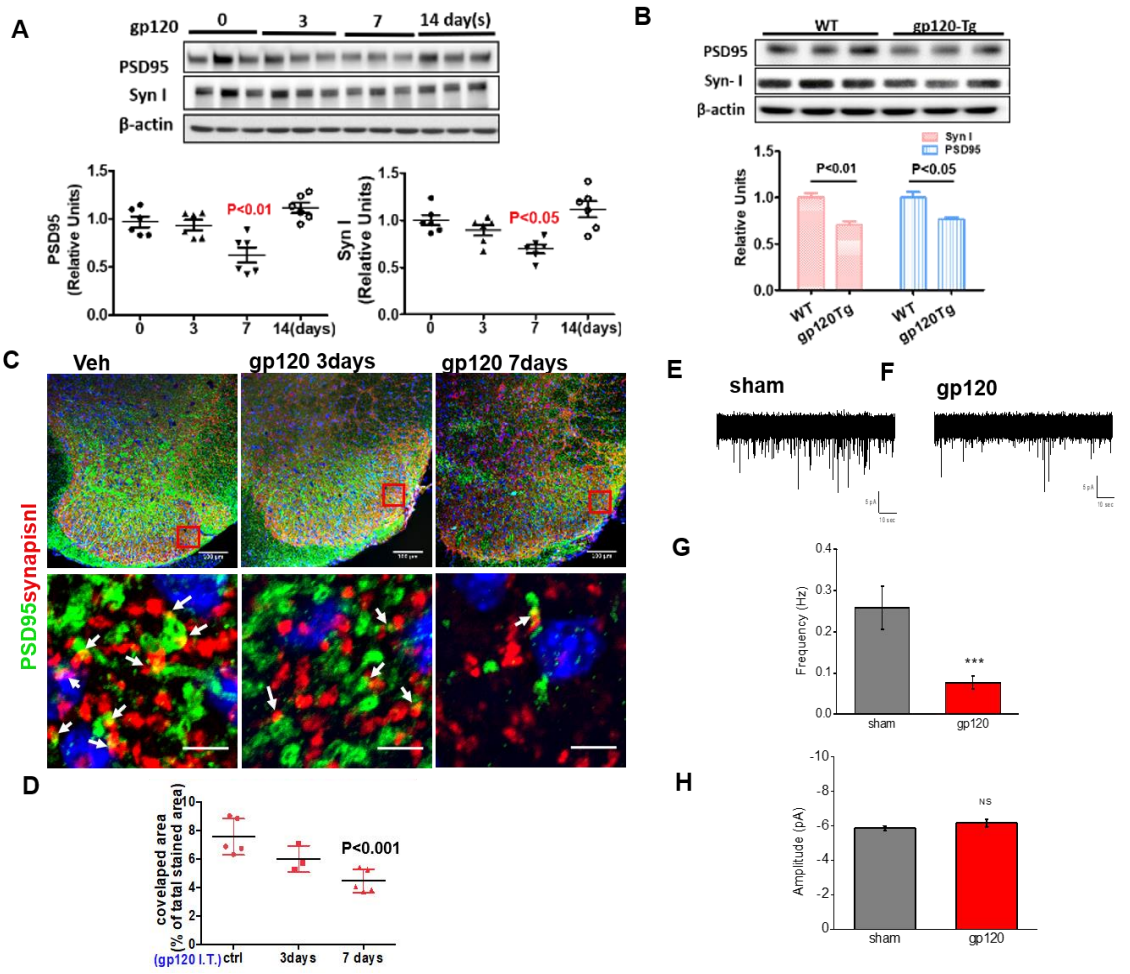

Fig 3. 2 Gp120 causes synapse decrease in the spinal dorsal horn. A. PSD95 and Syn I protein levels in the L4-L5 spinal cord after gp120 i.t. injection (4-5-month old mice were injected with gp120 (500 ng/injection/every other day for 7 days, N=6 mice per time point). B. PSD95 and Syn I protein levels in the L4-L5 spinal cord of the gp120 transgenic (Tg) and wild-type (WT) mice (N=3 mice per condition). C. Confocal images of SDH sections showing anti-Syn I and anti-PSD95 antibodies staining, co-localized areas of Syn I and PSD95 were calculated (white arrows). The scale bars for upper panels are 100 µm, lower panels are 5 µm. D. Quantification: Images of layers 1-2 of the SDH from 3-5 mice were included for each group. For each mouse, 3-4 spinal slices were included, and 2-3 images were obtained from each section. E, F. Representative whole cell recording of mEPSC from the SDH from mice treated via i.t. with vehicle (Sham) (E) or gp120 (F). 5 µl gp120 (500 ng) or PBS were i.t.-injected into GAD67/GFP mice once every other day for 7 days. GFP labeled $GA67^{+}$ cells were held at Vm=−70 mV. G, H. Summary graphs showing the differences of frequency (G) and amplitude (H) of mEPSCs between the sham- and gp120-treated mice. N=15 (sham) and *N*=31 (gp120) neurons were recorded from 3 sham and 5 gp120 i.t. mice for mEPSCs. E-H. Electrophsilogical experiments were conducted by Dr. Chilman Bae. Error bars represent SEM.

synapses with co-staining of SynI and PSD95 as described (Micheva et al., 2010; Okerlund et al., 2010; Galli et al., 2014). The results showed that gp120 exposure caused a significant loss of intact synapses (Fig. 3.1 G-L).

To determine the effects of gp120 on synapses in vivo, we injected gp120 (500 ng/injection) intrathecally into adult mice and measured the synaptic proteins PSD95 and Syn I in the L4-L5 spinal segments. Our results showed that both PSD95 and Syn I levels were lower at day 7 after gp120 injection and returned to the baseline at day 14 (Fig. 3.2 A). The restoring of PSD95 and Syn I at day 14 may result from the homeostatic mechanism of neurons, to restore synaptic connections. We also performed double staining of Syn I and PSD95 and quantified intact synapses with co-localized PSD95 and Syn I on confocal images. We observed that the synapse number was significantly decreased in the SDH at day 7 post injection (Fig. 3.2 C, 2 D). We also sought to confirm the gp120-induced synaptic degeneration in the gp120 transgenic (gp120 Tg) mice. We observed that both PSD95 and Syn I levels were lower in the spinal cord (Fig. 3.2 B) of transgenic mice. We further confirmed the gp120-induced synapse loss by electrophysiology. We recorded miniature excitatory postsynaptic currents (mEPSCs) of GABAergic neurons in the laminar 1-2 of SDH. These GABAergic neurons were labeled by GFP (Yowtak et al., 2011; Cadwell et al., 2016). Gp120 administration significantly decreased the frequency of mEPSCs (Fig. 2 E-H), indicating the reduction of functional synapses.

3.2.2 Microglia are critical for gp120-induced synapse loss.

Recent studies reveal a critical role of microglia in synapse pruning (Kettenmann et al., 2013; Brown and Neher, 2014; Chung et al., 2015b). Hence, we wanted to test the

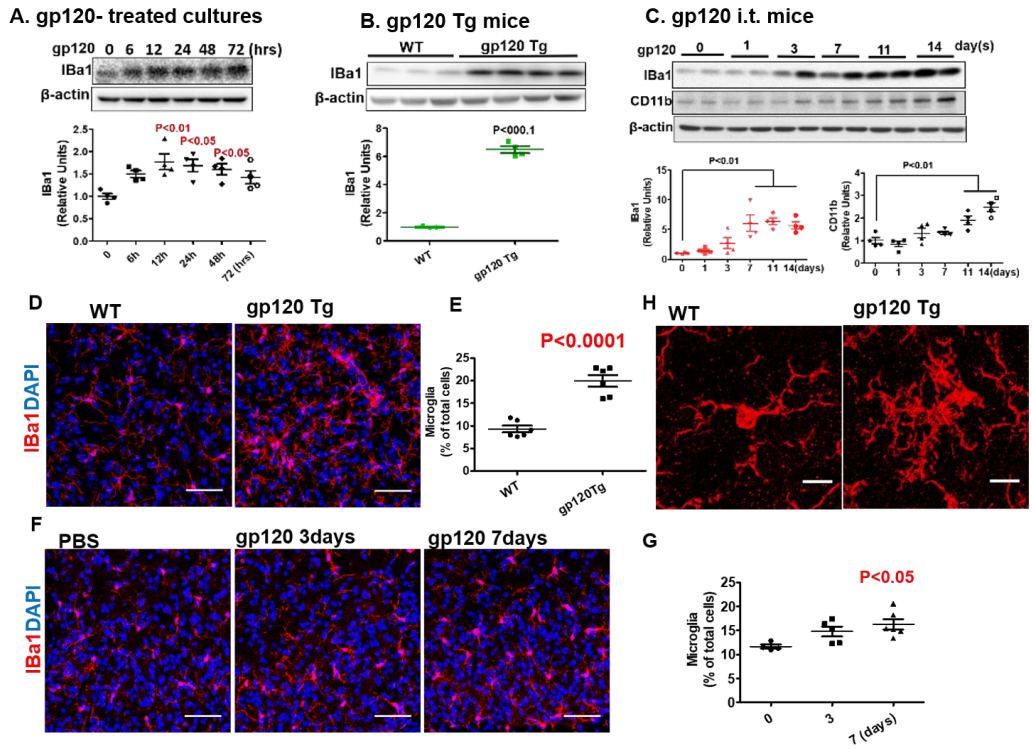

Fig 3. 3 Gp120 causes microglial activation. A. Levels of IBa1 in 200 pM gp120-treated primary cortical cultures (N= 4 cultures in each condition). B. IBa1 in L4-L5 spinal cords from gp120 transgenic and WT mice. WT, N=3 mice; gp120Tg, N=4 mice. C. IBaI and CD11b in L4-L5 spinal cords from mice after gp120 injection (i.t.) (500 ng/injection). N=4 mice per time point. D. Confocal images of IBa1-positive cells in the SDH from WT and gp120Tg mice. E. Quantitative summary of D (mean ± SEM); N=6 mice per group. F. Confocal images of IBa1-positive cells in the SDH of PBS- or gp120-injected (i.t.) mice. G. Quantitative summary of F (mean ± SEM); PBS, N=4 mice; gp120/3 days; N=5 mice; gp120/7 days, N=6 mice. H. High-magnification images showing morphological characteristics of reactive microglia. Scale bars: D & F, 50 µm; H, 10 µm.

potential involvement of microglia in gp120-induced synapse loss. Immunoblotting analysis on primary cortical cultures showed that the expression level of ionized calcium binding adaptor molecule 1 (IBa1), a protein up-regulated in reactive microglia, was significantly increased after gp120 treatment (Fig. 3.3 A). IBa1 was also up-regulated in the spinal cords of gp120 transgenic mice (Fig. 3.3 B) and gp120-injected (i.t.) mice (Fig. 3.3 C). Another microglial marker, CD11b, was also elevated after gp120 injection (Fig. 3.3 C). Immunofluorescent staining of the spinal sections revealed significant increases in

the number of microglia in gp120 Tg (Fig. 3.3 D, 3.3 E) and gp120-injected (i.t.) mice (Fig. 3.3 F, 3.3 G), with increased processes and enlarged soma (Fig. 3.3 H). These findings indicate that gp120 stimulates microglial activation.

Next, we set out to determine the role of microglia in gp120-induced synapse loss. As seen in previous experiments (Fig. 3.1 A, 3.1 B), gp120 caused transient decreases of PSD95 and Syn I in cortical cultures (Fig. 3.4 A, 3.4 B). The decreases diminished when cultures were pre-treated with minocycline (Fig. 3.4 A, 3.4 B) to inhibit microglial activation (Kobayashi et al., 2013). To determine the role of microglia in vivo, we generated the gp120/CD11b-DTR double transgenic mouse and ablated microglia in the mice by diphtheria toxin (DT) administration (Cailhier et al., 2005; Duffield et al., 2005). Similar to the gp120 Tg mice, the gp120/CD11b-DTR mice also displayed decreases of PSD95 and Syn I in spinal cord (Fig. 3.4 D). DT i.t. administration (20 ng/injection, once a day for 3 days) led to microglial atrophy (Supplemental Fig. 1). Importantly, DT administration reversed the reduction of the synaptic markers in the double transgenic mice (Fig. 3.4 D). These in vitro and in vivo data indicate that microglia play a crucial role in gp120-induced synapse loss.

3.2.3 The gp120-induced synapse loss is mediated by FKN/CX3CR1 signaling.

FKN/CX3CR1 signaling is critical for neuron-microglia interaction. CX3CR1 (receptor of FKN) is exclusively expressed on microglia in the CNS; whereas FKN is specifically in neurons (Harrison et al., 1998; Cardona et al., 2006; Ransohoff, 2009). To determine the effect of gp120 on fractalkine expression, we determined the FKN protein level in gp120-treated primary cortical cultures. Western blotting results revealed that FKN

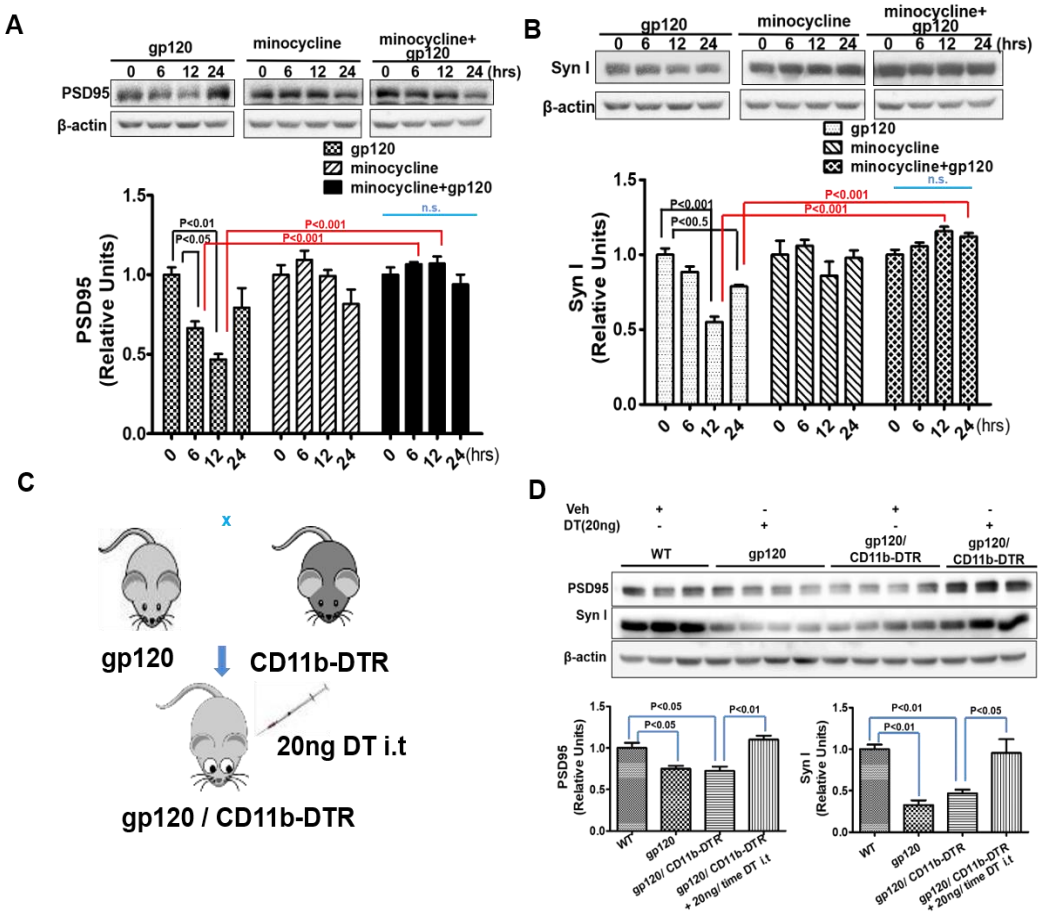

Fig 3. 4 Microglia are crucial for gp120-induced synapse loss. A-B. Pre-treatment of primary cortical cultures with minocycline prevented gp120-induced decreases in PSD95 (A) and Syn I (B). Cortical cultures (14 DIV) were pretreated with 30 µM minocycline, followed by co-incubation with 200 pM gp120, N=4 cultures per condition. C. Diagram showing the generation of gp120/CD11b-DTR mice for microglial ablation by DT. D. Effect of DT administration on PSD95 and Syn I level in the spinal cord of the gp120/CD11b-DTR mice. WT, gp120Tg, and gp120/CD11b-DTR mice were administrated (i.t.) 20 ng DT (in 5 µl PBS) or 5 µl PBS only once per day for 3 days. L4-L5 spinal cords were used for immunoblotting analysis of PSD95 and Syn I. N: WT/ PBS, 3; gp120Tg/DT, 4; gp120gp/CD11b-DTR/PBS, 4; gp120gp/CD11b-DTR/DT, 3. Quantitative graphs are shown as mean ± SEM.

was gradually up-regulated over time (Fig. 3.5 A). Time-dependent FKN up-regulation was also observed in the spinal cords following gp120 administration (i.t.) (Fig. 3.5 B). To determine the role of FKN signaling in gp120-induced synapse loss, we used a mouse strain in which the CX3CR1 gene was replaced by a green fluorescent protein (GFP) reporter gene (Jung et al., 2000a). Immunoblotting analysis showed that gp120 administration (i.t.)

for 7 days caused significant reduction of PSD95 and Syn I in the WT mice (Fig. 3.5 C). However, knocking out CX3CR1 blocked the effects of gp120 on PSD95 and Syn I (Fig. 3.5 C). Because synapse degeneration is associated with the development of HIV-related pain in patients (Yuan et al., 2014), we sought to test if the blockage of synapse degeneration by the CX3XR1 knockout is associated with an inhibition of the gp120-induced mechanical pain in animal models. Von Frey tests showed that gp120 (i.t.) increased the mechanical sensitivity in WT mice, as indicated by the decreased threshold

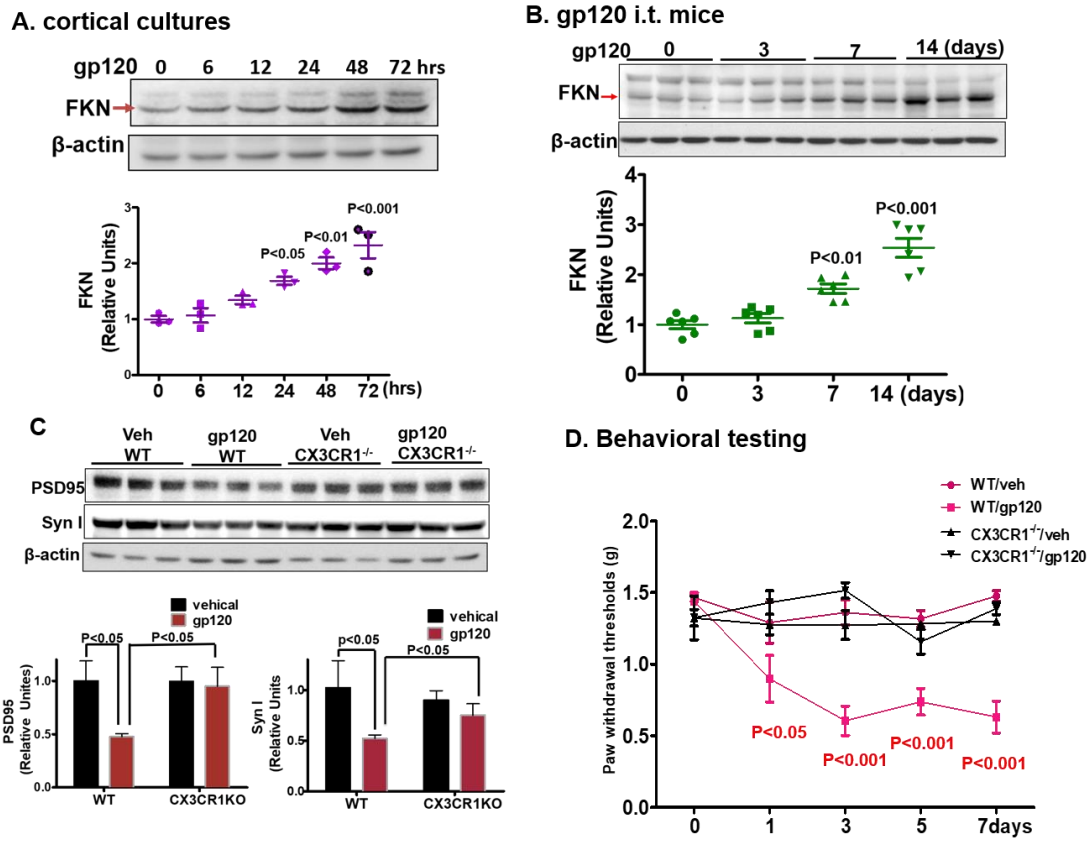

Fig 3. 5 FKN/CX3CR1 signaling is required for gp120-induced synaptic degeneration. A. gp120 stimulated FKN expression in cortical cultures (N=3 cultures per treatment). B. gp120 (i.t.) stimulated FKN expression in the mouse spinal cords (N=6 mice per time point). C. Protein levels of PSD 95 and Syn I in the spinal cord of CX3CR1$^{-/-}$ or WT mice at day 7 after Veh or gp120 injection (i.t.) (N=5 mice per). D. Behavioral tests of gp120-induced mechanical allodynia in WT and CX3CR1$^{-/-}$ mice. Threshold of mechanical sensitivity in the hind paw was measured by von Frey tests (N=6 mice per group; Error bars: mean ± SEM). The behavioral tests were performed by Dr. Xin Liu.

of responses to mechanical stimulation. However, it failed to cause a similar effect in the CX3CR1 knockout mice (Fig. 3.5 D). These results suggest that disruption of FKN/CX3CR1 signaling blocks gp120-induced synaptic degeneration and mechanical pain.

3.2.4 gp120 up-regulated FKN via the Wnt canonical pathway.

Wnt signaling regulates the FKN-CX3CR1 signal pathway in remifentanile-induced hyperalgesia (Gong et al., 2016). We sought to test the role of this pathway in gp120-induced FKN elevation. We observed that gp120 up-regulated the expression of the prototypic Wnt ligand for the canonical pathway, Wnt3a, in both cortical cultures (Fig. 3.6A) and spinal cords (Fig. 3.6 B). To determine the effects of disruption of the Wnt canonical pathway on gp120-induced FKN expression, we used the conditional knockout approach to delete β-catenin in neural cells by crossing the floxed β-catenin mouse with the nestin-Cre mouse line (Tronche et al., 1999). Only heterozygotes were obtained ($Cat^{+/-}$), indicating that the homozygotes died during the embryonic stages. The spinal β-catenin level in the heterozygotes was about 60% of that in the WT (Fig. 3.6 C). We found that, unlike the gp120-induced FKN up-regulation observed in the WT mice, gp120 (i.t.) failed to induce FKN elevation in the $Cat^{+/-}$ mice (Fig. 3.6D). This result suggests that gp120 up-regulates FKN expression via the Wnt/β-catenin pathway. Because FKN signaling is critical for gp120-induced synapse loss (Fig. 3.5), we hypothesized that the Wnt3a/β-catenin pathway might regulate gp120-induced synapse degeneration. To test this idea, we neutralized Wnt3a using a specific antibody and observed that the neutralization blocked the gp120-induced reduction of PSD95 and Syn I (Fig. 3.6 E). These results indicated that

the Wnt3a/β-catenin signaling pathway is crucial for gp120-induced FKN up-regulation and synaptic degeneration.

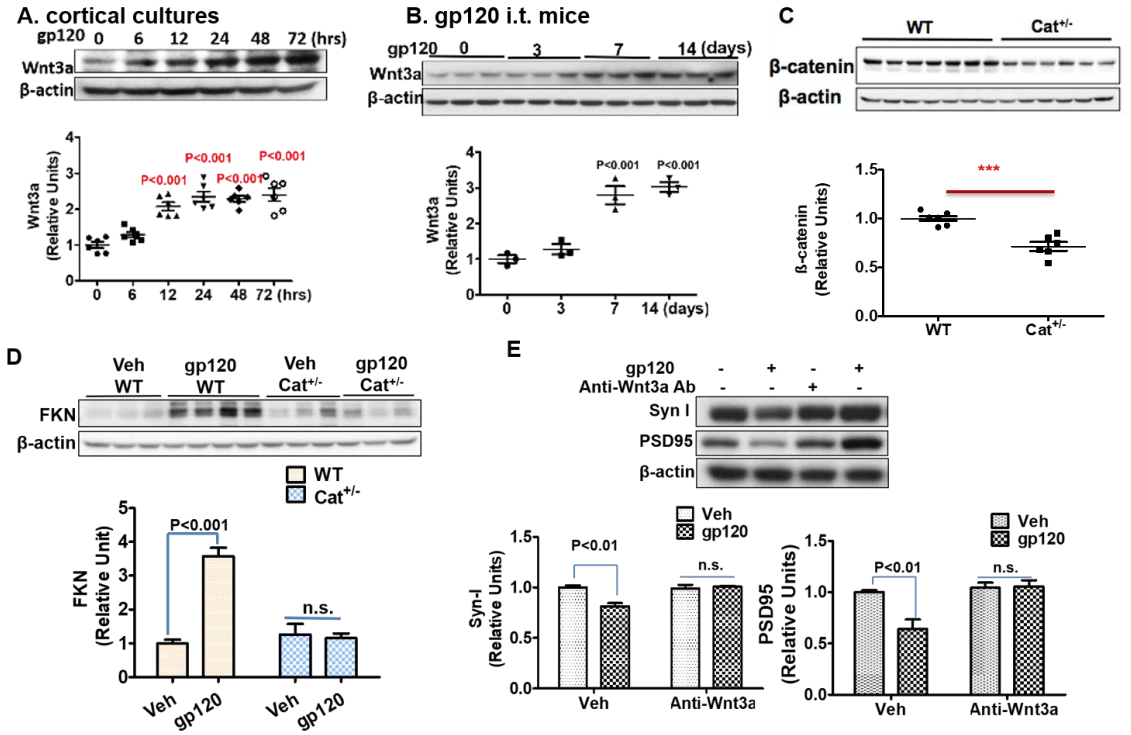

Fig 3. 6 Wnt3a/β-catenin pathway mediates gp120-induced FKN up-regulation and synaptic degeneration. A. Temporal profiles of Wnt3a expression in gp120-treated primary cortical cultures (N=6 cultures per group). B. Temporal profiles of Wnt3a expression in the spinal cords (L4-L5) from mice after gp120 injection (i.t.; N=3 mice per group). C. β-catenin protein levels in spinal cords (L4-L5) from WT and Cat$^{+/-}$ mice (N=6 mice for WT and N=7 mice for Cat$^{+/-}$). D. Comparison of the effect of gp120 on FKN expression in WT and Cat$^{+/-}$ mice. Mice was intrathecally treated with gp120 or vehicle every other day for 7 days. Spinal (L4-L5) FKN protein was analyzed by western blotting. N=3 mice per group for Veh/WT, Veh/Cat$^{+/-}$ and gp120/Cat$^{+/-}$, N=4 mice for gp120/WT. E. Effect of Wnt3a neutralizing antibody on gp120-induced synaptic degeneration in primary cortical cultures. Anti-Wnt3a antibody (2 μg/ml) was added to the cultures for 30 min, and then gp120 (200 pM) was added for an additional 12 hrs. N=3 independent cultures per group (mean ± SEM).

3.2.5 Gp120 induced FKN expression and synapse loss via NMDA receptor (NMDAR) activation.

Previous studies show that synaptic activity regulates Wnt3a/β-catenin signaling activation via NMDAR (Chen et al., 2006). It is known that gp120 can directly activate NMDARs by binding to their glycine binding sites (Fontana et al., 1997; Pattarini et al., 1998). Gp120 also can indirectly affect the activity of NMDARs after binding to its co-receptor, which triggers a series of signalling cascades as well as cytokine/chemokine release, thus facilitating NMDAR activation (Catani et al., 2000; Kaul et al., 2001; Nicolai et al., 2010; Marchionni et al., 2012; Maung et al., 2014; Ru and Tang, 2016). We observed that co-receptors CCR5 and CXCR4 were mainly located on the post-synapse, and blockage of CCR5 abolished gp120-induced synaptic degeneration (Supplemental Fig. 2). Then, we wanted to determine if gp120-induced Wnt3a and FKN up-regulation required NMDARs in the spinal cord. We found that injection (i.t.) of the NMDAR antagonist APV prevented gp120-induced increases of Wnt3a and FKN (Fig. 3.7 A, 3.7 B). These data suggest that gp120 induced both Wnt3a and FKN via NMDAR activation.

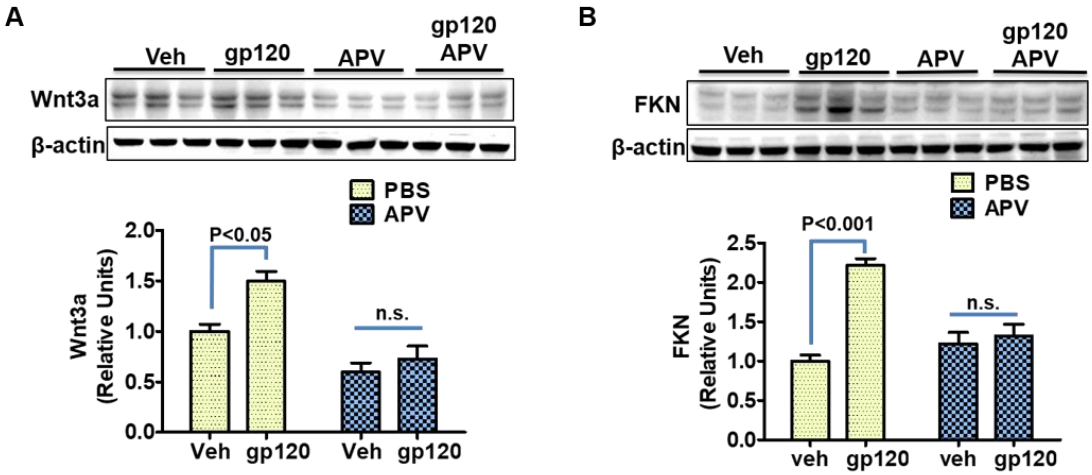

Fig 3. 7 NMDAR is crucial for gp120 to induce Wnt3a and FKN expression. Mice were injected (i.t.) with either APV (5 µg/injection in 5 µl PBS) or Veh (5 µl PBS/ injection) 30 min before gp120 injection (500 ng; i.t.; once every other day for 7 days). Spinal cords (L4-L5) were collected at day 7 for immunoblotting analysis of Wnt3a (A) and FKN (B). N=6 mice for the groups of Veh and APV, N=7 for the groups of gp120 and gp120+APV.

We next determined the potential role of NMDARs in gp120-induced synapse degeneration both in primary cortical cultures and in the spinal cords. We found that APV application to the cultures completely blocked the gp120-induced decreases of PSD95 (Fig. 3.8 A) and Syn I (Fig. 3.8 B). In addition, injection of APV (i.t.) also blocked the effect of gp120 on Syn I (Fig. 3.8 C) and PSD95 (Fig. 3.8 D). Thus, NMDAR activity is critical for gp120-induced synaptic degeneration both in vitro and in vivo.

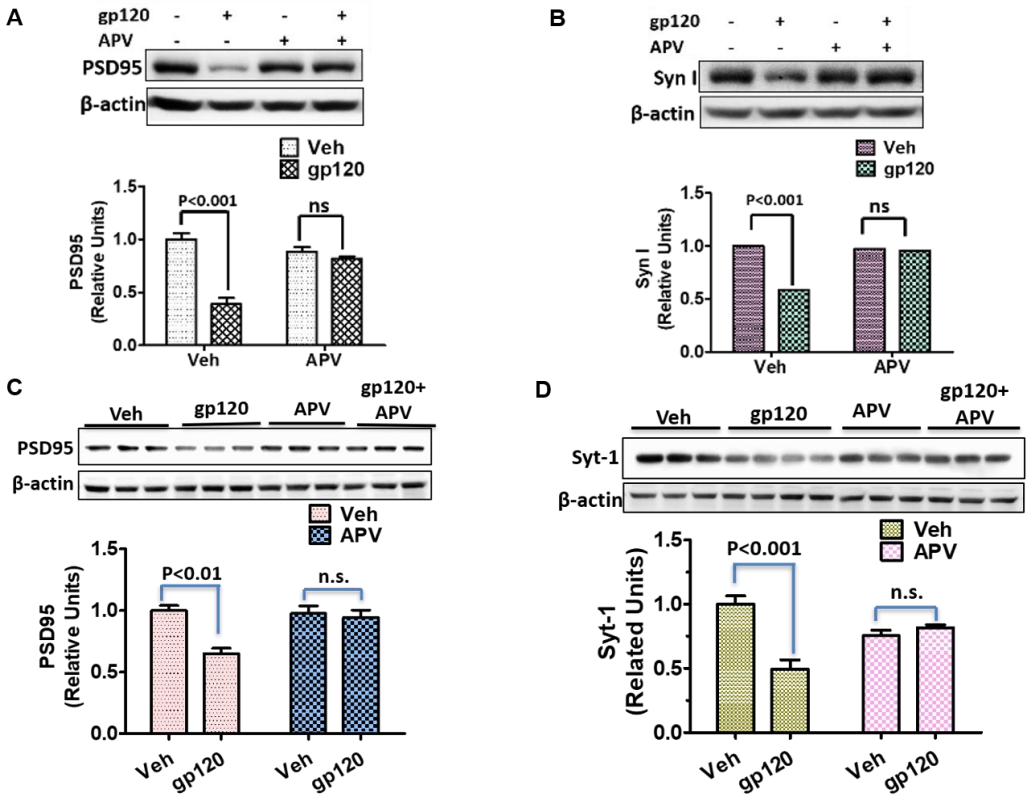

Fig 3. 8 Gp120-induced synapse loss depends on NMDAR activation. A, B. Effects of APV on gp120-induced decreases of PSD95 (A) and Syn I (B) in primary cortical cultures. APV (100 nM) was added to the cultures (14 DIV) 30 min before gp120 (200 pM) application. The cultures were exposed to gp120 for 12 h before harvesting for immunoblotting (N=4 independent cultures per group). C, D. Effects of APV on gp120-induced decreases of PSD95 (C) and Syn I (D) in the spinal cords (L4-L5). Mice were injected with APV (i.t.; 5 ug/injection in 5 µl PBS) or Veh (5 µl PBS/ injection) 30 min prior to gp120 injection (500 ng; i.t.; once every other day). L4-L5 spinal cords were collected for immunoblotting analysis of PSD95 (C) and Syt-1 (D). N=3 mice per group (mean ± SEM).

3.3 DISCUSSION

In this study, we have uncovered a critical role of microglia in HIV-1 gp120-induced synaptic degeneration, especially in the spinal pain neural circuits. We also elucidated an important mechanism that regulates the microglia-mediated synaptic degeneration. Specifically, our results indicate that gp120 stimulates the NMDAR-dependent Wnt3a/β-catenin pathway to up-regulate the FKN/CX3CR1 neuron-to-microglia signaling to activate microglia-mediated elimination of synapses (Fig. 3.9).

The synaptic alteration in the spinal cord contributes to central sensitization and pain hypersensitivity (Latremoliere and Woolf, 2009). Recent in vivo two-photon imaging revealed synaptic structural changes in cortical pain circuits following peripheral nerve injury, implicating structural change of cortical synapses in the development of neuropathic pain (Kim et al., 2012). At the spinal pain circuits, we observed significant reduction of synaptic markers in the SDH in HIV patients with chronic pain but not in HIV patients without pain (Yuan et al., 2014). This synaptic degeneration also developed in the mouse HIV-1 gp120 pain model (Yuan et al., 2014). The findings from this study identify the first potential molecular and cellular mechanisms that underlie synaptic degeneration during the pathogenesis of HIV-associated pain.

Our results show that microglial blockage by two different approaches protected synapses from gp120 toxicity (Fig. 3.4). These data suggest that microglia play an important role in gp120-induced synaptic degeneration. Prior studies revealed a contribution of neurotoxic immunomodulatory factors from reactive and/or infected microglia (Garden, 2002). More recent work identified a key role of microglial phagocytosis in synaptic remodeling and maturation (Paolicelli et al., 2011; Schafer et al.,

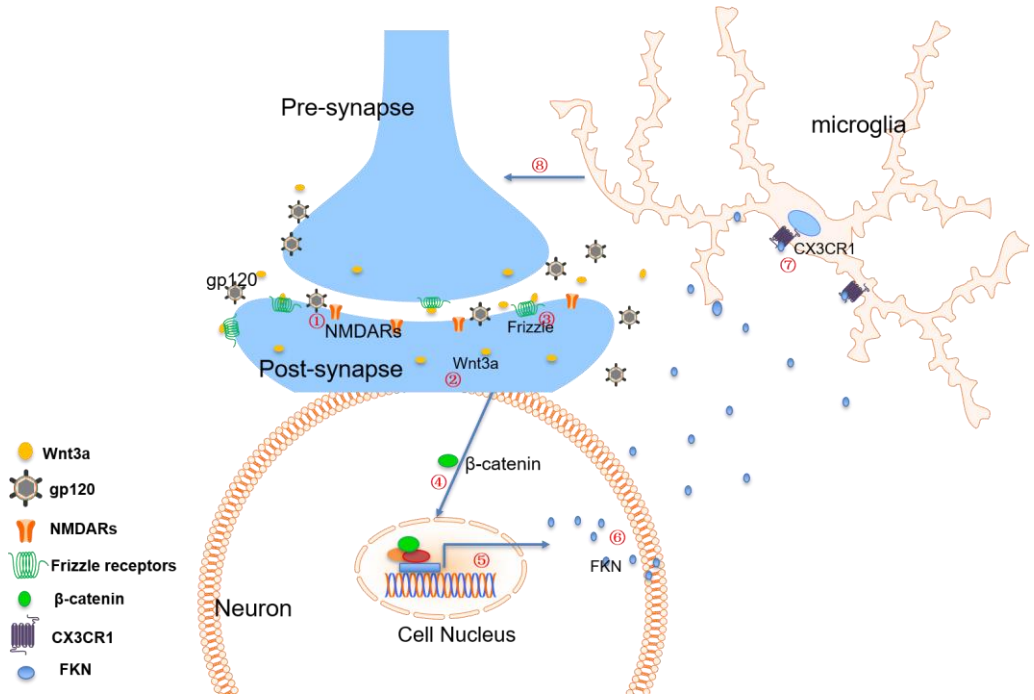

Fig 3. 9 Microglia-mediated synaptic degeneration in spinal pain neural circuits after gp120 exposure. ① Spinal synapses are exposed to gp120, which can directly or indirectly affect the activity of NMDRs and cause synaptic activation. ② Synaptic activation elicits Wnt3a release from synapses. This synaptic activity-induced rapid Wnt3a synthesis and secretion are dependent on NMDARs. ③ Wnt3a binds to Frizzle receptors and its co-receptor, low-density lipoprotein receptor related protein (LRP6/LRP5), on both the pre- and post-synaptic membrane. ④ Activation of the Wnt3a receptor complex causes inhibition of β-catenin phosphorylation and results in β-catenin stabilization and accumulation. Accumulated β-catenin is translocated to the nucleus. ⑤ In the nucleus, β-catenin binds to LEF/TCF transcription factors with additional co-activators to regulate specific targets expression. FKN is likely a target gene of Wnt3a/β-catenin. ⑥ FKN is expressed and released from neurons upon Wnt3a/β-catenin pathway activation. ⑦ FKN binds to CX3CR1 on microglia and regulates microglial activation and migration. Microglia also can be directly activated by gp120. ⑧ Activated microglia then remove the damaged synapses.

2012; Kettenmann et al., 2013; Hong et al., 2016a). The findings from this work significantly expand the understanding of the role of microglia by identifying their involvement in synapse remodeling in a specific disease condition caused by the HIV-1 coat toxic protein. These results also potentially connect the microglia-mediated synapse degeneration with the development of HIV-associated pathological pain.

We observed that FKN was significantly up-regulated by gp120 both in vitro and in vivo (Fig. 3.5), and deletion of the FKN receptor CX3CR1 blocked the synapse loss induced by gp120 (Fig. 3.5). The data suggest that FKN/CX3CR1 signaling is essential for gp120-induced synapse degeneration. FKN acts as both a membrane-tethered and a secreted chemokine that binds to its receptor, CX3CR1, to regulate microglial phagocytosis. Previous studies indicate that the FKN/CX3CR1 signaling modulates synapse pruning during development (Paolicelli et al., 2011; Hoshiko et al., 2012). It is thus possible that the FKN/CX3CR1 signaling stimulates microglial phagocytosis of damaged synapses caused by gp120 exposure, although the direct evidence for this is still lacking. Besides its regulatory role in microglial phagocytosis of synapses, FKN/CX3XR1 signaling may also regulate the microglial clearance of pathogens and extracellular protein aggregates (Lee et al., 2010; Liu et al., 2010). Therefore, another possibility is that FKN/CX3CR1 suppresses neurotoxin clearance and then promotes gp120-induced synaptic degeneration. FKN/CX3XR1 signaling also regulates microgliosis and the local neuroinflammatory milieu around the pathogenic insults (Lee et al., 2010; Tang et al., 2014) . Thus, a third possibility is that FKN/CX3CR1 signaling may facilitate gp120-induced synapse degeneration by enhancing neuroinflammation that is induced by gp120.

We further identified the Wnt/β-catenin signaling as a critical up-stream regulator of FKN expression induced by gp120. Our data show that β-catenin is required for gp120 to up-regulate FKN (Fig 3.6). Consistent with our findings, recent studies indicate that the spinal Wnt3a/β-catenin pathway modulates FKN/CX3CR1 signaling in opioid-induced hyperalgesia (Gong et al., 2016). In addition, we also showed that gp120-induced Wnt3a and FKN expression depends on NMDAR activation (Fig. 3.7). Because previous studies

have established that NMDAR-dependent synaptic activity activates Wnt/β-catenin signaling (Chen et al., 2006; Tang, 2014), we propose that gp120 induces the synaptic activity-regulated Wnt3a/β-catenin signaling that activates FKN expression.

3.4 SUPPLEMENTAL DATA.

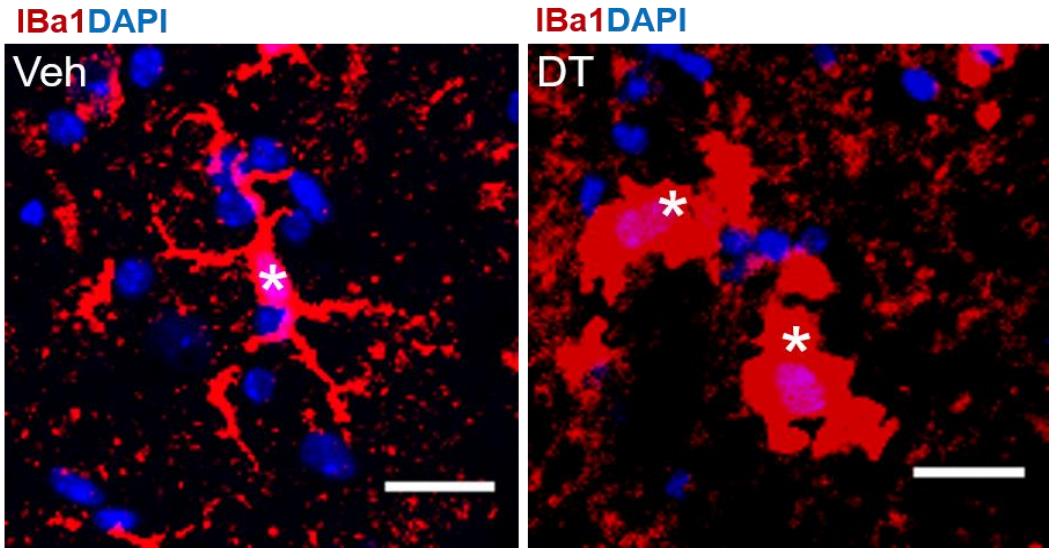

Supplemental Fig. 1 DT treatment caused microglial atrophy. 20 ng DT (in 5 µl PBS) or Veh (5 µl PBS) was i.t. injected into CD11b-DTR mice, once a day for 3 days. Twenty-four hours after the last treatment, spinal cords were harvested for immunofluorescent staining with IBa1. DT treatment showed significant loss of microglial processes and shrunken cell body (* indicates microglia). Scale bar: 20 µm.

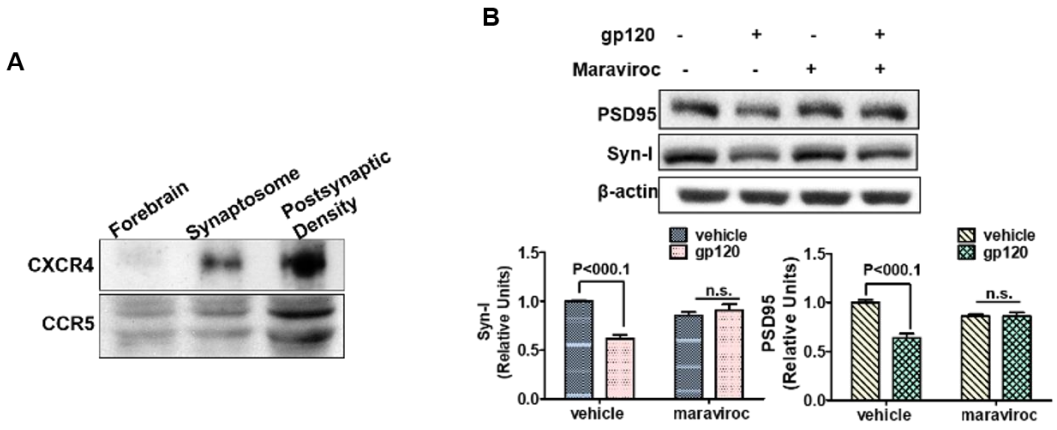

Supplemental Fig. 2 Gp120 induced synapse loss via its co-receptors. A. Immunoblots showed the expression level of CXCR4 and CCR5 in forebrain, synaptosome and postsynaptic density homogenate. B. Effects of maraviroc pre-treatment on gp120-induced decrease of PSD95 and Syn I. Cortical cultures were pre-treated with the maraviroc (50 µM) for 30 min and then co-treated with gp120 (200 pM) for another 12 hours. Cell lysates were analyzed by immunoblotting. N=3 cultures per condition. B. Data are expressed as mean ± SEM.

Chapter 4 The role of microglial phagocytosis in gp120-induced synapse elimination

4.1 INTRODUCTION

My previous study demonstrated that gp120 caused significant spinal synaptic degeneration, which likely contributes to HIV-associated pain. In this specific Aim, I shall focus on the brain to determine if gp120 leads to similar synaptic changes in the cortex and to further understand the underlying mechanism of gp120-induced synapse loss. A critical role of FKN/ CX3CR1-mediated microglia' activity in gp120-induced spinal synapse loss was identified in my studies described in Chapter 3. However, it is still unknown if microglia mediate synapse elimination via physical contacts, such as phagocytosis. Emerging evidence suggests a crucial role of microglia in synaptic pruning during development and under certain disease conditions (Harrison et al., 1998; Stevens et al., 2007b; Paolicelli et al., 2011; Schafer et al., 2012; Zhan et al., 2014; Hong et al., 2016b; Vasek et al., 2016a). The "un-wanted" synapses are usually labeled by phagocytic (so-called "eat-me") signals, which are recognized by the receptors on microglia to initiate synapses engulfment and phagocytosis. Based on such evidence I hypothesize that microglia mediate gp120-induced synaptic degeneration by phagocytosis.

Recently, several neuron-glia signaling pathways have been were identified to mediate synapse pruning (Harrison et al., 1998; Stevens et al., 2007b; Paolicelli et al., 2011; Schafer et al., 2012; Chung et al., 2013; Zhan et al., 2014; Chung et al., 2015b). Microglia, as professional phagocytes in the brain, are closely in contact with synapses and can

remove dead/dying neurons, neuronal debris as well as synapses or axons of alive neurons (Neumann et al., 2009; Fricker et al., 2012; Neniskyte and Brown, 2013; Sierra et al., 2013; Brown and Neher, 2014). Microglia promote synapse pruning in a manner dependent on CX3CR1 or complement receptor 3 (CR3) receptors. Complement component C1q is produced by neurons and localized at synapses (Stevens et al., 2007b). It initiates synapse pruning by promoting the deposition of C3 on synapses (Schafer et al., 2012), and triggering C3 receptor (CR3) binding and consequently synapse elimination by microglia (Stevens et al., 2007b; Schafer et al., 2012). The complement-initiated and microglia-mediated synapse elimination is also critical for synapse striping in various diseases models, including Alzheimer diseases (Hong et al., 2016b) and West Nile virus infection (Vasek et al., 2016a). FKN is the CX3CR1 ligand, and primarily expressed by neurons. In response to neuronal activity, FKN is rapidly released from neuron (Chapman et al., 2000). FKN-CX3CR1 interaction regulates microglial activation and phagocytosis of synapses (Harrison et al., 1998; Paolicelli et al., 2011; Zhan et al., 2014).

In addition to those CR3 and CX3CR1, microglia also express phagocytotic receptor MerTK (Grommes et al., 2008; Chung et al., 2013). MerTK was reported to regulate macrophage's activity in the clearance of apoptotic cells (Scott et al., 2001), microglial phagocytosis of stressed neurons (Neher et al., 2013; Nomura et al., 2017), and astrocytic elimination of excessive synapse during development (Chung et al., 2013). However, it is still unknown if MerTK mediates microglial phagocytosis of synapses.

I am therefore interested in further exploring the contribution of microglia to gp120-induced synapse loss and obtaining mechanistic insights into the molecular

pathways at both the microglial and neuronal levels that modulate synaptic degeneration. In particular, I want to address two key questions: 1) Is microglial phagocytosis responsible for the gp120-induced synapse loss? 2) How does gp120 induce microglial phagocytosis of synapse? I therefore compared the levels and distribution of synaptic proteins in frontal cortices of WT and gp120 Tg mice. Significant decrease of Syn-1, Syt-1, vGluT1 and PSD95 were observed in gp120 Tg mice. Consistent with these results, dramatic reduction of intact synapses was shown in gp120 Tg mice. To determine the role of microglial phagocytosis in the synapse loss, we measured the physical contacts between synapse and microglia, and found gp120 induced more neuron-microglia contacts. Interestingly, gp120 induced microglia to selectively engulf pre-synaptic elements (compared with post-synaptic elements). Importantly, ablation of microglia protected pre-synaptic component from gp120-induced elimination. I further determined the role of the FKN/CX3CR1 signaling and MerTK signaling in gp120 induced-microglial activation and synapses phagocytosis. The results revealed that MerTk played an important role in gp120- induced microglial phagocytosis of pre-synaptic elements. However, CX3CR1 deletion potentiate microglial activation and gp120-induced synaptic degeneration.

4.2 RESULTS:

4.2.1 Gp120 induced synapse loss in the frontal cortex.

To test gp120's activity in inducing synapse degeneration, the cortices from 6-month-old gp120 Tg and wildtype (WT) littermates were analyzed, by western blotting. we observed significant reduction of pre-synaptic markers synapsin I (Syn I), synaptogami-1 (Syt-1) and vesicular glutamate transporter 1 (vGluT1) in gp120Tg cortices (Fig. 4.1 A). Post-synaptic protein PSD95 decreased significantly, but to a less degree of magnitude

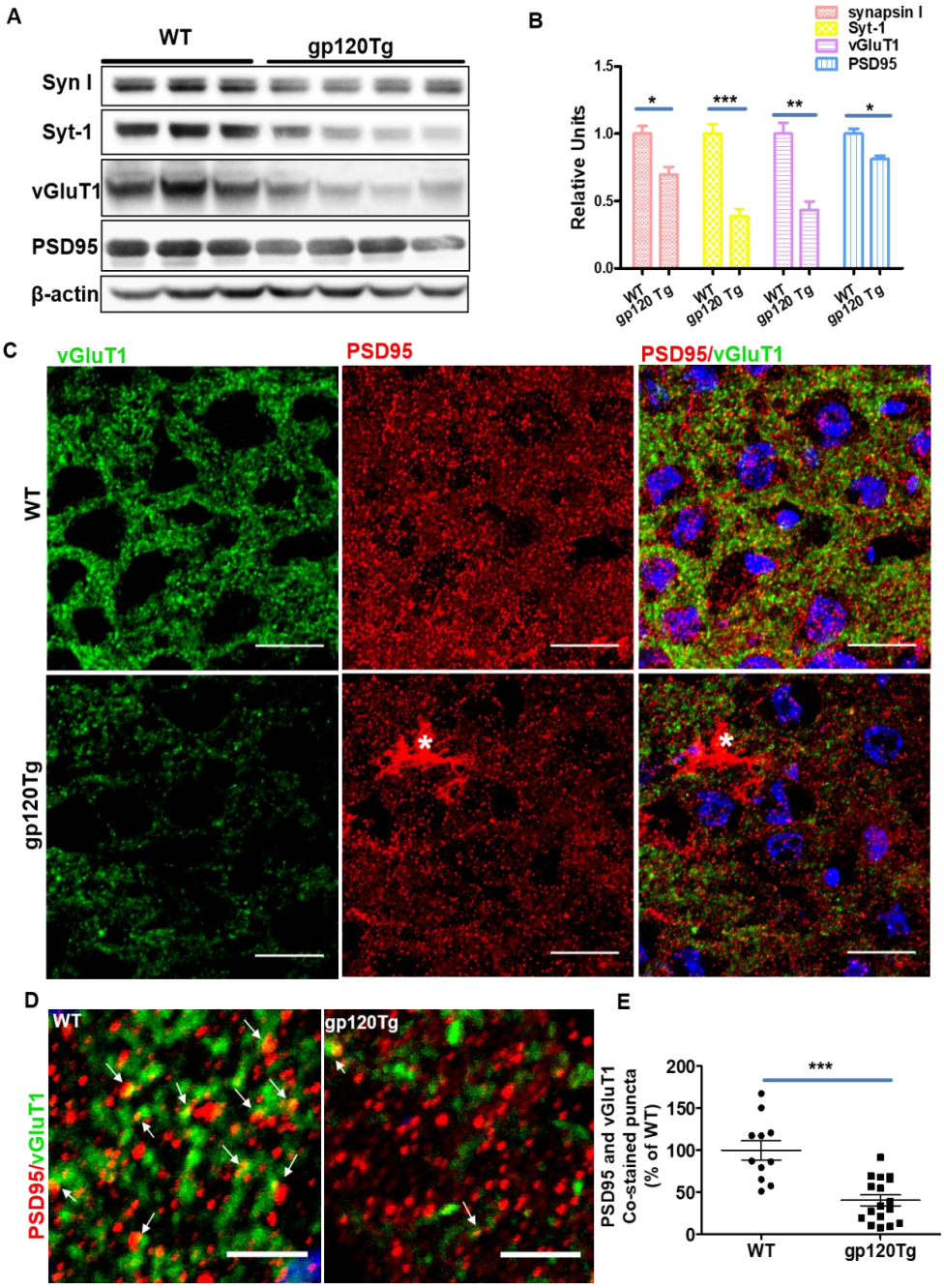

Fig 4. 1 gp120 causes synaptic degeneration in the frontal cortex. A. Protein levels of Syn I, Syt-1 vGluT1 and PSD95 in the frontal cortex of the WT and gp120 Tg mice at the age 6-months-old. B. Quantitative summary of A. C. Confocal micrographs of vGlutT1 (green) and PSD95 (red) immunostaining, stars show the $PSD95^{+}$ clumps (scale bar: 20 μm). D. Overlaps of vGluT1 and PSD95 signals (yellow) suggest intact synapses (indicated by arrows), which decreases in gp120 Tg mice. Immunostaining performed within the frontal cortex, confocal images captured the distribution of synapse in the layer I-II of cortex. E. Quantification of the overlapped vGluT1 and PSD95 signals. (All panels, data are expressed as mean ± SEM. *, $p<0.05$; **, $p<0.01$ ***, $p<0.001$; n =3 for WT, 4 mice for gp120 Tg).

(Fig. 4.1 A and 4.1 B). To visualize synapse loss in gp120 Tg mice cortices, we performed confocal imaging of synapses in cortical sections after double-staining of vGluT1 and PSD95. We observed dramatic decreases of synaptic puncta (Fig. 4.1 C). The vGluT1 and PD95 co-stained puncta were viewed as intact synapses (arrows in Fig. 4.1 D). The quantification of the vGluT1 and PSD95 co-stained puncta showed that gp120 exposure caused a significant loss of intact synapses (~41% of WT) (Fig 4.1 E). Interesting, we observed many $PSD95^+$ aggregates in gp120 Tg cortices (stars in Fig. 4.1 C). These data suggest that gp120 exposure lead to synaptic degeneration in the brain cortex.

4.2.2 Gp120 led to microglial activation.

To assess the potential involvement of microglia in HIV-1-gp120 induced synaptic degeneration, we performed immunostaining of IBa1 (Ito et al., 1998) in gp120Tg and WT mice cortical sections. Confocal imaging showed that the $IBa1^+$ cells significantly increased in gp120 Tg mice (Fig. 4.2 A, B). In addition, gp120 caused microglial morphological changes, with enlarged soma and thicker processes (Right panels of Fig. 4.2 A). As IBa1 is also expressed in macrophages, to rule out the possibility that the increased $IBa1^+$ cells was due to the peripheral macrophage infiltration after gp120 stimulation, we performed immunostaining of the transmembrane protein 119 (TMEM119), which is specifically expressed by microglial and was used to distinguish microglia from macrophages after CNS inflammation and injury (Bennett et al., 2016). $IBa1^+TMEM119^+$ cells were microglia, $IBa1^+TMEM119^-$ cells were macrophages (Fig. 4.2 C). We found that majority of cortical $IBa1^+$ cells were microglia in both WT and gp120 Tg mice (96.96 % in WT vs 89.30% in gp120 Tg mice) (Fig 4.2 D). Gp120 caused the number of both microglia and macrophages increase, with microglia increase at a much bigger magnitude

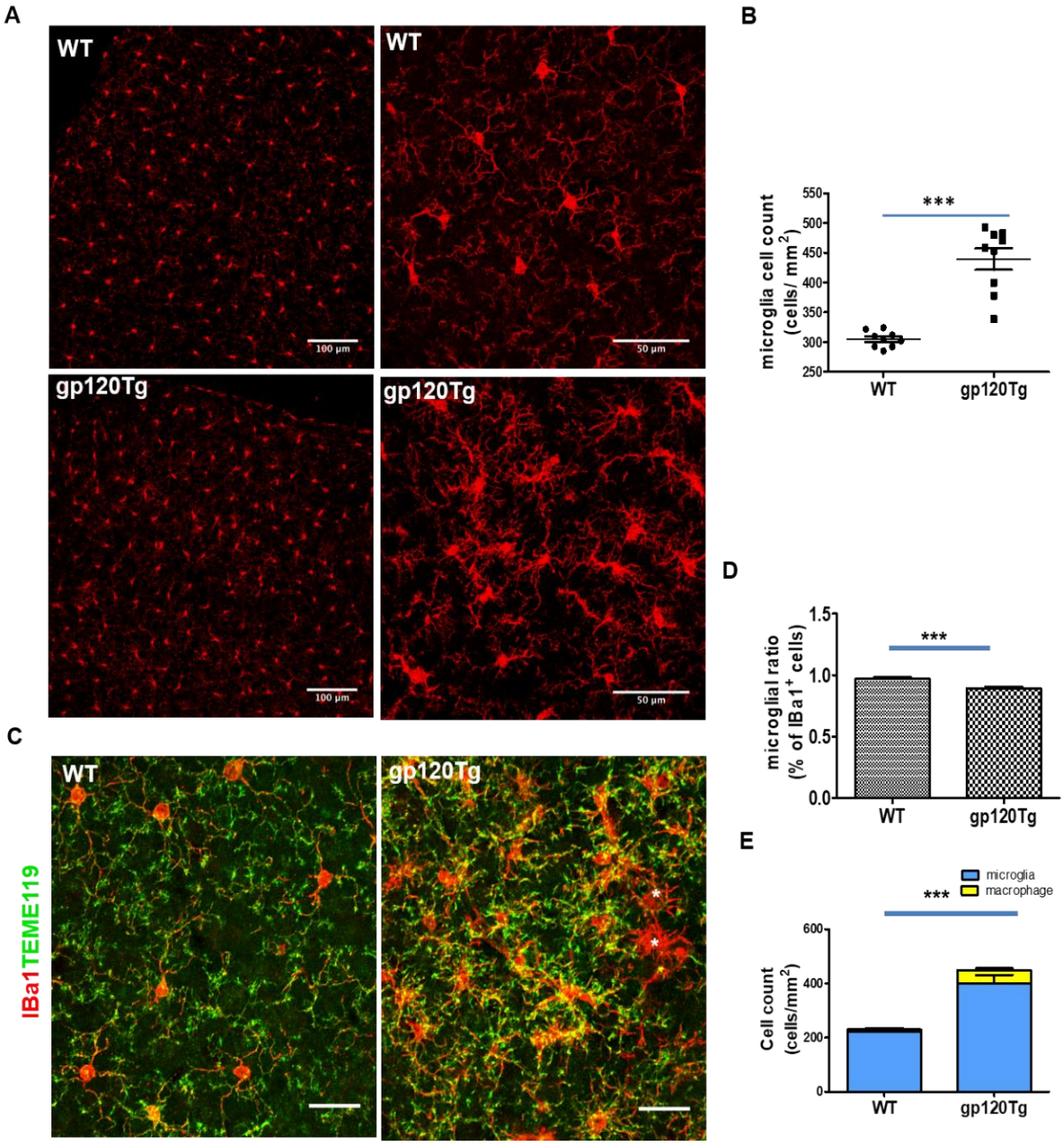

Fig 4. 2 Microglial activation in the cortex of gp120 transgenic mice. A. confocal images of IBa1$^+$ microglia in WT and gp120Tg mice at age of 6 months old. (n = 3 or 4 mice for WT or gp120Tg, respectively). Scale bar, 100 µm for left panels; 50 µm for right panels. B. Quantitative graph showing increased IBa1$^+$ cells in gp120 Tg mice. C. Immunostaining images showing the co-expression of IBa1 and TEME119 in microglia and only IBa1 expression in macrophages (indicated by *), scale bars, 25µm, n=4 mice per group. D. Quantification of the portion of microglial cells in IBa1$^+$ cells. E. Density of microglia and macrophages in WT and gp120Tg mice. Error bars, s.e.m; ***, p<0.001. Immunostaining and quantification performed within the frontal cortex.

(Fig. 4.2 E). These results suggested microglia were activated in gp120 Tg cortices. In the following experiments, we will use IBa1 to label microglia because IBa1 staining better demarcates microglial morphology.

4.2.3 Gp120-induced microglia-neuron contacts and microglial phagocytosis.

To gain insights about the potential physical interaction between neurons and microglia induced by gp120, we performed immunostaining of IBa1 in Thy1-YFP/gp120 double transgenic mice, in which cortical neurons are labeled by YFP. We observed that microglia in Thy1-YFP only mice had no obvious association with neuronal soma (Fig. 4.3 A). In Thy1-YFP/gp120Tg mice, however, we observed that some microglia closely appose to neuron (Fig 4.3 A). There were 12% cortical neurons in gp120 Tg mice in contact with microglia compared to 2% of neuron in WT associate with microglia (Fig. 4.3 B). These data indicated that gp120 induced microglia-neuron physical interaction. To assess if gp120 induces microglial phagocytosis, we performed immunostaining of galectin-3, a phagocytic biomarker (Sano et al., 2003; Morizawa et al., 2017). We observed that, while galectin-3^+ cells were rare in the cortices of WT mice, about 10% microglia expressed galectin-3 (Fig. 4.3 C, D). The increase of microglia-neuron contacts and galectin-3^+ microglia in gp120Tg mice indicated that gp120 may cause microglia to phagocytose damaged synapses.

4.2.4 Microglia predominantly phagocytosed presynaptic structures in the gp120 transgenic mice.

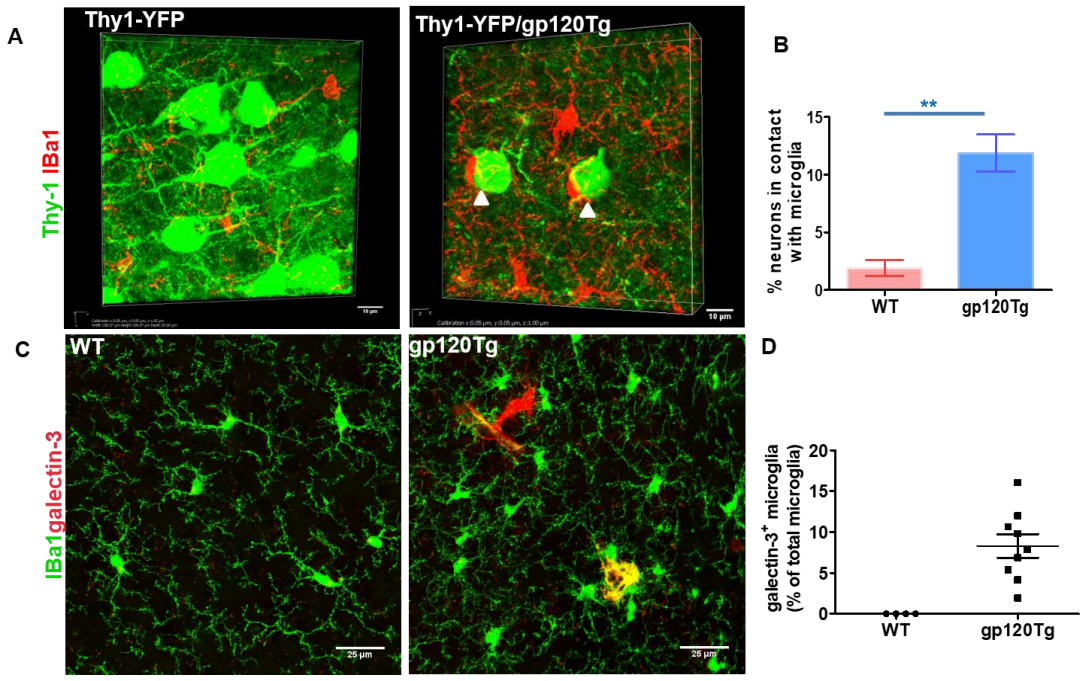

Fig 4. 3 Activated microglia target cortical neurons and show phagocytotic features in the gp120 Tg mouse. A. Representative 3D images show morphological changes of microglia (microglia) in the gp120 Tg mice. Triangle indicate the association of microglia with neuronal cell bodies (Green). N=4 mice per group, scale bars: 10 µm. B Quantitative graph shows the percentage of neuron in contact with microglia. C. Representative image of IBa1^{+}, galectin-3^{+} microglia in the WT and gp120 Tg mice. N=3 per group, scale bars: 25 µm. D. Quantification of C, IBa1^{+}Galectin-3^{+} cells are counted phagocytotic microglia, IBa1+cells are counted as microglia. Error bars, s.e.m.

To determine if gp120 induces microglial phagocytosis of synapses, we performed double-immunostaining of IBa1 and vGluT1 in cortical sections. Three-dimensional (3D) images were constructed to show the vGluT1^{+} IBa1^{+} colocalized puncta (arrows) (Fig. 4.4 A), which indicate the engulfed pre-synaptic elements by microglia. We observed the number of vGluT1^{+} IBa1^{+} colocalized puncta was increased in the transgenic mice compared to WT control (Fig. 4.4 B), suggesting gp120 stimulation activated microglia to engulf pre-synaptic components. To clearly show the microglial engulfment of pre-synaptic structure, we used Imaris software to reconstruct 3-D images to subtract only vGluT1 and only IBa1 expressed signals. Therefore, all the signals showing in Fig. 4.4 E

are vGluT1 and IBa1 colocalized signals. We observed that gp120 stimulation greatly increased the vGluT1 and IBa1 colocalized signals, indicating more presynaptic puncta internalized by microglia in gp120Tg mice (Fig. 4.4 E). The quantified results confirmed that gp120 enhanced microglial engulfment of presynaptic puncta (Fig. 4.4, F). Interestingly, 3-D images reconstructed from IBa1 and PSD95 double-immunostaining cortical sections showed PSD95 signals formed many clumps, but microglia clearly did not phagocytose them (Fig. 4.4 C, D). These striking findings suggest microglia selectively engulf and eliminate presynaptic structure but not postsynaptic part in the gp120 Tg mice. To rule out the other possible interpretation that vGluT1 was more stable in microglia and accumulated there, we performed immunostaining of additional presynaptic markers, including Syn I and Bassom. The results showed that gp120 induced similar increases of these markers inside the microglia (data not shown). Thus, the observation of selective accumulation of multiple presynaptic markers supports the idea of gp120-induced microglia predominantly phagocytosing presynaptic structures.

To rule out the possibility of imaging bias of a small number of cells, we performed flow cytometry analysis to quantify the microglial populations containing Syt-1 (a presynaptic marker) or PSD95 (a postsynaptic marker) staining signal. Single cell suspensions from WT and gp120 Tg mice's cortices were stained with anti-CD11b and anti-GFAP antibodies to label the microglia and astrocytes respectively, the group of $CD11b^+$ cell was counted as microglia (showing in the first quadrant in Fig. 4.5 A). The quantified result showed that microglia was significantly increased in gp120 Tg mice. (16% of total cortical cells were $CD11b^+$ cells in WT v.s 24% in gp 120Tg mice) (Fig 4.5 C). We then assessed the Syt-1 and PSD95 signals in the $CD11b^+$ cells (Fig 4.5 B). The right-

shift of the population curve in Fig 4.5 B indicated increased microglial population contained Syt-1 signal in transgenic mice. Compared to microglia in WT mice, there were 1.8 times of microglia in gp120 Tg mice containing Syt-1 signal (Fig 4.5 D). However, the

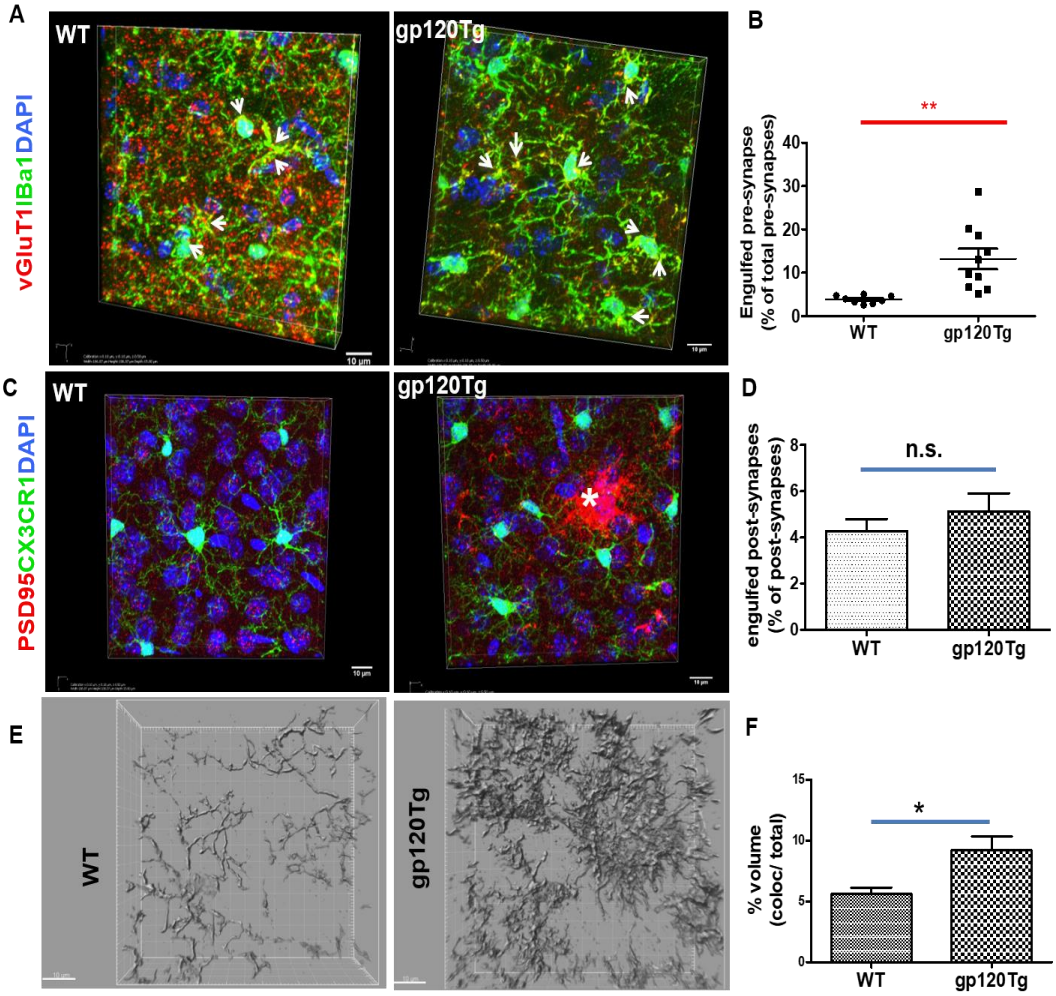

Fig 4. 4 Microglia in the gp120Tg mice predominantly phagocytose pre-synaptic elements. A. Evident vGluT1 staining in the IBa1-labeled microglia cell bodies (arrows). B. Quantification of the percentage of vGluT1 puncta in microglia. N=3 mice per group C. Microglia (labeled with CX3CR1) do not phagocytose PSD95 clumps (indicated by *). D. Quantification of the percentage of $PSD95^{+}$ post-synaptic component within microglia. N=5 mice per group. E. 3-D reconstruction images shown vGluT1 and IBa1 colocalized signal after subtracting only vGluT1 and only IBa1 expressed singals by using Imaris. F. Quantitative summary of E, N=5 mice per group Confocal z-stack images were taken at 60 × magnification using Nikon A1 inverted confocal microscopy, 30-50 consecutive optical sections with 0.5 µm interval thickness were obtained and e transformed into 3D reconstruction. For each mouse, at least 3 z-stack images were counted, which were derived from 3 fixed-frozen cortical sections. Scale bars: 10 µm. The analysis for E, F were performed by Lorenzo Ochoa.

microglial population curve showed the similar pattern in WT and gp120 Tg mice when we analyze the PSD95 signal distribution (Fig. 4.5 B, D), suggesting that gp120 does not affect the microglia to interact with PSD95^{+} post-synaptic component. These findings confirm that microglia selectively phagocytose presynaptic compartments.

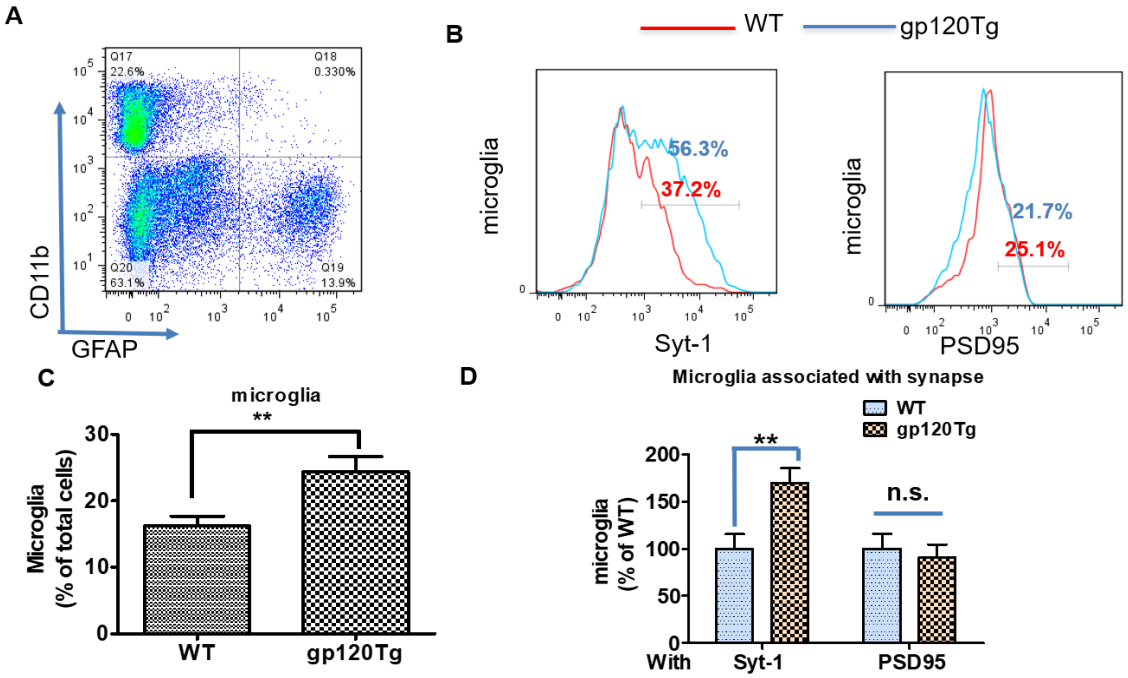

Fig 4. 5 Microglial population with Syt-1 staining markedly increases in the gp120 transgenic mice. A, B. Flow cytometry analysis of microglia associated with Syt-1 or PSD95. Microglia distribution is gated by CD11b and GFAP, CD11b^{+}GFAP^{-} cells (in the first quadrant) are counted as microglia (A). In microglial population, the signal intensity of Syt-1 and PSD95 are showed in B. The percentages showed in the graph represent the portion of microglia associate with Syt-1 signal or PSD95 signal (B). C and D. Quantitative summaries of the percentage of IBa1^{+} microglia (C) and the number of microglia associated with Syt-1 or PSD95 (D) in WT and gp120 Tg. N: 6 mice for WT, 8 mice for gp120 Tg.

4.2.5 Microglia is required for gp120-induced pre-synaptic elements elimination.

Adult mice administered with PLX5622, a specific colony-stimulating factor 1 receptor (CSF1R) inhibitor, show near-complete microglial elimination from the CNS (Dagher et al., 2015; Acharya et al., 2016; Hilla et al., 2017; Janova et al., 2017; Reshef et

al., 2017). To conclusively determine the role of microglia, six-month-old gp120 Tg and WT mice were treated with PLX5622 (formulated at 1200 mg/kg of chow) or control chow for 3 weeks. Cortical sections then were immunostained against microglial markers: IBa1 and TMEM119 (Fig 4.6 A). We observed the number of $IBa1^{+}TMEM119^{+}$ microglia were dramatically decreased in the gp120 Tg mice with PLX5622 chow administration (compared with mice receiving control chow) (Fig. 4.6 A and B), which demonstrated microglial depletion in the brain cortex of gp120 Tg mouse with PLX5622 administration. Next, we performed the double immunostaining of IBa1 and vGluT1 in cortical sections (Fig. 4.6 C), we found $vGluT1^{+}$ puncta were decreased in gp120 Tg mice receiving control chow compared to WT mice with control show administration, however, gp120 Tg mice administrated with PLX5622 to deplete microglia showed similar vGluT1 signal density (Fig. 4.6. D) as WT mice treated with control chow. These findings indicate that microglia depletion attenuated $vGluT^{+}$ presynaptic puncta loss in gp120Tg mice and further demonstrate a crucial role of microglia in gp120-induced synaptic degeneration, especially presynaptic degeneration.

4.2.6 FKN/CX3CR1 signaling regulates pre-synapse loss in gp120 Tg mice.

Next, we wanted to understand the mechanism that regulates microglial activity in synaptic phagocytosis. FKN/CX3CR1 signaling pathway mediates neuron- microglia interaction and the dysregulation of FKN/CX3CR1 contributes to neurodegeneration (Meucci et al., 2000; Dénes et al., 2008; Tang et al., 2014; Febinger et al., 2015). In

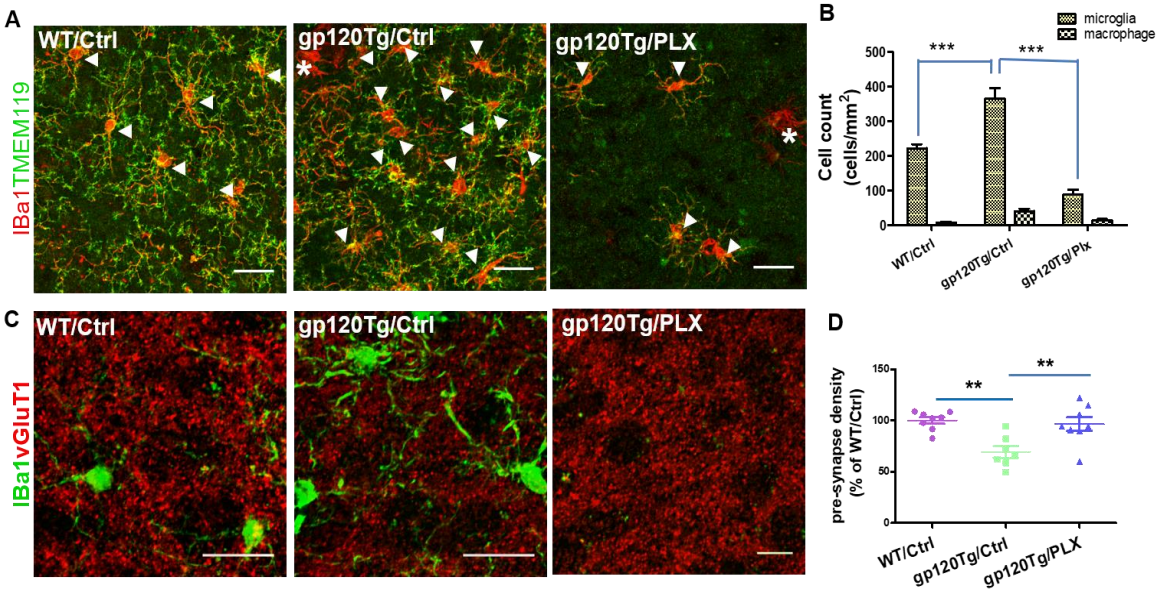

Fig 4. 6 CSF1R inhibitor PLX5622 depleted microglia and blocked pre-synaptic degeneration in the cortex of gp120Tg mice. A. Representative images show IBa1^{+}TMEM119^{+} microglia and IBa1^{+}TMEM119^{-} macrophages in the frontal cortex, scale bar: 25μm. B. Quantification of microglia and macrophage density in the frontal cortex. C. Confocal images of vGluT^{+} pre-synaptic puncta in the mouse cortex, scale bar: 10μm. D. Quantitative summaries of vGluT1^{+} puncta density in cortical sections. WT/ctrl: WT mice administrated with control chow; gp120Tg/Ctrl: gp120Tg mice administrated with control chow and gp120Tg/PLX: gp120Tg mice administrated with PLX5622 containing chow. N=4 mice per group.

addition, FKN/CX3CR1 regulates microglial phagocytosis and synapse elimination (Harrison et al., 1998; Paolicelli et al., 2011; Zhan et al., 2014). In previous studies, we observed that FKN is up-regulated by gp120 in both cortical cultures and mouse spinal cords, and that disruption of FKN/CX3CR1 signaling by CX3CR1 knockout attenuated gp120-induced synapse degeneration (Fig.3.6). We were interested in extending these findings and tested here the potential contribution of FKN/CX3CR1 to phagocytose gp120 injured synapses in the cortex. Therefore, we generated gp120Tg/CX3CR1KO mice. Interestingly, we found CX3CR1 knockout potentiated gp120 induced-microglial activation, indicated by increased microglial density in the cortex, 509.8 ± 22.76 microglia per mm^2 in gp120Tg/ CX3CR1$^{-/-}$ mice vs. 426.5 ± 25.77 microglia per mm^2

in gp120Tg/ CX3CR1$^{+/-}$ mice (Fig.4.7 A and B). We observed that gp120Tg/CX3CR1KO mice only had 38.04 ± 6.53% pre-synaptic puncta (labeled by Syn I) of gp120Tg/CX3CR1$^{+/-}$ mice, indicating CX3CR1 KO lead to significant decline of pre-synaptic structure (Fig. 4.7 C-F). In addition, we performed western blotting to validate our immunostaining results. We examined the pre-synaptic marker, vGluT1, protein levels in CX3CR$^{+/-}$, CX3CR1$^{-/-}$, gp120Tg/CX3CR1$^{+/-}$ and gp120Tg/CX3CR1$^{-/-}$ mice. We found CX3CR1$^{-/-}$ did not affect the protein level of vGluT1 (no significant difference was observed between CX3CR$^{+/-}$ and CX3CR1$^{-/-}$ mice), however, gp120 exposure induced vGluT1 decrease in gp120Tg/CX3CR1$^{+/-}$, knockout of CX3CR1 exaggerated gp120-indeced vGluT1 decline (gp120Tg/CX3CR1$^{-/-}$ mice showed lower vGluT1 expression than gp120Tg/CX3CR1$^{+/-}$ mice) (Fig.4.7 F, G). Immunostaining and western blotting results collectively demonstrated CX3CR1 knockout exacerbated gp120-caused pre-synapse loss. These results suggest that the FKN/ CX3CR1 signaling pathway plays an important role in regulating microglial activation and synaptic degeneration.

4.2.7 MerTK is involved in gp120 -induced pre-synaptic degeneration.

MerTK is a phagocytotic receptor expressed by microglia, astrocytes and endothelial cells in the brain (Chung et al., 2013). Recent studies revealed a regulatory role of MerTK in microglial phagocytosis of apoptotic cells and stressed neurons (Scott et al., 2001; Neher et al., 2013; Fourgeaud et al., 2016; Nomura et al., 2017). MerTK pathway is also involved in the engulfment and elimination of synapses by astrocytes (Chung et al., 2013). Thus, we performed western blots to test if gp120 stimulation activates the MerTK pathway. Indeed, MerTK showed activated format in gp120Tg mice indicated by the slightly up-shifted blotting bands (Fig.4.8 A) and elevated phosphorylated MerTK (Fig. 4.8 B). Moreover, galectin-3, a newly identified MerTK ligand and opsonin (Caberoy et

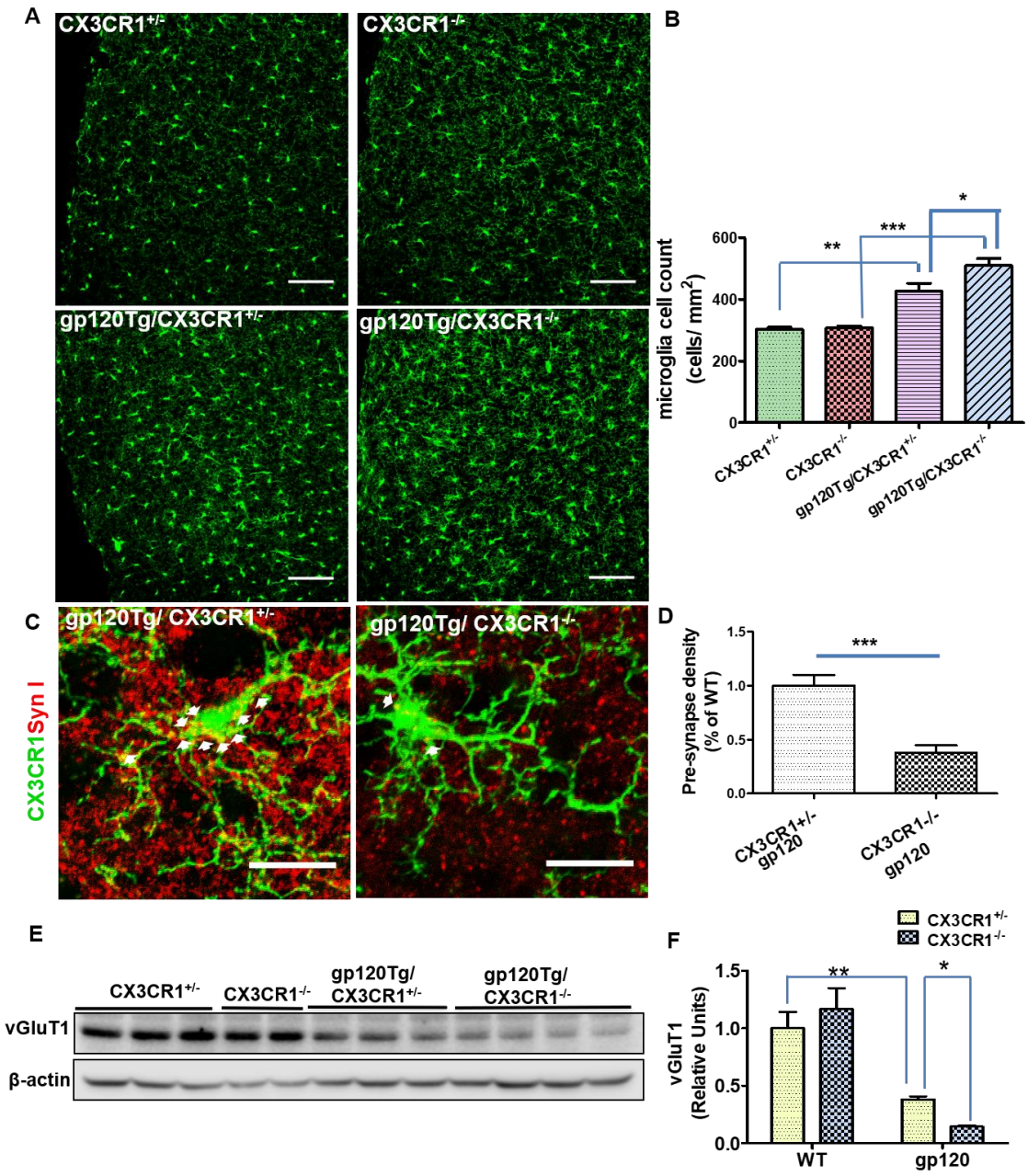

Fig 4. 7 CX3CR1 deficit enhanced gp120-induced microglial activation and pre-synaptic degeneration. A. Confocal images showing IBa1^{+} microglia in the frontal cortex of CX3CR$^{+/-}$, CX3CR$^{-/-}$, gp120Tg/ CX3CR$^{-/-}$ and gp120Tg/ CX3CR$^{-/-}$ mice. Scale bar: 100μm. B. Quantitative summary of A. N=6 mice per group. C. Confocal images of Syn I-labeled pre-synaptic puncta in the frontal cortex, scale bar: 15μm. D. Quantification of pre-synapse density, N=6 mice per each group. E. immunoblots of vGluT1 and β-actin. F. Quantitative summary of E. N=6 mice for CX3CR$^{+/-}$and CX3CR$^{-/-}$. N= 7 for gp120 Tg/ CX3CR$^{-/-}$ and gp120 Tg/ CX3CR$^{-/-}$.

al., 2012), was highly expressed in some microglia (10% of total microglial) in gp120 Tg mice, but no microglia in the WT was found to express immunostaining-detectable galectin-3 (Fig. 4.3 C). Galectin-3 is known to release from microglia to regulate microglial engulfment of target cells (Nomura et al., 2017). Those results highly suggest that microglia may mediate the engulfment and elimination of pre-synaptic element in gp120 Tg through MerTK pathway. To test this hypothesis, we generated gp120 Tg/MerTK KO mice by crossing the gp120 Tg mice with MerTK KO mice. The absence of MerTK was validated in gp120 Tg/MerTK KO mice by using the western blotting technique (Fig. 4.8 C). We found that only MerTK knockout did not affect the pre-synaptic marker: Syn I's expression level, showing as no significant difference was observed between WT and MerTK KO mice (Fig. 4.8 D). However, MerTK KO almost completely blocked gp120 induced decrease of Syn I (no significant difference was observed about the protein level of Syn I between the gp120 Tg/MerTK KO and WT mice) (Fig 4,8 D). To confirm our observation, we performed immunostaining of vGluT1 (pre-synaptic marker) and IBa1 (microglial marker) in cortical sections (Fig. 4.8 E). Similarly, the density of vGluT1 stained pre-synaptic puncta in the gp120Tg/MerTK$^{-/-}$ mice was greater than gp120Tg mice and almost reach to the WT mice' s level (Fig. 4.8 F). More importantly, single plane images showed a dramatic decline of vGluT1 and IBa1 colocalized signals in gp120 Tg/MerTK KO mice (compared to gp120 Tg mice) indicating the attenuated engulfment of pre-synaptic elements by microglia in gp120 Tg/MerTK KO mice (compared to gp120 Tg mice) (Fig. 4.8 G, H). These results demonstrate that MerTK pathway mediates, at least partially, gp120- induced microglial phagocytosis of pre-synaptic degeneration.

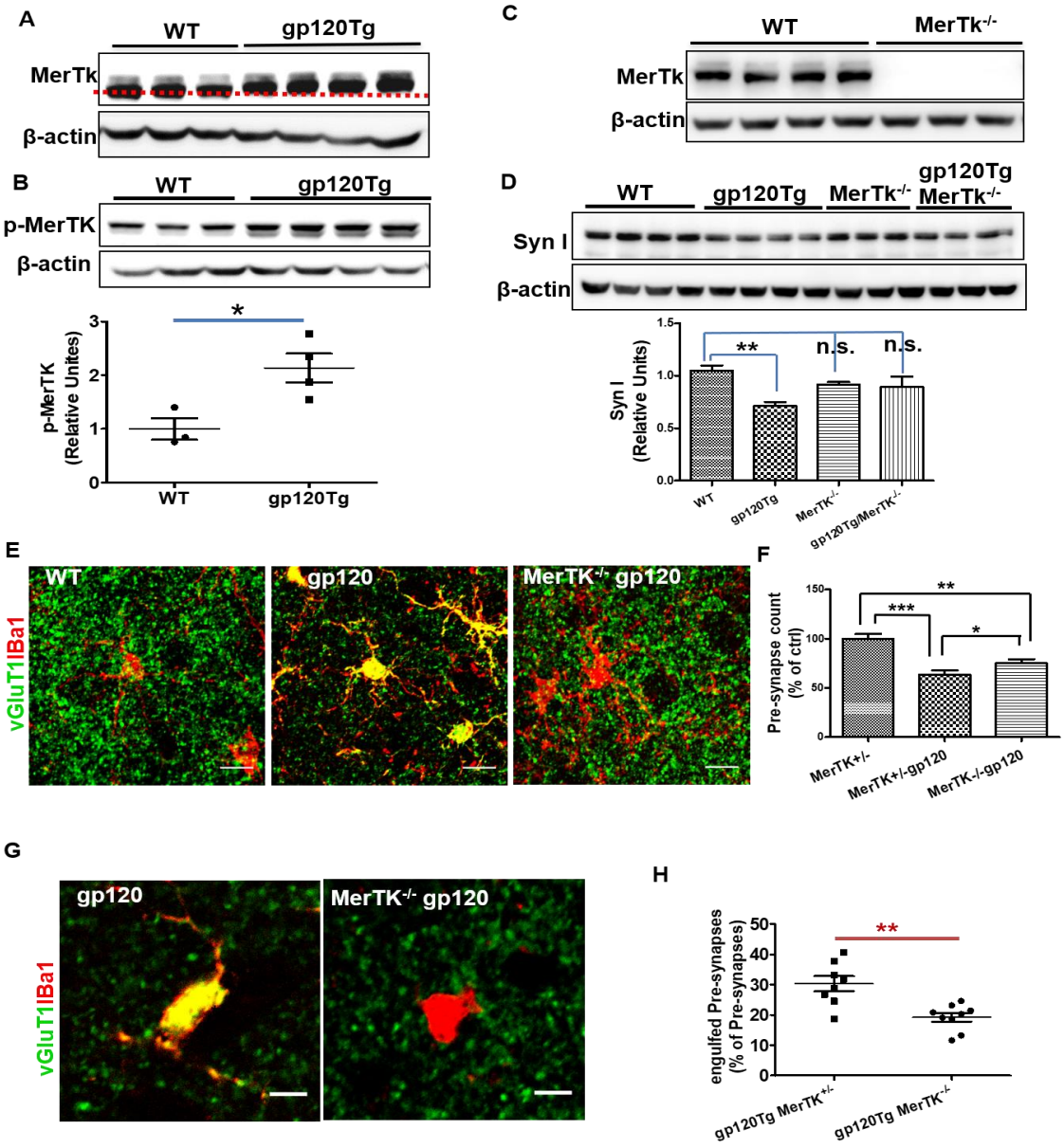

Fig 4. 8 MerTK KO prevents, at least partially, gp120 -induced pre-synaptic degeneration. A. Immunoblots of MerTK in WT and gp120 Tg mice. B. The expression level of phospho-MerTK (Y749 + Y753 + Y754) in cortices from gp120 transgenic and WT mice. A and B. WT, N=3 mice; gp120Tg, N=4 mice. C. The protein level of MerTK in the cortex from WT and MerTK$^{-/-}$ mice. (N=4 mice for WT and N=3 mice for MerTK$^{-/-}$. D. Comparison of the effect of gp120 on Syn I protein levels in WT and MerTK$^{-/-}$ mice. WT and gp120 Tg, N=4 mice; MerTK$^{-/-}$ and gp120Tg/MerTK$^{-/-}$, N=3 mice. E. Confocal images showing vGluT1 labeled glutamatergic pre-synaptic components in the frontal cortex. Scale bar: 10µm. F. Quantification of the density of vGluT1^{+} puncta in WT (N=3), gp120 Tg (N=5), and gp120 Tg MerTk$^{-/-}$ (N=5) mice. G. Single plane images showing the vGluT1^{+} pre-synapse engulfment by microglia. MerTK intact and null mice were immunostained for vGluT1 and IBa1 with yellow staining depicting colocalization. Scale bar: 5µm. H. Quantification of engulfed vGluT1^{+} pre-synapses. N=3 mice for each group.

4. 3 DISCUSSION

The results obtained suggests that microglia actively contribute to synapses (especially the presynaptic compartment) engulfment and elimination in the HIV1-gp120 Tg mice. These results also indicate critical roles of the MerTK and CX3CR1 signaling pathways in regulating the microglial phagocytosis of synapses. Such findings establish the key role of microglia in gp120-induced synapses loss and suggest a new microglia-mediated extrinsic mechanism in neural circuit remodeling during HIV infection. The new insights may shed light on the pathogenic mechanism of synapse loss in the brain of HIV-infected patients.

Although growing evidence suggests a crucial role of microglia in synaptic pruning during development and under certain disease conditions (Stevens et al., 2007b; Stevens et al., 2007a; Hong et al., 2016c; Vasek et al., 2016b)， no study has segmentally studied the mechanism (s) that regulate synapse loss from pre- and post-synaptic sites. Interestingly, our results found microglia selectively engulf and eliminate pre-synaptic component in gp120 Tg mice, which is consistent with recent findings that West-Nile virus infection causes microglia activation and significant pre-synaptic terminal loss (Vasek et al., 2016a). Blockage of complement-microglial axis inhibits infection induced- synaptic degeneration (Vasek et al., 2016a). This study also observed unsynchronized loss of pre- and post-synaptic terminal, the significant reduction of pre-synaptic structure but not post-synaptic part was demonstrated (Vasek et al., 2016a). These findings suggest synaptic degeneration may initiate from the pre-synaptic part and the distinct mechanisms may be involved in pre- and post-synaptic degeneration. However, microglia were observed engulf and eliminate post-synaptic elements during the synapse

loss in Alzheimer disease mouse models (Hong et al., 2016b) and during postnatal development (Paolicelli et al., 2011). Those observations indicate that the microglia-mediated synapse loss is context-dependent, during the infection, pre-synaptic terminal may be the primary target for microglial phagocytosis (Stevens et al., 2007b; Stevens et al., 2007a; Hong et al., 2016a; Vasek et al., 2016a).

Pre-synaptic elements engulfment by microglia is evident in our study (Fig.4.4), this important finding raised many questions. How does microglia selectively recognize pre-synaptic structures? Do "un-wanted" pre-synaptic elements present "eat-me" signals locally? What is the signaling pathway that controls microglial phagocytosis of synapses? Notably, our data indicate that the MerTK pathway regulates microglial activity in phagocytosing pre-synaptic compartments. MerTK is critical for microglia and macrophages to remove apoptotic cells (Scott et al., 2001), stressed neurons (Neher et al., 2013), our data indicate a novel role of the MerTK pathway in microglia-mediated synapse phagocytosis. Consistent with our finding, Chung et al reported the involvement of MerTK pathway in astrocytic phagocytosis of synapses (Chung et al., 2013), suggesting MerTK is a universal pathway that mediates different types of phagocytes to clear the "un-wanted" synapses. MerTK can initiate phagocytosis by binding to phosphatidylserine on the target cells or cell debris. Arrest-specific gene 6 (GAS6) or protein S are two known ligands of MerTK-mediated phosphatidylserine binding (Chen et al., 1997; Hafizi and Dahlbäck, 2006; Grommes et al., 2008). More recently, galectin-3 was identified as a new MerTK ligand (Caberoy et al., 2012) that is expressed by and released from microglia to opsonize cells for phagocytosis (Nomura et al., 2017). We observed that galectin-3 was highly expressed in about 10% of microglia in

gp120Tg mice but not in WT mice. We speculate that galectin-3 is expressed by and released from gp120 activated microglia and opsonizes damaged pre-synaptic compartments, and that MerTK on microglia then binds to galectin-3-labeled elements for phagocytosis. Because desialylated sugar chains on plasma membranes are the target binding site of galectin-3 (Nomura et al., 2017), we envision that gp120 may up-regulate desialyation of the pre-synaptic compartment to facilitate galectin-3 binding. Consequently, the galectin-3-labeled damaged pre-synaptic structures are recognized by MerTK on microglia to initiate phagocytosis (Fig. 4.8).

FKN/CX3CR1 is a neuron-to-microglia signal that mediates the crosstalk between microglia and neurons (Jung et al., 2000b; Cook et al., 2001; Sheridan and Murphy, 2013). Dysregulation of the FKN/CX3CR1 pathway was observed in HIV-infected brains (Cotter

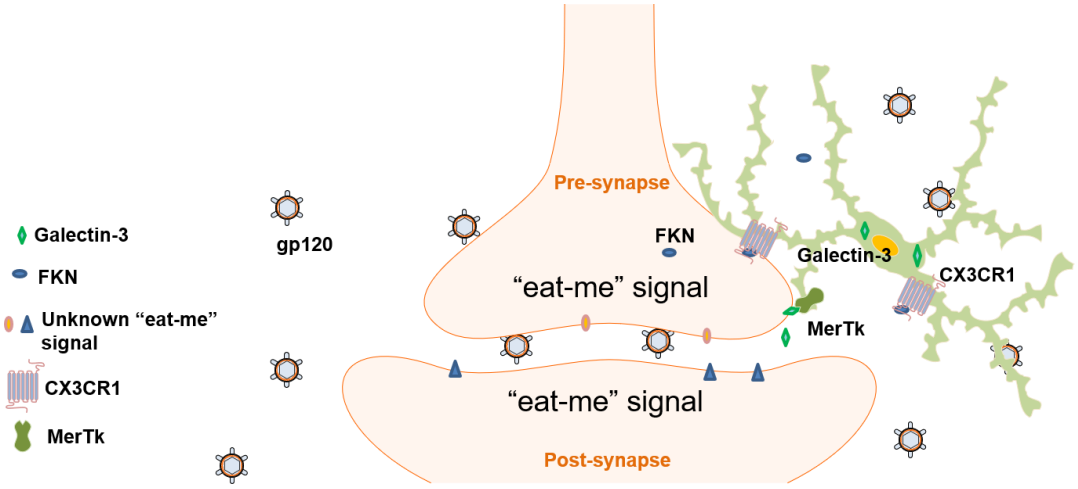

Fig 4. 9 Diagram depicts potential mechanisms by which microglia engulf and phagocytose pre-synaptic compartments. Gp120 causes the synaptic damage and pre-synaptic desialylation. Meanwhile, microglia are also activated by gp120, the activated microglia express and secrete galectin-3. Released galectin-3 binds to the desialylated pre-synaptic membranes, and the MerTK receptor on microglia then mediates microglial engulfment of the damaged pre-synaptic compartment. Gp120 may also induce the pre- and post-synaptic structures to express other "eat-me" signals to initiate synapse elimination through different signal pathways. Notably, FKN/CX3CR1 pathway is very important to control microglial activity, including migration and clearance of damaged debris.

et al., 2002) . Because the FKN/CX3CR1 pathway regulates microglial phagocytosis (Harrison et al., 1998; Paolicelli et al., 2011; Zhan et al., 2014), we hypothesized that gp120 induced synapse elimination through the FKN/CX3CR1 pathway, and predicted that CX3CR1 deficit ought to inhibit gp120-induced synaptic degeneration. Surprisingly, different from our speculation, CX3CR1 KO potentiated gp120-induced microglial activation and synapse loss (Fig. 4.6). One possibility is that after CX3CR1 KO, microglia lose their neuronal regulation, and gp120 stimulation causes excessive microglial activation that lead to overwhelming synapse loss. This idea is supported by the findings that binding of soluble FKN to CX3CR1 maintains microglia in a "resting" state (Bachstetter et al., 2011; Valero et al., 2016) and CX3CR1 KO enhances microglial activation and neurotoxicity (Cardona et al., 2006; Wu et al., 2013; Reshef et al., 2014). In addition, FKN has chemoattractant properties (Paolicelli et al., 2014; Sokolowski et al., 2014). CX3CR1 deficit may impair microglial migration (Paolicelli et al., 2011; Pagani et al., 2015) and interaction with damaged synapses. It is also possible that absence of CX3CR1 may promote pro-inflammatory phenotype of microglia to cause neurotoxicity and synapse loss. It is reported that $CX3CR1^{-/-}$ exacerbate microglial neurotoxicity by up-regulating NO, IL-6, IL-1β and TNF-α production (Cho et al., 2011; Rogers et al., 2011). We will test these hypotheses with further studies.

Moreover, significant and dramatic reduction of post-synapse was observed in the gp120Tg mice. The selectively engulfment of pre-synaptic compartment by microglia indicated that gp120 causes post-synaptic elimination by other mechanisms. Identifying these mechanisms is of importance for future studies.

Chapter 5. The role of astrocytic phagocytosis in gp120-induced synapse elimination

5.1 INTRODUCTION

Astrocytes constitute the most abundant cell type of human brain and physically associate with synapses (Araque et al., 1999; Ventura and Harris, 1999; Halassa et al., 2007; Witcher et al., 2010). The close interaction of astrocytes and synapses suggest important roles of astrocytes in the regulation of synaptic transmission and plasticity (Beattie et al., 2002; Haber et al., 2006; Stellwagen and Malenka, 2006; Jones et al., 2011; Allen, 2014; Araque et al., 2014). Recent studies revealed the involvement of astrocytes in synapse formation and elimination (Ullian et al., 2001; Chung et al., 2013; Chung et al., 2015a; Chung et al., 2015c; Chung et al., 2016; Allen and Eroglu, 2017; Farhy-Tselnicker and Allen, 2018). Dysfunction of astrocytes may contribute to the development of neurological disorders.

Astrocytes regulate the neuronal activity by buffering potassium and up-taking neurotransmitters (glutamate and GABA)(Rothstein et al., 1996; Walz, 2000; Liang et al., 2006). They also release gliotransmitters such as D-serine to stimulate neurons (Yang et al., 2003). Dysfunction of these processes is linked to the pathogenesis of epilepsy, stroke and other neurological disorders (Bambrick et al., 2004; David et al., 2009; Ricci et al., 2009; Coulter and Eid, 2012). In addition, astrocytes secrete other factors to regulate synapse development and function. For example, thrombospondins, the major extracellular matrix proteins secreted by astrocytes, promote glutamatergic synapse formation (Christopherson et al., 2005; Eroglu et al., 2009; Xu et al., 2010). SPARC (secreted

protein acidic, rich in cysteine) protein and D-serine secreted by astrocytes are also reported to modulate synaptogenesis and synaptic plasticity. While hevin (also known as SPARC-like 1) can induce structural formation of excitatory synapses, SPARC antagonizes hevin activity and inhibits glutamatergic synapse formation (Kucukdereli et al., 2011). Besides its regulatory role in glutamatergic synapse formation, SPARC prevents cholinergic presynaptic maturation (Albrecht et al., 2012) and inhibits post-synaptic recruitment of AMPA receptors (Jones et al., 2011; Kucukdereli et al., 2011).

During development, neurons initially form excessive synapses, which are eliminated during critical time periods to form the refined and mature neural circuits (Neniskyte and Gross, 2017). Recent studies highlight the important roles of astrocytes in synapse elimination. In the developing visual system, microglia phagocytose extra synapses through the complement pathway (Paolicelli et al., 2011). The "unwanted" synapses are labeled by C1q and C3, which then are recognized and eliminated by microglia through C3R-mediated phagocytosis (Stevens et al., 2007b; Schafer et al., 2012). Astrocytes modulate this process by controlling the expression of C1q in retinal ganglion cell (RGC). Transforming growth factor-β (TGF-β) released by astrocytes controls C1q expression in RGC (Bialas and Stevens, 2013). In addition, mounting evidence indicates the phagocytotic ability of astrocytes in removing apoptotic neurons, cell debris (Al-Ali et al., 1988; Cheng et al., 1994; Nguyen et al., 2011; Lööv et al., 2012; Morizawa et al., 2017; Ponath et al., 2017). Astrocytes are enriched with expressed genes in phagocytic pathways (Cahoy et al., 2008). A recent study shows that astrocytes eliminate synapses by direct phagocytosis, via the MEGF10 and MERTK pathways (Chung et al., 2013). Mice with

MEGF10 and MERTK deficits fail to refine retinogenicular connections and retain excess functional weak synapses (Chung et al., 2013).

It is still unknown if astrocytic phagocytosis plays a role in disease-associated synapse loss. Current investigation of astrocytic role in HIV-associated neural injury is mainly focused on the release of proinflammatory cytokines such as TNF-α, IL-6 (Nottet et al., 1995; Shah et al., 2011b), chemokine CCL5 (Shah et al., 2011a) and neurotoxic nitric oxide (NO) (Reddy et al., 2012) after HIV infection. In this study, I reveal a novel role of astrocytes in gp120-induced synaptic degeneration. I show that in the gp120 Tg mice astrocytes engulf synapses. In contrast to microglia, astrocytes predominantly phagocytose post-synaptic elements. This observation indicates astrocytes actively participate in the gp120-induced synapse degeneration by selectively removing the post-synaptic compartments of the degenerating synapses. To futher identify the signal pathway that regulates astrocytic phagocytosis of gp120-induced synapase elimination, we test the role of the MerTK signaling, a known pathway that regulates astrocytic phagocytosis (Chung et al., 2013). The activaiton of MerTK pathway was suggested by the shift immunoblotting bands of MerTk and elevated p-MerTk, and up-regulated galectin-3 (a ligand of MerTK receptor) in our gp120 Tg mice. However, MerTK knockout did not affect gp120-indeced astrocytic activation and synapse elimination. These resultes suggest MerTK pathway is not the main signaling pathway medating gp120-induced actrocytic phagocytosis of synapses.

5.1 RESULTS

5.1.1 Astrocytes are activated in gp120 transgenic mice.

In the last chapter, I showed significant synapse loss in the frontal cortices of gp120 transgenic mice (Fig.4.1), and microglia mediated the synaptic degeneration by predominately phagocytosing pre-synaptic components (Fig. 4.4). To assess if astrocytes contribute to the synaptic degeneration in the gp120 transgenic mice, I first measured astrocytic activation by immunostaining and western blotting, with the astrocyte marker glial fibrillary acidic protein (GFAP). I observed a marked increase of $GFAP^+$ cells in the fontal cortex of gp120 Tg mice (Fig. 5.1 A and B), and the $GFAP^+$ cells displayed

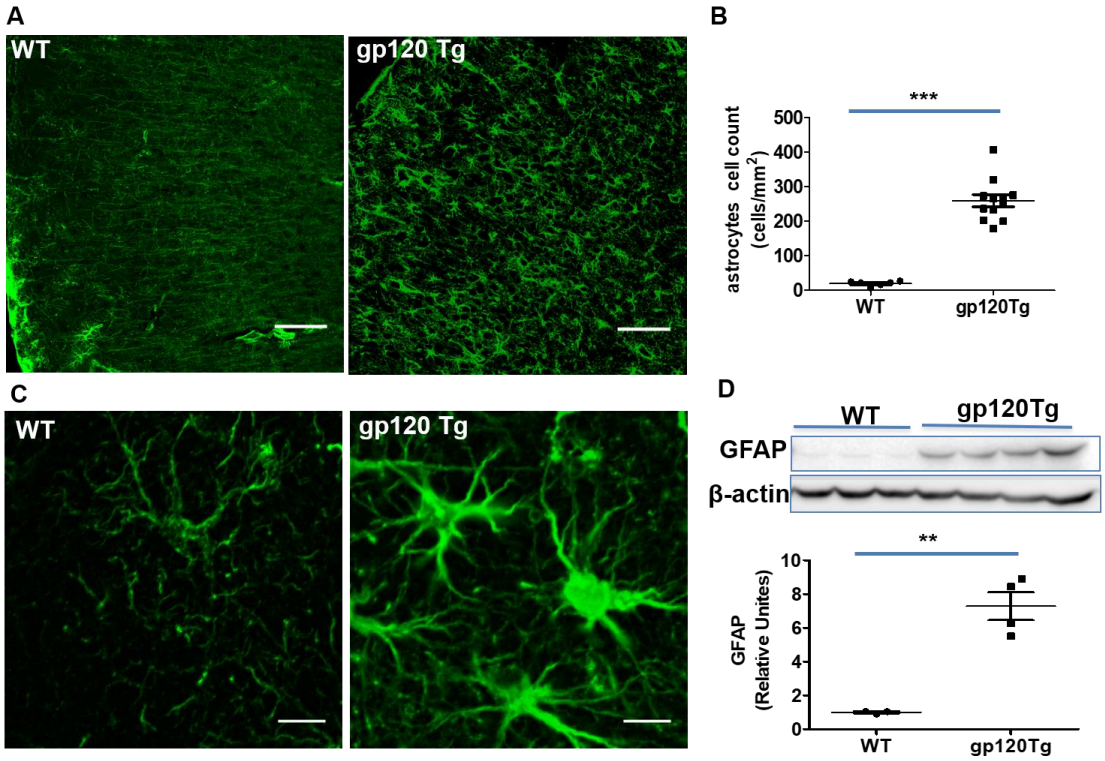

Fig 5. 1 Astrocytes activation in the cortex of gp120 transgenic mice. A. confocal images of $GFAP^+$ astrocytes in WT and gp120 Tg mice at the age of 6 months old. Scale bar, 100 µm. B. Quantitative graph showing increased $GFAP^+$ cells in gp120 Tg mice. C. High-power representative images from WT and gp120 Tg mice showing hypertrophic morphology of astrocytes in the cortex of gp120 Tg mice. Scale bar, 100 µm. D. Immunoblots and quantification of GFAP protein level in WT and gp120 Tg mice's cortices. D. The quantitative summary of graph C. N= 3 mice for WT, 4 mice for gp120 Tg. Immunostaining performed within the frontal cortex, confocal images captured the distribution of synapse in the layer I-II of cortex. Error bars, s.e.m; **, $p<0.01$; ***, $p<0.001$.

hypertrophic morphology (Fig. 5.1 C). Compared to WT mice, in which astrocytes displayed a bushy morphology with many thin processes, astrocytes in gp120 Tg mice increased expression of GFAP and loss the bushy appearance but exhibited stellate morphology with shorter and thicker processes (Fig. 5.1 C). In addition, western blotting results showed the protein level of GFAP was dramatically elevated in the cortex of gp120 Tg mice, gp120 Tg mice expressed 5 times GFAP as much as WT mice (Fig 5.1 D). These observations confirm the findings of the previous studies (Toggas et al., 1994), and suggest the activation of astrocytes in the brain of gp120 transgenic mice.

5.2.2 Astrocytes in the gp120 Tg mice predominantly engulf and eliminate post-synaptic structure.

To evaluate the potential role of astrocytic phagocytosis in synapse loss in the gp120 transgenic mouse, I performed double-staining of GFAP and PSD95 in the frontal cortex of the WT and gp120 Tg mice. I found that PSD95 aggregated in the transgenic mice, and most of PSD95 clumps were colocalized with GFAP-labeled astrocytes, mainly in the somatic regions (indicated by arrowheads in Fig. 5.2A). In contrast, microglia did not seem to associate with PSD95 clumps (Fig. 4.4C). The similar staining pattern was observed with another post-synaptic marker, NMDA receptor subunit 1 (NR1) (Fig. 5.2 B). Triple-immunostaining of GFAP, PSD95 and Syn I revealed gp120 stimulation induced astrocyte to engulf synapses. Compared to WT mice, gp120 Tg mice showed more pre- and post-synaptic puncta labeled by anti-Syn I or anti-PSD95 antibody in the astrocytes, however, reactive astrocytes in the transgenic mice predominately engulfed $PSD95^+$ elements, with much fewer Syn I signals (Fig. 5.2 C, D). The portion of $PSD95^+$ synaptic structure inside $GFAP^+$ astrocytes (showed as colocalized volume) in gp120 Tg mice were

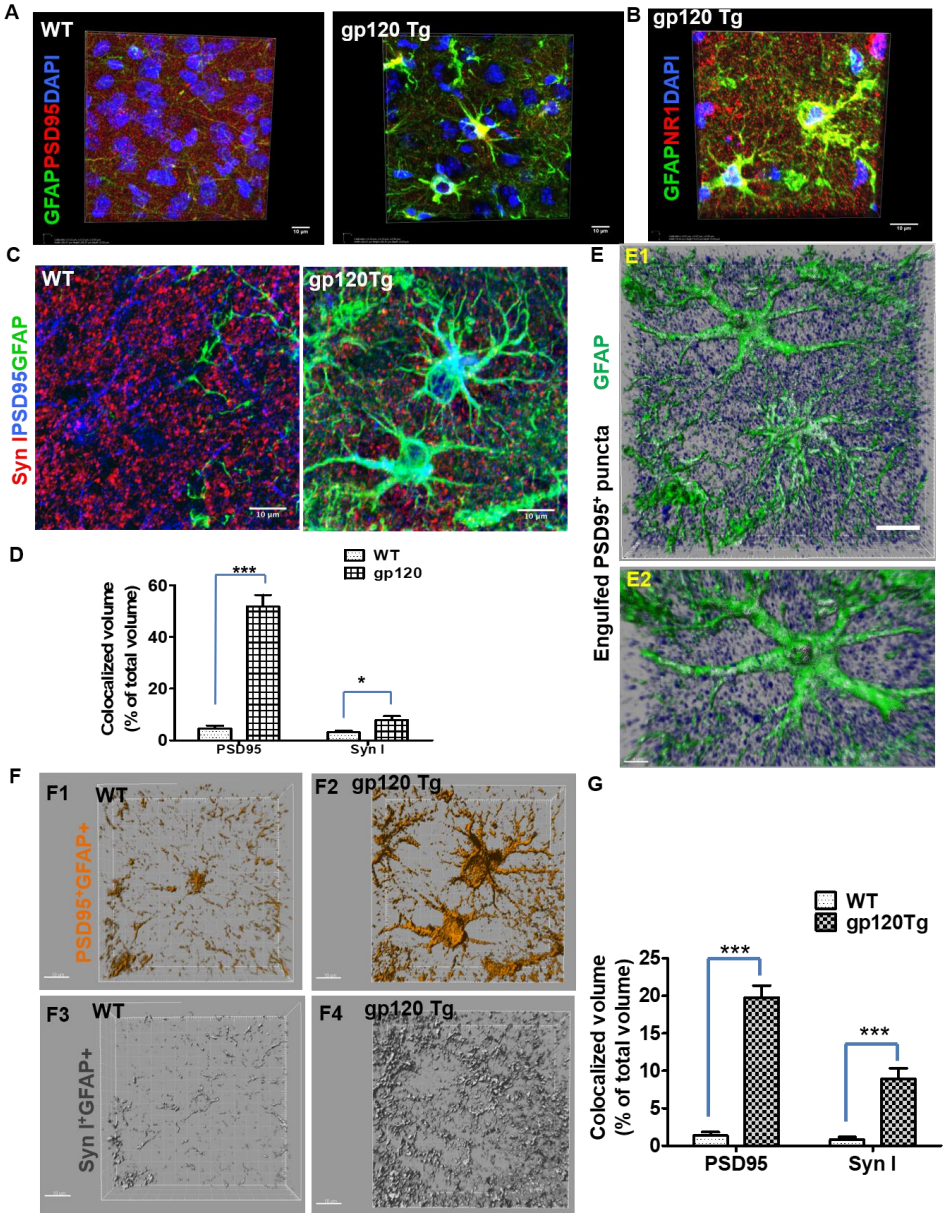

Fig 5. 2 Astrocytes in the gp120Tg mice predominantly contain post-synaptic signal. A. Double-immunostaining confocal images of GFAP (green) and PSD95 (red) to show PSD95 clumps in the cell bodies of astrocytes (yellow), scale bar: 10 µm. B. Representative images showed NR1-labed post-synaptic terminal located in GFAP$^+$ astrocytes, scale bar: 10 µm. C. Triple-immunostaining confocal images of GFAP (green), Syn1 (red) and PSD95 (blue) to show astrocytes mainly contain PSD95$^+$ puncta (cyan) but a little Syn1 signal, 10 µm. D. Quantitative summary of C. E. 3-D surface rendering (Imaris) to show the astrocyte-engulfed PSDD95$^+$ puncta (white singals), scale bars: 10 µm for E1; 4 µm for E2. F. 3-D reconstruction images (Imaris) showing the overlapped signals of PSD95 and GFAP (E1-E2) or Syn I and GFAP (E3-E4) F. Quantification of SynI or PSD95 signals in 3-D images N: 6 mice for WT, 7 mice for gp120Tg. The 3-D images analysis showed in E-G were conducted by Lorenzo Ochoa.

4 times as much as in WT mice (Fig. 5.2D). To visualize enclosed structures of astrocytes and exclude the PSD95 or Syn I signal outside astrocytes, Imaris was used to perform surface rendering. As the Fig. 5.2 E showing, many $PSD95^{+}$ synaptic components are localized in astrocytes in gp120 Tg mice (showed as white puncta), these colocalized puncta indicate the engulfment of post-synaptic terminal by astrocytes in gp120 Tg mice. To perform 3-D images quantification and rule out the possibility of including the PSD95 or Syn I signals outside the astrocytes during quantification in Fig. 5.2 D, Imaris was also used to reconstruct 3-D images from Z-stacks images to visualize the overlaps of PSD95 and GFAP signals (Fig. 5.2 F1-F2) or Syn I and GFAP signals (Fig. 5.2 F3-F4). In Fig. 5.2 F1-F2, signals that only had PSD95 expression and only had GFAP expression was subtract from the images; in Fig. 5.2 F3-F4, signals only had Syn I expression and only had GFAP expression were removed. 3-D image-based quantification confirmed that reactive astrocytes in the transgenic mice predominately engulfed post-synaptic elements (Fig. 5.2 G). Interesting, we found most PSD95 clumps were in the soma of gp120Tg astrocytes, (Fig. 5.2 C and F2). On the other hand, the Syn I puncta overlapping with the GFAP signals mainly located in the process of astrocytes (Fig. 5.2 C and F4). Those data collectively indicate that astrocytes predominately phagocytose post-synaptic terminal in gp120 Tg mice.

I also performed flow cytometry to quantify the astrocytic populations containing Syt-1 or PSD95 staining signals (Fig. 5.3 A-C). Single cell suspensions from the cortex of WT and gp120 Tg were stained with anti-CD11b and anti-GFAP antibodies to label the microglia and astrocytes respectively, the group of $CD11b^{-}$ $GFAP^{+}$ cells (The fourth quadrant of Fig. 5.3 A) was counted as astrocytes. The results showed that the cell counts

of GFAP$^+$ astrocytes was dramatically increased in gp120 Tg mice (Fig.5.3 D). Similarly, to examine the astrocytic population that contain PSD95 or Syt-1 signal, single cell suspensions from the cortex of WT and gp120Tg were stained with anti-GFAP, anti-PSD95 and anti-Syt-1 antibodies to label astrocytes, pre- and post-synaptic terminal. The GFAP$^+$ Syt-1$^+$ cells (the third quadrant of Fig. 5.3 B) were counted as astrocytes associated with pre-synaptic structure and the GFAP$^+$PSD95$^+$ cells (the third quadrant of Fig. 5.3 C) were counted as astrocytes associated with post-synaptic structure. Increased astrocytic

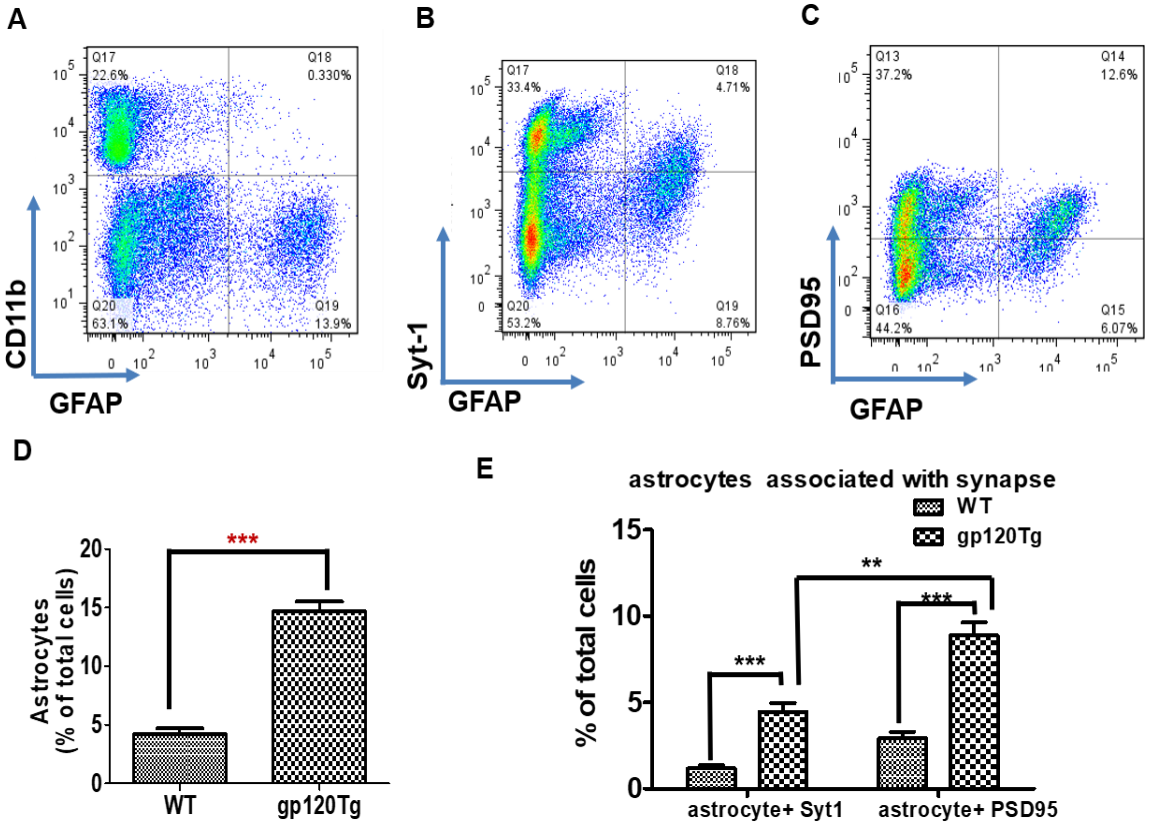

Fig 5. 3 Astrocytic population with PSD95 staining markedly increases in the gp120 transgenic mice. A-C. Flow cytometry strategies to gate astrocytes (GFAP$^+$CD11b$^-$) (A), astrocytic population associated with pre-synaptic element (GFAP$^+$Syt-1$^+$) (B) and astrocytic population associated with post-synaptic structure (GFAP$^+$PSD95$^+$) (C). D. Quantitative results shows increased astrocytes in gp120Tg mice. E. Quantification shows that both PSD95 and Syt-1 containing astrocytes are increased in the gp120 mice, but the number of astrocytes with PSD95 is much greater than the astrocytes with Syt-1. N: 6 mice for WT, 8 mice for gp120 Tg.

population was observed in gp120 Tg mice (2 times greater than WT mice). The number of astrocytes that contain PSD95 signal (8.9% of total cells in gp120 Tg mice v.s. 2.9 % in WT mice) and that contain Syt-1 signal (4.5% of total cells in gp120 Tg mice v.s. 1.2 in WT mice) were up-regulated in gp120 Tg mice (Fig. 5.3 E). But importantly, more astrocytes associated with post-synaptic structure than that associated with pre-synaptic structure. The number of astrocytes associated with PSD95 took up 8.9% of total cortical cells, whereas astrocytes associated with Syn I only took up 4.5% of total cortical cells (Fig. 5.3E). These findings demonstrated that astrocytes predominantly phagocytose postsynaptic element in the gp120 transgenic mice.

5.2.3. MerTK signaling is not involved in post-synaptic elimination by astrocyte.

Next, I wanted to understand the mechanism by which astrocytes phagocytose gp120-damaged post-synaptic terminal. Recently transcriptome analysis revealed that astrocytes express a number of genes in phagocytotic pathways including MEGF10 and MERTK (Hochreiter-Hufford and Ravichandran, 2013). Phagocytotic receptors MEGF10 and MERTK have been reported to regulate phagocytosis of apoptotic cells and cell debris by recognizing 'eat me signals', such as phosphatidylserine on targets (Hochreiter-Hufford and Ravichandran, 2013; Tung et al., 2013). The study further demonstrated that astrocytes mediated synapse engulfment and elimination thorough MERTK and MEGP10 pathways and mice with either receptor deficit failed to refine synapses (Chung et al., 2013). On immunoblots, the MerTK bands from gp120 Tg cortical homogenates were slightly shifted up (Fig. 4.7 A), plus the evidence of increased p-MerTK (Fig. 4.7 B) in gp120 Tg mice, we demonstrated gp120 caused MerTK pathway activation. On the other hand, the expression level of MEGF10 showed no obvious quantitative differences

between gp120 Tg and WT mice (Fig.5.4A). In addition, a MerTK receptor ligand, galectin-3, was up-regulated in the astrocytes in gp120 Tg mice. While 10% astrocytes in gp120 Tg showed marked galectin-3 expression (Fig.5.4 B and C), almost none astrocytes in the WT cortices had such galectin-3 expression patterns (Fig.5.4 B and C). Importantly, most galectin-3^{+} astrocytes overlapped with PSD95 clumps (Fig.5.4 B, arrow). These findings indicate that the galectin-3/MerTK axis is activated in gp120 Tg mice and may regulate astrocytic phagocytosis to eliminate synapses. To test this hypothesis, gp120 TgMerTK$^{-/-}$ mice were generated thoough the hybridaizaiton of gp120 Tg mice and MerTK$^{-/-}$ mice. However, MerTK konockout did not affect gp120-induced astrocytes acitviation, the number of astrocytes showed no significat difference between gp120 Tg mice and gp120 Tg MerTK$^{-/-}$ mice (Fig.5.4 E and F). The engulfment of PSD95^{+} structure by astrocytes were clearly seen in the gp120 Tg MerTK$^{-/-}$ mice (Fig. 5.4 F) and the portion of emgulfed PSD95^{+} puncta showed no significant difference between gp120 Tg and gp120 Tg MerTK$^{-/-}$ mice (Fig.5.4 G). To confirm this observation, I performed western blotting to examine the protein level of PSD95 in WT, MerTK$^{-/-}$, gp120 Tg and gp120 Tg MerTK$^{-/-}$ mice. I found gp120 caused significant reduction of PSD95 in both gp120 Tg and gp120 Tg MerTK$^{-/-}$ mice, PSD95 showed similar reduction degree between gp120 Tg and gp120 Tg MerTK$^{-/-}$ mice (Fig. 5.4 I, J). Those results suggest that MerTK pathway is not the main pathway that regualtes astrocytes to elimiante gp120-damaged post-synaptic structure.

5.3 DISCUSSION:

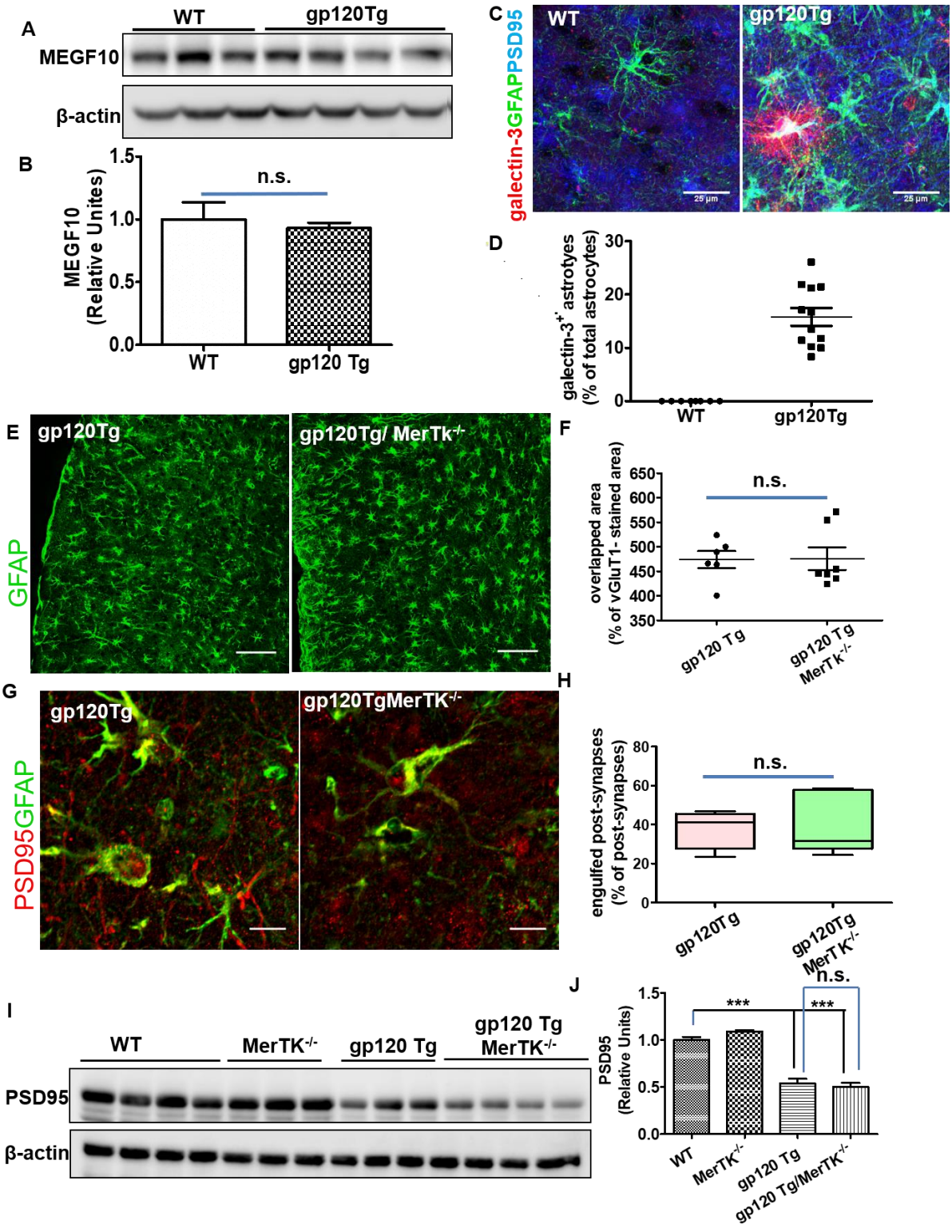
A
WT
gp120Tg
MEGF10
β-actin
B
MEGF10 (Relative Unites)
n.s.
WT
gp120 Tg
C
galectin-3GFAPPSD95
WT
gp120Tg
25 μm
D
galectin-3+ astrotyes (% of total astrocytes)
WT
gp120Tg
E
GFAP
gp120Tg
gp120Tg/ MerTk-/-
F
overlapped area (% of vGluT1- stained area)
n.s.
gp120 Tg
gp120 Tg MerTk-/-
G
PSD95GFAP
gp120Tg
gp120TgMerTK-/-
H
engulfed post-synapses (% of post-synapses)
n.s.
gp120Tg
gp120Tg MerTK-/-
I
WT
MerTK-/-
gp120 Tg
gp120 Tg MerTK-/-
PSD95
β-actin
J
PSD95 (Relative Units)
n.s.
***
***
WT
MerTK-/-
gp120 Tg
gp120 Tg/MerTK-/-

Fig 5. 4 MerTK is not required by astrocytes to engulf and eliminate post-synaptic terminal in gp120Tg mice. A. Immunoblots of MEGF10 in WT and gp120Tg mice. B. Quantificative summary of A. C. Triple immunostaining confocal images of galectin-3 (red), GFAP (green) and PSD95(blue) to show the overlapped signal (white) in the frontal cortex of WT and gp120 Tg mice. Scale bar: 25μm. D. Quantification of galectin-3^+ astrocytes in WT and gp120 Tg mice. E. Confocal images showing the $GFAP^+$ in gp120 Tg and gp120 Tg $MerTK^{-/-}$ mice. Scale bar: 100μm. F. Quantification of astrocytes represented in D. G. Confocal images of GFAP (red) and PSD95 (green) to show the overlapped signal (yellow) in cortical section of gp120 Tg and gp120 Tg $MerTK^{-/-}$ mice. Scale bar: 50μm. H. Quantification of overlapped $PSD95^+$ puncta. I and J. Immunoblots and quantification of the protein level of PSD95 in WT and $MerTK^{-/-}$, gp120 Tg and gp120 Tg $MerTK^{-/-}$ mice. For panels A-D N=3 mice for WT, 4 mice for gp120 Tg. Other panels, N=4 mice for WT and gp120 Tg $MerTK^{-/-}$; N=3 mice MerTK-/- and gp120 Tg.

As microglial cells, astrocytes have phagocytotic ability and express many phagocytic receptors like MerTK, MEGF10 and Bai1 (Cahoy et al., 2008). But the role of astrocytic phagocytosis is less studied especially under disease conditions. I demonstrated that astrocytes in gp120 Tg mice actively engulf and phagocytose synapses, especially post-synaptic structure. This finding reveals a previously unknown role of astrocytes in HIV-associated synapse loss. The galectin-3/MerTK axis seems to be activated in gp120 Tg but which is not required by astrocytes to mediate synapse elimination.

Interestingly, we found abundant post-synaptic clamps inside the astrocytes' soma in gp120 Tg mice, indicating astrocytes actively engulf and phagocytose post-synaptic element. Astrocyte/pre-synaptic interaction also enhanced in the gp120Tg mice. Pre-synaptic staining signals showed random distribution along the astrocyte processes, indicating the astrocytes/pre-synaptic colocalization may not result from phagocytosis. Why do activated astrocytes selectively phagocytose post-synaptic elements? It was reported that astrocytic processes predominantly interact with post-synaptic compartments, compared with their interaction with the pre-synaptic terminals (Lehre and Rusakov, 2002). The asymmetric contacts of astrocytic processes at synapses may facilitate the recognition

and engulfment of the post-synaptic structure by astrocytes during synaptic degeneration. Another possibility is that different "eat-me" signals are expressed by pre- and post-synapses, which trigger distinct phagocytic pathways used by microglia or astrocytes. Microglia and astrocytes reportedly mediate synapse phagocytosis through distinct pathways (Chung et al., 2015b). It is thereby important to identify the potential "eat-me" signals on synapse and "find-me" receptors on the glial cells to completely elucidate the mechanism by which glial cells mediate HIV-associated synaptic degeneration.

MerTK is a phagocytotic receptor found on astrocytes and regulates synapse pruning in developing and adult CNS (Chung et al., 2013). Galectin-3 is a secreted ligand of MerTK that mediates phagocytosis by binding the target debris and phagocytic cell (Caberoy et al., 2012; Nomura et al., 2017). The galectin-3/MerTK axis seems activated in gp120 Tg mice as indicated by the activation of MerTK and the significant up-regulation of galectin-3 in reactive astrocytes in gp120Tg mice (Fig. 5.4). However, we found MerTK deficits did not affect gp120-induced astrocytes activation nor astrocytic phagocytosis of synapses (Fig. 5.4), suggesting MerTK pathway is not required by astrocyte to engulf and eliminate synapses in gp120Tg mice, at least, MerTK pathway is not the major regulator that is involved in asytocytic phagocytosis. The deficit of MerTK can be compensated by other phgocytotic pathways. It thus becomes important and interesting to identify the signal pathway that regulates astrocytic phagocytosis in response to gp120 stimulation. Although phagocytic receptor: MEGF10 in gp120 Tg mice showed similar expression level as in WT mice, we can not exclude the involvment of MEGF10 pathway in astrocytes-mediated synapse elimination. It is possilbe that gp120 alters MEGF10 activity but not total expression level of MEGF10 or gp120 up-regulates the

expression of MEGF10 ligands. The involvement of MEGF10 needs to be tested in future studies. In addition, astrocytes express APOE phagocytosis pathway that is implicated in synapse pruning (Chung et al., 2016). The low-density lipoprotein receptor-related protein 1 receptor (LRP1), APOE membrane receptor, is enriched in astrocytes and mediates Aβ's clearanc e(Martiskainen et al., 2013; Liu et al., 2017). APOE/LRP1 phagocytotic pathway may participate in astrocytes-mediated synapse phagocytosis.

Chapter 6 Summary and Future Directions

6.1 SUMMARY

Synapse degeneration is one of the most relevant neuropathologies associated with HIV-associated neurological disorders. However, the mechanism by which HIV infection causes synapse loss is largely unknown. The results I have obtained reveal that HIV-1 gp120 activates glial cells, including microglia and astrocytes, and the reactive glia may contribute to gp120 induced synaptic degeneration by engulf and eliminate gp120-damaged synapses.

In the pain neural circuit at the SDH, I demonstrated that microglia play an important role in gp120-induced synaptic degeneration, and this process is probably regulated by FKN/CX3CR1 signaling. I further elucidated that activity-dependent Wnt3a/β-catenin signaling controlled gp120-induced FKN up-regulation. These findings collectively suggest a critical role of Wnt3a-FKN-CX3CR1 intercellular signaling from neurons to microglia in modulating gp120-induced synaptic degeneration.

Using gp120 transgenic mice, I also revealed a crucial role of glial phagocytosis in gp120-induced synaptic loss. I found that gp120 induced microglia to selectively engulf and eliminate pre-synaptic terminal but not post-synaptic terminal, while reactive astrocytes act predominantly at the postsynaptic compartment. Ablation of microglia protected pre-synaptic terminal from gp120-induced elimination, demonstrating an essential role of microglia in this process. The MerTK signal pathway participated in gp120- induced microglial phagocytosis of pre-synaptic structure but did not regulate astrocytes phagocytosis of post-synaptic part. These newly identified roles of microglial

and astrocytic phagocytosis along with regulatory molecular pathways provide significant insights on understating the mechanism of HIV-associated synaptic degeneration. Potentially, our findings may help identify glial phagocytotic pathways-based therapeutic targets for HIV-associated synaptic degeneration.

We found in gp120 Tg frontal cortices, microglia selectively phagocytosis of pre-synaptic element, while astrocytes predominately phagocytosis of post-synaptic element. The selective phagocytotic activities of microglia and astrocytes probably depends on the cross-talks between synapses and glial cells, as well as the interaction between microglia and astrocytes. Multiple "eat-me" signals and phagocytotic receptors are found at synapses, microglia and astrocytes (Vilalta and Brown, 2017). The specific "eat-me" signals on synaptic structures and the phagocytotic receptors on glia likely coordinate the selective interaction between pre- or post- synaptic terminal and microglia and/or astrocytes. Recent studies also revealed bidirectional interaction between microglia and astrocytes during the neurogenesis and neurodegeneration. For example, astrocytes regulate microglial phagocytosis of excess synapse by controlling the expression of C1q at synapses (Bialas and Stevens, 2013). On the other hand, secreted factors such as Il-1α, TNFα, and C1q from activated microglia are required and sufficient to induce reactive astrocytes (Liddelow et al., 2017). In addition, during the traumatic brain injury (TBI), microglia-derived cytokines can transform astrocytes to protective phenotype via down-regulating P2Y1 receptor (Shinozaki et al., 2017) . The selective phagocytosis of pre- or post- synaptic elements by microglia or astrocytes may also be due to their asymmetric interaction with pre- or post-synaptic compartments. Astrocytic processes at the post-synaptic site is 3-4 times higher than at pre-synaptic site (Lehre and Rusakov, 2002). This asymmetric interaction may

facilitate astrocytes to phagocytose post-synaptic component during the synaptic degeneration. The cooperative effects of microglia and astrocytes probably enhance the efficacy of synapses elimination, via multiple phagocytic pathways. Therefore, the manipulation of a specific cell type is probably insufficient to intervene the synapse degeneration. This may provide a potential explanation for the failures of clinical trials of therapeutic agents targeting one cell type or pathway. For example, treatment of HIV patients with minocycline that targets to reduce microglial activation showed no improvement to HIV-associated cognitive impairment (Nakasujja et al., 2013).

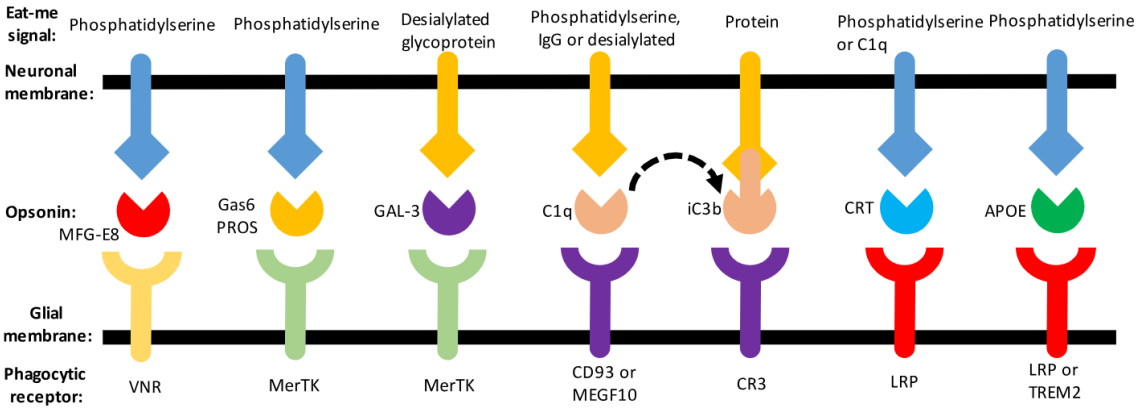

Fig 6. 1 Intercellular phagocytic signaling. (Adapted from Vilalta and Brown, 2017. FEBS J. FEBS J. vol: pages)(Vilalta and Brown, 2017).

My data indicate that the FKN/CX3CR1 pathway plays different roles in synapse elimination in different animal models (i.t.-gp120 mice vs. gp120Tg mice). Knockout of CX3CR1 protected synapses from gp120-induced degeneration in the SDH of i.t.-gp120 mice. In contrast, CX3CR1 KO potentiated microglial activation and synapse loss in the frontal cortex of gp120Tg mice. Those different observations may be contributed by multiple factors. For instance, different pathogenic processes may be involved in different models. In the i.t.-gp120 mouse model, 7 days of gp120 administration will cause acute

inflammation in the spinal cord. During the acute inflammatory episodes, FKN/CX3CR1 appears to promote synaptic degeneration by activating microglia, and CX3CR1 deletion may prevent microglia- neuron interaction and synapse loss. Similar results was reported in an ischemic stroke model, where disruption of FKN/CX3CR1 pathways suppressed microglial activation and neuronal loss (Tang et al., 2014). On the other hand, the gp120Tg mice have developed a chronic and slowly progress of neurodegeneration in the CNS. It takes 6 months to show synaptic degeneration. Instead of rapid microglial activation as in the i.t.-gp120 model, the microglia in gp120Tg mice are in a chronic activated state and likely transformed to M2 microglia suggesting by their evident phagocytosis (Fig. 4.4, 4.5). Lack of CX3CR1 on microglia in the transgenic model may cause them to become more active and transform to pro-inflammatory version (M1). Previous studies report that CX3CR1 deficit exacerbates microglial neurotoxicity by up-regulating NO, IL-6, IL-1β and TNF-α production (Cho et al., 2011; Rogers et al., 2011). Therefore, it is possible that the FKN/CX3CR1 signaling is neuroprotective in the gp120 Tg model but becomes neurotoxic in the i.t.-gp120 model. Since potentiated microglial activation was observed in the cortex of CX3CR1 knockout mice indicated by increased microglial population (Fig .4.7), but microglia did not exhibit higher proliferative activity in the i.t.-gp120 spinal cord (data is not shown), another possible mechanism is CX3CR1 knockout up-regulates microglial phagocytic capacity by enhancing microglial proliferation in the gp120 Tg model. Thus, results in increased microglial number surrounding gp120-damaged synapses. This is supported by the finding that CX3CR1 deficit reduced amyloid deposits through selectively phagocytosing proto-fibrillar amyloid-β in an Alzheimer's model mouse (Liu et al., 2010). However, in the transient gp120 injection mouse model, microglia

were rapidly activated by changing their activated status and lack of CX3CR1 may interrupt the microglial migration but not affect the proliferative activity of microglia during the short-term of gp120 stimulation. Therefore, CX3CR1 KO suppressed the microglia-synapse interaction. In addition, it is important to note that the different effects of CX3CR1 knockout were observed in different CNS regions. It is possible that microglia may show biological differences in different regions after gp120 stimulation. Indeed, spared nerve injury elicits differential microglial responses in spinal cords and brains (Li et al., 2016) and the region-dependent heterogeneity of microglia was demonstrated in a lipopolysaccharide-induced Inflammation model (Furube et al., 2018).

The MerTK receptor and its ligands, including arrest-specific gene 6 (GAS6) (Chen et al., 1997), Protein S (Hafizi and Dahlbäck, 2006) and recently identified galectin-3 (Caberoy et al., 2012), play critical roles in recognition and elimination of apoptotic cells and cell parts (Scott et al., 2001; Chung et al., 2013; Neher et al., 2013; Dransfield et al., 2015). The ligands act as molecular "bridges" that bind to MerTK on phagocytes as well as to the "eat-me" signals expressed on the targets to opsonize the targets for phagocytosis (Dransfield et al., 2015; Nomura et al., 2017). MerTK receptors are expressed by multiple cell types such as microglia and astrocytes in the CNS (Chung et al., 2013). We found galectin-3 is up-regulated in microglia and astrocytes in gp120 Tg mice (Fig. 4.3 and Fig. 5.4). However, our studies suggest that the MerTK pathway contributes to gp120-induced microglial phagocytosis of pre-synaptic terminal but not required for the astrocytic phagocytosis of post-synaptic terminal. It is possible that distinct "eat-me" signals are present on pre- and post-synaptic terminals after gp120 stimulation. Desialylated glycoprotein on the neuronal surface binds galectin-3 and triggers MerTK-

mediated microglial engulfment (Nomura et al., 2017) (Fig. 6.1). Phosphatidylserine, however, can interact with multiple opsonins that bind to different phagocytotic receptors (Fig. 6.1). I speculate that gp120 stimulates pre-synaptic terminals to express "eat-me" signals such as disialylated glycoprotein, which only activates MerTK-mediated microglial phagocytosis (Caberoy et al., 2012; Nomura et al., 2017; Vilalta and Brown, 2017). Thus, knockout of MerTK alleviates gp120-induced pre-synaptic loss. On contrary, post-synaptic compartments may be induced to present phosphatidylserine or other unknown "eat-me" signals that can activate multiple phagocytotic pathway by binding to different opsonin. In this case, the effects of MerTK deletion could be compensated by other phagocytotic pathways.

Overall, I have demonstrated the important roles of microglia and astrocytes in gp120-induced synaptic degeneration. The glial cells-mediated phagocytosis may contribute to the synapse elimination caused by gp120. My results show that the MerTK pathway is implicated in the microglial phagocytosis of pre-synaptic terminals, and that the FKN/CX3CR1 pathway plays an important role in regulating microglial activation and their activity in the synapse phagocytosis. The expression of FKN is regulated by neuronal wnt3a/β-catenin pathway. Current research has mainly been focused on the potential roles of HIV-induced inflammation or excitotoxicity in neuronal damages and synapse loss. Results from this study provide novel insights into the pathogenic mechanisms of HIV-associated synaptic degeneration by revealing a critical contribution of glial phagocytosis. The new knowledge may help improve our understanding of the pathogenesis HIV-associated neurological complications such as HAND and chronic pain in HIV patients.

6.2 FUTURE DIRECTIONS

Many important questions about gp120-induced glial phagocytosis of synapses remain. For example, how does gp120 induce astrocytes, non-professional phagocytes, to gain phagocytotic ability? If not MerTK, what are the signaling pathways that control gp120-induced astrocytic phagocytosis? Since the microglial activation is dynamic and heterogenous over the course of neurodegeneration (Mathys et al., 2017; Furube et al., 2018), do microglia show region-dependent heterogeneity and temporal difference during the gp120-induced synaptic degeneration? How are microglial and astrocytic phagocytosis coordinated during gp120-stimulated synapse elimination?

One important problem that remains to be solved is to determine the signaling pathways that regulate the phagocytotic activity of astrocytes. Astrocytes can be activated to an A1 neuroinflammatory reactive state or an A2 immunosuppressive reactive state (Liddelow and Barres, 2017). It would be interesting to determine if gp120 induces A1-like or A2-like reactive astrocytes. C3 is a specific marker for A1 astrocytes, while Emp1 for A2 astrocytes (Liddelow et al., 2017; Clarke et al., 2018). Immunofluorescent straining and/or *in situ* hybridization of these markers can be used to visualize A1 or A2 astrocytes in gp120Tg cortices. In addition, triple immunofluorescent staining (GFAP, PSD95 and C3/ Emp1) could be used to identify if posts-synaptic terminal is specifically engulfed and eliminated by A1-like or A2-like astrocytes. Recent studies suggest that STAT3 mediates A2 reactive astrocytes polarization (Anderson et al., 2016), whereas NF-κB (nuclear factor kappalight-chain-enhancer of activated B cells) signaling induces A1 neuroinflammatory reactive astrocytes (Lian et al., 2015; Liddelow et al., 2017). My preliminary studies indicated that STAT3 in astrocytes was up-regulated in gp120Tg mice (Fig. 6.2). It is meaningful to determine if STAT3 is a pathway that regulates astrocytic

phagocytosis, which has not been reported yet. One potentially informative study is to test if disruption of the STAT3 pathway alters the profiles of reactive astrocytes (ratio of A1 and A2 in total astrocytes), and determine if STAT3 deletion attenuates gp120-induced synaptic degeneration.

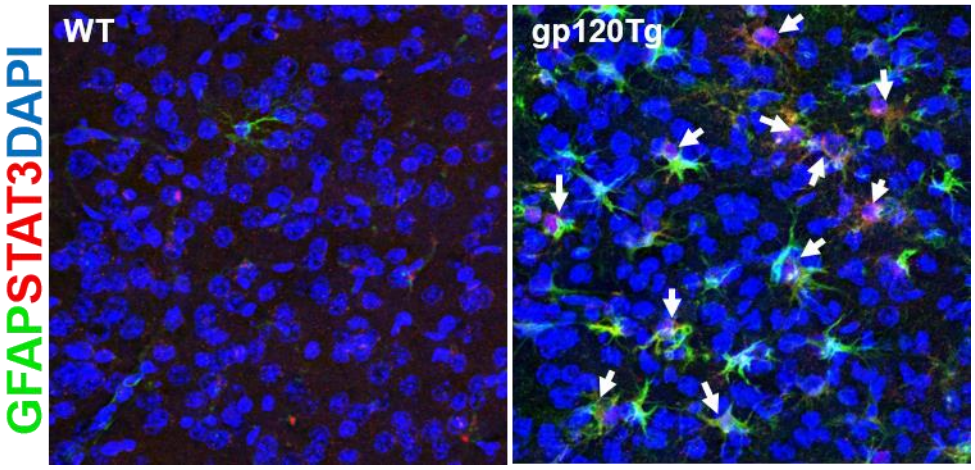

Fig 6. 2 The expression pattern of STAT3 in the frontal cortex of WT and gp120 Tg mouse.

Proteomic analysis of isolated astrocytes by laser capture microdissection (LCM)-mass spectrometry (MS) (Mukherjee et al., 2013) may helpful to identify novel phagocytotic pathways activated by gp120. Cortical sections from WT and gp120 Tg mice can be double-stained for GFAP and PSD95, and astrocytes with or without PSD95 clumps from gp120Tg mice are captured using LCM techniques. Mass spectrometry (MS) analysis of the captured cells would generate protein profiles of specific cell populations. Data mining of the protein profiles may reveal the up- or down-regulation of proteins in specific phagocytotic pathways. Single cell transcriptome analysis (scRNA-seq) (Macosko et al., 2015; Potter, 2018) is potentially another powerful approach to elucidate the novel phagocytotic pathways. Transcriptome profile of individual astrocytes from WT and gp120Tg mice will provide information about how gp120 influence astrocytes. Therefore,

scRNA-seq combined with LCM-MS hopefully will provide insights about the activated phagocytic pathway in astrocyte in gp120 Tg. Then the phagocytic pathway that regulates astrocytes in gp120 Tg mice could be validated by further pathway manipulation.

Another direction could be to examine and compare the phenotypic heterogeneity of microglial cells in the WT and gp120 Tg mice. Using single-cell RNA sequencing, transcriptome profiles of individual microglial cells isolated from the cortex of WT mice and of gp120 Tg mice at multiple time points during the synaptic degeneration could be obtained. Those transcriptome profile could be used to identify disease-specific and stage-specific microglial subtype and activated states. Moreover, these transcriptome profiles also could be used to identify novel phagocytotic pathways that regulate microglial activity to eliminate gp120-damaged synapse. In addition, phenotypic heterogeneity of microglial cells in the cortex of gp120Tg mice and in the spinal cord of i.t.-gp120 mice can be compared by scRNA-seq. The region-dependent heterogeneity and model- specific microglia subtype could be identified. This study will also be helpful to understand the opposite effects of CX3CR1 knockout on gp120-induced synapse loss in spinal pain circuit and in the frontal cortex of brain.

How are microglia and astrocytes coordinated during gp120-induced synaptic degeneration? Regulation of astrocytes by microglia has been suggested by recent studies. Liddelow et al. showed neuroinflammatory microglia regulated the induction of A1 astrocytes by secreting Il-1α, TNF and C1q (Liddelow et al., 2017). Another group found microglia-derived cytokines could transform astrocytes to A2 phenotype by down-regulating astrocyte-specific P2Y1 receptor P2Y1 (Shinozaki et al., 2017). Therefore, it would be interesting to examine how microglial ablation would affect astrocytic activation

and phagocytosis of synapses. Since PLX5622 can almost completely deplete microglia in the cortex after 3-weeks of administration (Fig. 4.5), WT and gp120Tg mice after PLX5622-induced microglia depletion can be used to measure the effects on total astrocytes, A1 or A2 populations by immunostaining of GFAP, C3 or Emp1, respectively. In addition, double-staining of GFAP and PSD-95 could be performed to determine if microglial ablation affects astrocytic phagocytosis of post-synaptic components. Astrocyte also regulate microglial activity. Bialas and Stevens demonstrated that astrocyte was essential for microglial phagocytosis of synapse by controlling the expression of C1q at synapses (Bialas and Stevens, 2013). Thus, it would be informative to investigate how astrocyte ablation would affect microglial activity and synapse elimination. Gancyclovir (GCV) can deplete reactive astrocytes in GFAP-TK transgenic mice (Bush et al., 1998). Gp120/GFAP-TK double transgenic mice can be generated to determine the effect of GCV administration on the microglial activation (by IBa1 staining) and pre-synaptic density (by vGluT1 staining).

REFERENCES

Acharya MM, Green KN, Allen BD, Najafi AR, Syage A, Minasyan H, Le MT, Kawashita T, Giedzinski E, Parihar VK, West BL, Baulch JE, Limoli CL (2016) Elimination of microglia improves cognitive function following cranial irradiation. Scientific Reports 6:31545.

Adle-Biassette H, Levy Y, Colombel M, Poron F, Natchev S, Keohane C, Gray F (1995) Neuronal apoptosis in HIV infection in adults. Neuropathol Appl Neurobiol 21:218-227.

Adle-Biassette H, Chrétien F, Wingertsmann L, Héry C, Ereau T, Scaravilli F, Tardieu M, Gray F (1999) Neuronal apoptosis does not correlate with dementia in HIV infection but is related to microglial activation and axonal damage. Neuropathol Appl Neurobiol 25:123-133.

Aksenov MY, Hasselrot U, Bansal AK, Wu G, Nath A, Anderson C, Mactutus CF, Booze RM (2001) Oxidative damage induced by the injection of HIV-1 Tat protein in the rat striatum. Neurosci Lett 305:5-8.

Al-Ali SY, Al-Zuhair AG, Dawod B (1988) Ultrastructural study of phagocytic activities of young astrocytes in injured neonatal rat brain following intracerebral injection of colloidal carbon. Glia 1:211-218.

Albrecht D, López-Murcia FJ, Pérez-González AP, Lichtner G, Solsona C, Llobet A (2012) SPARC prevents maturation of cholinergic presynaptic terminals. Mol Cell Neurosci 49:364-374.

Alkhatib G, Combadiere C, Broder CC, Feng Y, Kennedy PE, Murphy PM, Berger EA (1996) CC CKR5: a RANTES, MIP-1alpha, MIP-1beta receptor as a fusion cofactor for macrophage-tropic HIV-1. Science 272:1955-1958.

Allen NJ (2014) Astrocyte regulation of synaptic behavior. Annu Rev Cell Dev Biol 30:439-463.

Allen NJ, Eroglu C (2017) Cell Biology of Astrocyte-Synapse Interactions. Neuron 96:697-708.

An SF, Ciardi A, Giometto B, Scaravilli T, Gray F, Scaravilli F (1996) Investigation on the expression of major histocompatibility complex class II and cytokines and

detection of HIV-1 DNA within brains of asymptomatic and symptomatic HIV-1-positive patients. Acta Neuropathol 91:494-503.

Anders KH, Guerra WF, Tomiyasu U, Verity MA, Vinters HV (1986) The neuropathology of AIDS. UCLA experience and review. Am J Pathol 124:537-558.

Anderson MA, Burda JE, Ren Y, Ao Y, O'Shea TM, Kawaguchi R, Coppola G, Khakh BS, Deming TJ, Sofroniew MV (2016) Astrocyte scar formation aids central nervous system axon regeneration. Nature 532:195-200.

Antinori A et al. (2007) Updated research nosology for HIV-associated neurocognitive disorders. Neurology 69:1789-1799.

Araque A, Parpura V, Sanzgiri RP, Haydon PG (1999) Tripartite synapses: glia, the unacknowledged partner. Trends Neurosci 22:208-215.

Araque A, Carmignoto G, Haydon PG, Oliet SH, Robitaille R, Volterra A (2014) Gliotransmitters travel in time and space. Neuron 81:728-739.

Argyris EG, Acheampong E, Nunnari G, Mukhtar M, Williams KJ, Pomerantz RJ (2003) Human immunodeficiency virus type 1 enters primary human brain microvascular endothelial cells by a mechanism involving cell surface proteoglycans independent of lipid rafts. J Virol 77:12140-12151.

Bachis A, Major EO, Mocchetti I (2003) Brain-derived neurotrophic factor inhibits human immunodeficiency virus-1/gp120-mediated cerebellar granule cell death by preventing gp120 internalization. J Neurosci 23:5715-5722.

Bachstetter AD, Morganti JM, Jernberg J, Schlunk A, Mitchell SH, Brewster KW, Hudson CE, Cole MJ, Harrison JK, Bickford PC, Gemma C (2011) Fractalkine and CX 3 CR1 regulate hippocampal neurogenesis in adult and aged rats. Neurobiol Aging 32:2030-2044.

Bambrick L, Kristian T, Fiskum G (2004) Astrocyte mitochondrial mechanisms of ischemic brain injury and neuroprotection. Neurochem Res 29:601-608.

Bandaru VV, McArthur JC, Sacktor N, Cutler RG, Knapp EL, Mattson MP, Haughey NJ (2007) Associative and predictive biomarkers of dementia in HIV-1-infected patients. Neurology 68:1481-1487.

Beattie EC, Stellwagen D, Morishita W, Bresnahan JC, Ha BK, Von Zastrow M, Beattie MS, Malenka RC (2002) Control of synaptic strength by glial TNFalpha. Science 295:2282-2285.

Bennett ML, Bennett FC, Liddelow SA, Ajami B, Zamanian JL, Fernhoff NB, Mulinyawe SB, Bohlen CJ, Adil A, Tucker A, Weissman IL, Chang EF, Li G, Grant GA, Hayden Gephart MG, Barres BA (2016) New tools for studying microglia in the mouse and human CNS. Proc Natl Acad Sci U S A 113:E1738-1746.

Bialas AR, Stevens B (2013) TGF-β signaling regulates neuronal C1q expression and developmental synaptic refinement. Nat Neurosci 16:1773-1782.

Blomster LV, Vukovic J, Hendrickx DA, Jung S, Harvey AR, Filgueira L, Ruitenberg MJ (2011) CX_3CR1 deficiency exacerbates neuronal loss and impairs early regenerative responses in the target-ablated olfactory epithelium. Mol Cell Neurosci 48:236-245.

Bobardt MD, Salmon P, Wang L, Esko JD, Gabuzda D, Fiala M, Trono D, Van der Schueren B, David G, Gallay PA (2004) Contribution of proteoglycans to human immunodeficiency virus type 1 brain invasion. J Virol 78:6567-6584.

Boche D, Perry VH, Nicoll JA (2013) Review: activation patterns of microglia and their identification in the human brain. Neuropathol Appl Neurobiol 39:3-18.

Bokhari SM, Yao H, Bethel-Brown C, Fuwang P, Williams R, Dhillon NK, Hegde R, Kumar A, Buch SJ (2009) Morphine enhances Tat-induced activation in murine microglia. J Neurovirol 15:219-228.

Bokhari SM, Hegde R, Callen S, Yao H, Adany I, Li Q, Li Z, Pinson D, Yeh HW, Cheney PD, Buch S (2011) Morphine potentiates neuropathogenesis of SIV infection in rhesus macaques. J Neuroimmune Pharmacol 6:626-639.

Bomsel M (1997) Transcytosis of infectious human immunodeficiency virus across a tight human epithelial cell line barrier. Nat Med 3:42-47.

Boska MD, Dash PK, Knibbe J, Epstein AA, Akhter SP, Fields N, High R, Makarov E, Bonasera S, Gelbard HA, Poluektova LY, Gendelman HE, Gorantla S (2014) Associations between brain microstructures, metabolites, and cognitive deficits during chronic HIV-1 infection of humanized mice. Mol Neurodegener 9:58.

Bozzette SA, Santangelo J, Villasana D, Fraser A, Wright B, Jacobsen C, Hayden E, Schnack J, Spector SA, Richman DD (1991) Peripheral nerve function in persons with asymptomatic or minimally symptomatic HIV disease: absence of zidovudine neurotoxicity. J Acquir Immune Defic Syndr 4:851-855.

Brabers NA, Nottet HS (2006) Role of the pro-inflammatory cytokines TNF-alpha and IL-1beta in HIV-associated dementia. Eur J Clin Invest 36:447-458.

Brew BJ, Rosenblum M, Cronin K, Price RW (1995) AIDS dementia complex and HIV-1 brain infection: clinical-virological correlations. Ann Neurol 38:563-570.

Brown GC, Neher JJ (2014) Microglial phagocytosis of live neurons. Nat Rev Neurosci 15:209-216.

Bruce-Keller AJ, Turchan-Cholewo J, Smart EJ, Geurin T, Chauhan A, Reid R, Xu R, Nath A, Knapp PE, Hauser KF (2008) Morphine causes rapid increases in glial activation and neuronal injury in the striatum of inducible HIV-1 Tat transgenic mice. Glia 56:1414-1427.

Buch S, Pinson D, Hou Y, Adany I, Li Z, Mukherjee S, Jia F, Mackay G, Silverstein P, Kumar A, Narayan O (2000) Neuropathogenesis of chimeric simian human immunodeficiency virus infection in rhesus macaques. J Med Primatol 29:96-106.

Buch SJ, Villinger F, Pinson D, Hou Y, Adany I, Li Z, Dalal R, Raghavan R, Kumar A, Narayan O (2002) Innate differences between simian-human immunodeficiency virus (SHIV)(KU-2)-infected rhesus and pig-tailed macaques in development of neurological disease. Virology 295:54-62.

Budka H (1986) Multinucleated giant cells in brain: a hallmark of the acquired immune deficiency syndrome (AIDS). Acta Neuropathol 69:253-258.

Budka H (1991) Neuropathology of human immunodeficiency virus infection. Brain Pathol 1:163-175.

Bush TG, Savidge TC, Freeman TC, Cox HJ, Campbell EA, Mucke L, Johnson MH, Sofroniew MV (1998) Fulminant jejuno-ileitis following ablation of enteric glia in adult transgenic mice. Cell 93:189-201.

Caberoy NB, Alvarado G, Bigcas JL, Li W (2012) Galectin-3 is a new MerTK-specific eat-me signal. J Cell Physiol 227:401-407.

Cadwell CR, Palasantza A, Jiang X, Berens P, Deng Q, Yilmaz M, Reimer J, Shen S, Bethge M, Tolias KF, Sandberg R, Tolias AS (2016) Electrophysiological, transcriptomic and morphologic profiling of single neurons using Patch-seq. Nat Biotechnol 34:199-203.

Cahoy JD, Emery B, Kaushal A, Foo LC, Zamanian JL, Christopherson KS, Xing Y, Lubischer JL, Krieg PA, Krupenko SA, Thompson WJ, Barres BA (2008) A transcriptome database for astrocytes, neurons, and oligodendrocytes: a new resource for understanding brain development and function. J Neurosci 28:264-278.

Cailhier JF, Partolina M, Vuthoori S, Wu S, Ko K, Watson S, Savill J, Hughes J, Lang RA (2005) Conditional macrophage ablation demonstrates that resident macrophages initiate acute peritoneal inflammation. J Immunol 174:2336-2342.

Callahan BL, Gil AS, Levesque A, Mogil JS (2008) Modulation of mechanical and thermal nociceptive sensitivity in the laboratory mouse by behavioral state. J Pain 9:174-184.

Cardona AE, Pioro EP, Sasse ME, Kostenko V, Cardona SM, Dijkstra IM, Huang D, Kidd G, Dombrowski S, Dutta R, Lee JC, Cook DN, Jung S, Lira SA, Littman DR, Ransohoff RM (2006) Control of microglial neurotoxicity by the fractalkine receptor. Nat Neurosci 9:917-924.

Carey AN, Sypek EI, Singh HD, Kaufman MJ, McLaughlin JP (2012) Expression of HIV-Tat protein is associated with learning and memory deficits in the mouse. Behav Brain Res 229:48-56.

Carne CA, Tedder RS, Smith A, Sutherland S, Elkington SG, Daly HM, Preston FE, Craske J (1985) Acute encephalopathy coincident with seroconversion for anti-HTLV-III. Lancet 2:1206-1208.

Carr A, Miller J, Law M, Cooper DA (2000) A syndrome of lipoatrophy, lactic acidaemia and liver dysfunction associated with HIV nucleoside analogue therapy: contribution to protease inhibitor-related lipodystrophy syndrome. AIDS 14:F25-32.

Carr A, Samaras K, Burton S, Law M, Freund J, Chisholm DJ, Cooper DA (1998) A syndrome of peripheral lipodystrophy, hyperlipidaemia and insulin resistance in patients receiving HIV protease inhibitors. AIDS 12:F51-58.

Catani MV, Corasaniti MT, Navarra M, Nisticò G, Finazzi-Agrò A, Melino G (2000) gp120 induces cell death in human neuroblastoma cells through the CXCR4 and CCR5 chemokine receptors. J Neurochem 74:2373-2379.

Cenker JJ, Stultz RD, McDonald D (2017) Brain Microglial Cells Are Highly Susceptible to HIV-1 Infection and Spread. AIDS Res Hum Retroviruses 33:1155-1165.

Chapman GA, Moores K, Harrison D, Campbell CA, Stewart BR, Strijbos PJ (2000) Fractalkine cleavage from neuronal membranes represents an acute event in the inflammatory response to excitotoxic brain damage. J Neurosci 20:RC87.

Chen J, Carey K, Godowski PJ (1997) Identification of Gas6 as a ligand for Mer, a neural cell adhesion molecule related receptor tyrosine kinase implicated in cellular transformation. Oncogene 14:2033-2039.

Chen J, Park CS, Tang SJ (2006) Activity-dependent synaptic Wnt release regulates hippocampal long term potentiation. J Biol Chem 281:11910-11916.

Cheng HW, Jiang T, Brown SA, Pasinetti GM, Finch CE, McNeill TH (1994) Response of striatal astrocytes to neuronal deafferentation: an immunocytochemical and ultrastructural study. Neuroscience 62:425-439.

Cherner M, Masliah E, Ellis RJ, Marcotte TD, Moore DJ, Grant I, Heaton RK (2002) Neurocognitive dysfunction predicts postmortem findings of HIV encephalitis. Neurology 59:1563-1567.

Cho SH, Sun B, Zhou Y, Kauppinen TM, Halabisky B, Wes P, Ransohoff RM, Gan L (2011) CX3CR1 protein signaling modulates microglial activation and protects against plaque-independent cognitive deficits in a mouse model of Alzheimer disease. J Biol Chem 286:32713-32722.

Choe H, Farzan M, Sun Y, Sullivan N, Rollins B, Ponath PD, Wu L, Mackay CR, LaRosa G, Newman W, Gerard N, Gerard C, Sodroski J (1996) The beta-chemokine receptors CCR3 and CCR5 facilitate infection by primary HIV-1 isolates. Cell 85:1135-1148.

Choi DW (1992) Excitotoxic cell death. J Neurobiol 23:1261-1276.

Chompre G, Cruz E, Maldonado L, Rivera-Amill V, Porter JT, Noel RJ (2013) Astrocytic expression of HIV-1 Nef impairs spatial and recognition memory. Neurobiol Dis 49:128-136.

Christopherson KS, Ullian EM, Stokes CC, Mullowney CE, Hell JW, Agah A, Lawler J, Mosher DF, Bornstein P, Barres BA (2005) Thrombospondins are astrocyte-secreted proteins that promote CNS synaptogenesis. Cell 120:421-433.

Chung WS, Allen NJ, Eroglu C (2015a) Astrocytes Control Synapse Formation, Function, and Elimination. Cold Spring Harb Perspect Biol 7:a020370.

Chung WS, Welsh CA, Barres BA, Stevens B (2015b) Do glia drive synaptic and cognitive impairment in disease? Nat Neurosci 18:1539-1545.

Chung WS, Welsh CA, Barres BA, Stevens B (2015c) Do glia drive synaptic and cognitive impairment in disease? Nat Neurosci 18:1539-1545.

Chung WS, Verghese PB, Chakraborty C, Joung J, Hyman BT, Ulrich JD, Holtzman DM, Barres BA (2016) Novel allele-dependent role for APOE in controlling the rate of synapse pruning by astrocytes. Proc Natl Acad Sci U S A 113:10186-10191.

Chung WS, Clarke LE, Wang GX, Stafford BK, Sher A, Chakraborty C, Joung J, Foo LC, Thompson A, Chen C, Smith SJ, Barres BA (2013) Astrocytes mediate synapse elimination through MEGF10 and MERTK pathways. Nature 504:394-400.

Churchill MJ, Gorry PR, Cowley D, Lal L, Sonza S, Purcell DF, Thompson KA, Gabuzda D, McArthur JC, Pardo CA, Wesselingh SL (2006) Use of laser capture microdissection to detect integrated HIV-1 DNA in macrophages and astrocytes from autopsy brain tissues. J Neurovirol 12:146-152.

Cinque P, Brew BJ, Gisslen M, Hagberg L, Price RW (2007) Cerebrospinal fluid markers in central nervous system HIV infection and AIDS dementia complex. Handb Clin Neurol 85:261-300.

Clarke LE, Liddelow SA, Chakraborty C, Münch AE, Heiman M, Barres BA (2018) Normal aging induces A1-like astrocyte reactivity. Proc Natl Acad Sci U S A 115:E1896-E1905.

Colton CA (2009) Heterogeneity of microglial activation in the innate immune response in the brain. J Neuroimmune Pharmacol 4:399-418.

Conant K, Tornatore C, Atwood W, Meyers K, Traub R, Major EO (1994) In vivo and in vitro infection of the astrocyte by HIV-1. Adv Neuroimmunol 4:287-289.

Cook DN, Chen SC, Sullivan LM, Manfra DJ, Wiekowski MT, Prosser DM, Vassileva G, Lira SA (2001) Generation and analysis of mice lacking the chemokine fractalkine. Mol Cell Biol 21:3159-3165.

Cook-Easterwood J, Middaugh LD, Griffin WC, Khan I, Tyor WR (2007) Highly active antiretroviral therapy of cognitive dysfunction and neuronal abnormalities in SCID mice with HIV encephalitis. Exp Neurol 205:506-512.

Cornblath DR, McArthur JC (1988) Predominantly sensory neuropathy in patients with AIDS and AIDS-related complex. Neurology 38:794-796.

Cotter R, Williams C, Ryan L, Erichsen D, Lopez A, Peng H, Zheng J (2002) Fractalkine (CX3CL1) and brain inflammation: Implications for HIV-1-associated dementia. J Neurovirol 8:585-598.

Coulter DA, Eid T (2012) Astrocytic regulation of glutamate homeostasis in epilepsy. Glia 60:1215-1226.

D'hooge R, Franck F, Mucke L, De Deyn PP (1999) Age-related behavioural deficits in transgenic mice expressing the HIV-1 coat protein gp120. Eur J Neurosci 11:4398-4402.

Dagher NN, Najafi AR, Kayala KM, Elmore MR, White TE, Medeiros R, West BL, Green KN (2015) Colony-stimulating factor 1 receptor inhibition prevents microglial plaque association and improves cognition in 3xTg-AD mice. J Neuroinflammation 12:139.

Dalakas MC, Illa I, Pezeshkpour GH, Laukaitis JP, Cohen B, Griffin JL (1990) Mitochondrial myopathy caused by long-term zidovudine therapy. N Engl J Med 322:1098-1105.

Dash PK, Gorantla S, Gendelman HE, Knibbe J, Casale GP, Makarov E, Epstein AA, Gelbard HA, Boska MD, Poluektova LY (2011) Loss of neuronal integrity during progressive HIV-1 infection of humanized mice. J Neurosci 31:3148-3157.

David Y, Cacheaux LP, Ivens S, Lapilover E, Heinemann U, Kaufer D, Friedman A (2009) Astrocytic dysfunction in epileptogenesis: consequence of altered potassium and glutamate homeostasis? J Neurosci 29:10588-10599.

Denning DW, Anderson J, Rudge P, Smith H (1987) Acute myelopathy associated with primary infection with human immunodeficiency virus. Br Med J (Clin Res Ed) 294:143-144.

Deshmane SL, Kremlev S, Amini S, Sawaya BE (2009) Monocyte chemoattractant protein-1 (MCP-1): an overview. J Interferon Cytokine Res 29:313-326.

Di Rocco A, Simpson DM (1998) AIDS-associated vacuolar myelopathy. AIDS Patient Care STDS 12:457-461.

Dragic T, Litwin V, Allaway GP, Martin SR, Huang Y, Nagashima KA, Cayanan C, Maddon PJ, Koup RA, Moore JP, Paxton WA (1996) HIV-1 entry into CD4+ cells is mediated by the chemokine receptor CC-CKR-5. Nature 381:667-673.

Dransfield I, Zagórska A, Lew ED, Michail K, Lemke G (2015) Mer receptor tyrosine kinase mediates both tethering and phagocytosis of apoptotic cells. Cell Death Dis 6:e1646.

Dreyer EB, Lipton SA (1995) The coat protein gp120 of HIV-1 inhibits astrocyte uptake of excitatory amino acids via macrophage arachidonic acid. Eur J Neurosci 7:2502-2507.

Duffield JS, Forbes SJ, Constandinou CM, Clay S, Partolina M, Vuthoori S, Wu S, Lang R, Iredale JP (2005) Selective depletion of macrophages reveals distinct, opposing roles during liver injury and repair. J Clin Invest 115:56-65.

Dénes Á, Ferenczi S, Halász J, Környei Z, Kovács KJ (2008) Role of CX3CR1 (fractalkine receptor) in brain damage and inflammation induced by focal cerebral ischemia in mouse. Journal of Cerebral Blood Flow & Metabolism 28:1707-1721.

Edwards JP, Zhang X, Frauwirth KA, Mosser DM (2006) Biochemical and functional characterization of three activated macrophage populations. J Leukoc Biol 80:1298-1307.

Ellis R, Langford D, Masliah E (2007) HIV and antiretroviral therapy in the brain: neuronal injury and repair. Nature Reviews Neuroscience 8:33-44.

Ellis RJ, Calero P, Stockin MD (2009) HIV infection and the central nervous system: a primer. Neuropsychol Rev 19:144-151.

Erichsen D, Lopez AL, Peng H, Niemann D, Williams C, Bauer M, Morgello S, Cotter RL, Ryan LA, Ghorpade A, Gendelman HE, Zheng J (2003) Neuronal injury regulates fractalkine: relevance for HIV-1 associated dementia. J Neuroimmunol 138:144-155.

Eroglu C, Allen NJ, Susman MW, O'Rourke NA, Park CY, Ozkan E, Chakraborty C, Mulinyawe SB, Annis DS, Huberman AD, Green EM, Lawler J, Dolmetsch R, Garcia KC, Smith SJ, Luo ZD, Rosenthal A, Mosher DF, Barres BA (2009) Gabapentin receptor alpha2delta-1 is a neuronal thrombospondin receptor responsible for excitatory CNS synaptogenesis. Cell 139:380-392.

Eugenin EA, Berman JW (2007) Gap junctions mediate human immunodeficiency virus-bystander killing in astrocytes. J Neurosci 27:12844-12850.

Eugenin EA, Clements JE, Zink MC, Berman JW (2011) Human immunodeficiency virus infection of human astrocytes disrupts blood-brain barrier integrity by a gap junction-dependent mechanism. J Neurosci 31:9456-9465.

Everall IP, Heaton RK, Marcotte TD, Ellis RJ, McCutchan JA, Atkinson JH, Grant I, Mallory M, Masliah E (1999) Cortical synaptic density is reduced in mild to moderate human immunodeficiency virus neurocognitive disorder. HNRC Group. HIV Neurobehavioral Research Center. Brain Pathol 9:209-217.

Farhy-Tselnicker I, Allen NJ (2018) Astrocytes, neurons, synapses: a tripartite view on cortical circuit development. Neural Dev 13:7.

Febinger HY, Thomasy HE, Pavlova MN, Ringgold KM, Barf PR, George AM, Grillo JN, Bachstetter AD, Garcia JA, Cardona AE, Opp MR, Gemma C (2015) Time-dependent effects of CX3CR1 in a mouse model of mild traumatic brain injury. J Neuroinflammation 12:154.

Feng Y, Broder CC, Kennedy PE, Berger EA (1996) HIV-1 entry cofactor: functional cDNA cloning of a seven-transmembrane, G protein-coupled receptor. Science 272:872-877.

Fitting S, Xu R, Bull C, Buch SK, El-Hage N, Nath A, Knapp PE, Hauser KF (2010) Interactive comorbidity between opioid drug abuse and HIV-1 Tat: chronic

exposure augments spine loss and sublethal dendritic pathology in striatal neurons. Am J Pathol 177:1397-1410.

Fitting S, Ignatowska-Jankowska BM, Bull C, Skoff RP, Lichtman AH, Wise LE, Fox MA, Su J, Medina AE, Krahe TE, Knapp PE, Guido W, Hauser KF (2013) Synaptic dysfunction in the hippocampus accompanies learning and memory deficits in human immunodeficiency virus type-1 Tat transgenic mice. Biol Psychiatry 73:443-453.

Fontana G, Valenti L, Raiteri M (1997) Gp120 can revert antagonism at the glycine site of NMDA receptors mediating GABA release from cultured hippocampal neurons. J Neurosci Res 49:732-738.

Fourgeaud L, Través PG, Tufail Y, Leal-Bailey H, Lew ED, Burrola PG, Callaway P, Zagórska A, Rothlin CV, Nimmerjahn A, Lemke G (2016) TAM receptors regulate multiple features of microglial physiology. Nature 532:240-244.

Foussat A, Bouchet-Delbos L, Berrebi D, Durand-Gasselin I, Coulomb-L'Hermine A, Krzysiek R, Galanaud P, Levy Y, Emilie D (2001) Deregulation of the expression of the fractalkine/fractalkine receptor complex in HIV-1-infected patients. Blood 98:1678-1686.

Fox HS (2008) Virus-host interaction in the simian immunodeficiency virus-infected brain. J Neurovirol 14:286-291.

Fricker M, Neher JJ, Zhao JW, Théry C, Tolkovsky AM, Brown GC (2012) MFG-E8 mediates primary phagocytosis of viable neurons during neuroinflammation. J Neurosci 32:2657-2666.

Fuhrmann M, Bittner T, Jung CK, Burgold S, Page RM, Mitteregger G, Haass C, LaFerla FM, Kretzschmar H, Herms J (2010) Microglial Cx3cr1 knockout prevents neuron loss in a mouse model of Alzheimer's disease. Nat Neurosci 13:411-413.

Furube E, Kawai S, Inagaki H, Takagi S, Miyata S (2018) Brain Region-dependent Heterogeneity and Dose-dependent Difference in Transient Microglia Population Increase during Lipopolysaccharide-induced Inflammation. Sci Rep 8:2203.

Galli S, Lopes DM, Ammari R, Kopra J, Millar SE, Gibb A, Salinas PC (2014) Deficient Wnt signalling triggers striatal synaptic degeneration and impaired motor behaviour in adult mice. Nat Commun 5:4992.

Garden GA (2002) Microglia in human immunodeficiency virus-associated neurodegeneration. Glia 40:240-251.

Garden GA, Guo W, Jayadev S, Tun C, Balcaitis S, Choi J, Montine TJ, Möller T, Morrison RS (2004) HIV associated neurodegeneration requires p53 in neurons and microglia. FASEB J 18:1141-1143.

Garden GA, Budd SL, Tsai E, Hanson L, Kaul M, D'Emilia DM, Friedlander RM, Yuan J, Masliah E, Lipton SA (2002) Caspase cascades in human immunodeficiency virus-associated neurodegeneration. J Neurosci 22:4015-4024.

Gelman BB (1993) Diffuse microgliosis associated with cerebral atrophy in the acquired immunodeficiency syndrome. Ann Neurol 34:65-70.

Gendelman HE (2012) The neurology of AIDS, 3rd Edition. Oxford: Oxford University Press.

Gisslén M, Rosengren L, Hagberg L, Deeks SG, Price RW (2005) Cerebrospinal fluid signs of neuronal damage after antiretroviral treatment interruption in HIV-1 infection. AIDS Res Ther 2:6.

Giulian D, Vaca K, Noonan CA (1990) Secretion of neurotoxins by mononuclear phagocytes infected with HIV-1. Science 250:1593-1596.

Goffinet C, Allespach I, Keppler OT (2007) HIV-susceptible transgenic rats allow rapid preclinical testing of antiviral compounds targeting virus entry or reverse transcription. Proc Natl Acad Sci U S A 104:1015-1020.

Gold LH, Fox HS, Henriksen SJ, Buchmeier MJ, Weed MR, Taffe MA, Huitrón-Resendiz S, Horn TF, Bloom FE (1998) Longitudinal analysis of behavioral, neurophysiological, viral and immunological effects of SIV infection in rhesus monkeys. J Med Primatol 27:104-112.

Gong G, Hu L, Qin F, Yin L, Yi X, Yuan L, Wu W (2016) Spinal WNT pathway contributes to remifentanil induced hyperalgesia through regulating fractalkine and CX3CR1 in rats. Neurosci Lett 633:21-27.

Gorantla S, Makarov E, Finke-Dwyer J, Castanedo A, Holguin A, Gebhart CL, Gendelman HE, Poluektova L (2010) Links between progressive HIV-1 infection of humanized mice and viral neuropathogenesis. Am J Pathol 177:2938-2949.

Gorry P, Purcell D, Howard J, McPhee D (1998) Restricted HIV-1 infection of human astrocytes: potential role of nef in the regulation of virus replication. J Neurovirol 4:377-386.

Gorry PR, Ong C, Thorpe J, Bannwarth S, Thompson KA, Gatignol A, Vesselingh SL, Purcell DF (2003) Astrocyte infection by HIV-1: mechanisms of restricted virus replication, and role in the pathogenesis of HIV-1-associated dementia. Curr HIV Res 1:463-473.

Gorry PR, Bristol G, Zack JA, Ritola K, Swanstrom R, Birch CJ, Bell JE, Bannert N, Crawford K, Wang H, Schols D, De Clercq E, Kunstman K, Wolinsky SM, Gabuzda D (2001) Macrophage tropism of human immunodeficiency virus type 1 isolates from brain and lymphoid tissues predicts neurotropism independent of coreceptor specificity. J Virol 75:10073-10089.

Grant I, Atkinson JH, Hesselink JR, Kennedy CJ, Richman DD, Spector SA, McCutchan JA (1987) Evidence for early central nervous system involvement in the acquired immunodeficiency syndrome (AIDS) and other human immunodeficiency virus (HIV) infections. Studies with neuropsychologic testing and magnetic resonance imaging. Ann Intern Med 107:828-836.

Gray F, Chimelli L, Mohr M, Clavelou P, Scaravilli F, Poirier J (1991a) Fulminating multiple sclerosis-like leukoencephalopathy revealing human immunodeficiency virus infection. Neurology 41:105-109.

Gray F, Geny C, Lionnet F, Dournon E, Fenelon G, Gherardi R, Poirier J (1991b) [Neuropathologic study of 135 adult cases of acquired immunodeficiency syndrome (AIDS)]. Ann Pathol 11:236-247.

Gray F, Lescs MC, Keohane C, Paraire F, Marc B, Durigon M, Gherardi R (1992) Early brain changes in HIV infection: neuropathological study of 11 HIV seropositive, non-AIDS cases. J Neuropathol Exp Neurol 51:177-185.

Gray F, Scaravilli F, Everall I, Chretien F, An S, Boche D, Adle-Biassette H, Wingertsmann L, Durigon M, Hurtrel B, Chiodi F, Bell J, Lantos P (1996) Neuropathology of early HIV-1 infection. Brain Pathol 6:1-15.

Gray L, Roche M, Churchill MJ, Sterjovski J, Ellett A, Poumbourios P, Sherieff S, Sheffief S, Wang B, Saksena N, Purcell DF, Wesselingh S, Cunningham AL,

Brew BJ, Gabuzda D, Gorry PR (2009) Tissue-specific sequence alterations in the human immunodeficiency virus type 1 envelope favoring CCR5 usage contribute to persistence of dual-tropic virus in the brain. J Virol 83:5430-5441.

Grommes C, Lee CY, Wilkinson BL, Jiang Q, Koenigsknecht-Talboo JL, Varnum B, Landreth GE (2008) Regulation of microglial phagocytosis and inflammatory gene expression by Gas6 acting on the Axl/Mer family of tyrosine kinases. J Neuroimmune Pharmacol 3:130-140.

Haase AT (1986) Pathogenesis of lentivirus infections. Nature 322:130-136.

Haber M, Zhou L, Murai KK (2006) Cooperative astrocyte and dendritic spine dynamics at hippocampal excitatory synapses. J Neurosci 26:8881-8891.

Hadas E, Chao W, He H, Saini M, Daley E, Saifuddin M, Bentsman G, Ganz E, Volsky DJ, Potash MJ (2013) Transmission of chimeric HIV by mating in conventional mice: prevention by pre-exposure antiretroviral therapy and reduced susceptibility during estrus. Dis Model Mech 6:1292-1298.

Hafizi S, Dahlbäck B (2006) Gas6 and protein S. Vitamin K-dependent ligands for the Axl receptor tyrosine kinase subfamily. FEBS J 273:5231-5244.

Hagberg L, Fuchs D, Rosengren L, Gisslén M (2000) Intrathecal immune activation is associated with cerebrospinal fluid markers of neuronal destruction in AIDS patients. J Neuroimmunol 102:51-55.

Halassa MM, Fellin T, Takano H, Dong JH, Haydon PG (2007) Synaptic islands defined by the territory of a single astrocyte. J Neurosci 27:6473-6477.

Harbison C, Zhuang K, Gettie A, Blanchard J, Knight H, Didier P, Cheng-Mayer C, Westmoreland S (2014) Giant cell encephalitis and microglial infection with mucosally transmitted simian-human immunodeficiency virus SHIVSF162P3N in rhesus macaques. J Neurovirol 20:62-72.

Harrison JK, Jiang Y, Chen S, Xia Y, Maciejewski D, McNamara RK, Streit WJ, Salafranca MN, Adhikari S, Thompson DA, Botti P, Bacon KB, Feng L (1998) Role for neuronally derived fractalkine in mediating interactions between neurons and CX3CR1-expressing microglia. Proc Natl Acad Sci U S A 95:10896-10901.

Hatziioannou T, Evans DT (2012) Animal models for HIV/AIDS research. Nat Rev Microbiol 10:852-867.

Haughey NJ, Holden CP, Nath A, Geiger JD (1999) Involvement of inositol 1,4,5-trisphosphate-regulated stores of intracellular calcium in calcium dysregulation and neuron cell death caused by HIV-1 protein tat. J Neurochem 73:1363-1374.

Helke KL, Queen SE, Mankowski JL (2013) 14-3-3 Protein in CSF reflects SIV-mediated pre-synaptic damage. Curr HIV Res 11:281-287.

Hilla AM, Diekmann H, Fischer D (2017) Microglia Are Irrelevant for Neuronal Degeneration and Axon Regeneration after Acute Injury. The Journal of Neuroscience 37:6113-6124.

Ho DD, Sarngadharan MG, Resnick L, Dimarzoveronese F, Rota TR, Hirsch MS (1985) Primary human T-lymphotropic virus type III infection. Ann Intern Med 103:880-883.

Hochreiter-Hufford A, Ravichandran KS (2013) Clearing the dead: apoptotic cell sensing, recognition, engulfment, and digestion. Cold Spring Harb Perspect Biol 5:a008748.

Hollenbach R, Sagar D, Khan ZK, Callen S, Yao H, Shirazi J, Buch S, Jain P (2014) Effect of morphine and SIV on dendritic cell trafficking into the central nervous system of rhesus macaques. J Neurovirol 20:175-183.

Hong S, Dissing-Olesen L, Stevens B (2016a) New insights on the role of microglia in synaptic pruning in health and disease. Curr Opin Neurobiol 36:128-134.

Hong S, Beja-Glasser VF, Nfonoyim BM, Frouin A, Li S, Ramakrishnan S, Merry KM, Shi Q, Rosenthal A, Barres BA, Lemere CA, Selkoe DJ, Stevens B (2016b) Complement and microglia mediate early synapse loss in Alzheimer mouse models. Science 352:712-716.

Hong S, Beja-Glasser VF, Nfonoyim BM, Frouin A, Li S, Ramakrishnan S, Merry KM, Shi Q, Rosenthal A, Barres BA, Lemere CA, Selkoe DJ, Stevens B (2016c) Complement and microglia mediate early synapse loss in Alzheimer mouse models. Science 352:712-716.

Horn TF, Huitron-Resendiz S, Weed MR, Henriksen SJ, Fox HS (1998) Early physiological abnormalities after simian immunodeficiency virus infection. Proc Natl Acad Sci U S A 95:15072-15077.

Hoshiko M, Arnoux I, Avignone E, Yamamoto N, Audinat E (2012) Deficiency of the microglial receptor CX3CR1 impairs postnatal functional development of thalamocortical synapses in the barrel cortex. J Neurosci 32:15106-15111.

Iskander S, Walsh KA, Hammond RR (2004) Human CNS cultures exposed to HIV-1 gp120 reproduce dendritic injuries of HIV-1-associated dementia. J Neuroinflammation 1:7.

Ito D, Imai Y, Ohsawa K, Nakajima K, Fukuuchi Y, Kohsaka S (1998) Microglia-specific localisation of a novel calcium binding protein, Iba1. Brain Res Mol Brain Res 57:1-9.

Ito M, Hiramatsu H, Kobayashi K, Suzue K, Kawahata M, Hioki K, Ueyama Y, Koyanagi Y, Sugamura K, Tsuji K, Heike T, Nakahata T (2002) NOD/SCID/gamma(c)(null) mouse: an excellent recipient mouse model for engraftment of human cells. Blood 100:3175-3182.

Janova H et al. (2017) Microglia ablation alleviates myelin-associated catatonic signs in mice. The Journal of Clinical Investigation 128.

Jay C, Ropka M, Dalakas MC (1994) The drugs 2',3'-dideoxyinosine (ddI) and 2',3'-dideoxycytidine (ddC) are safe alternatives in people with AIDS with zidovudine-induced myopathy. J Acquir Immune Defic Syndr 7:630-631.

Jin J, Lam L, Sadic E, Fernandez F, Tan J, Giunta B (2012) HIV-1 Tat-induced microglial activation and neuronal damage is inhibited via CD45 modulation: A potential new treatment target for HAND. Am J Transl Res 4:302-315.

Jones EV, Bernardinelli Y, Tse YC, Chierzi S, Wong TP, Murai KK (2011) Astrocytes control glutamate receptor levels at developing synapses through SPARC-beta-integrin interactions. J Neurosci 31:4154-4165.

Jones HR, Ho DD, Forgacs P, Adelman LS, Silverman ML, Baker RA, Locuratolo P (1988) Acute fulminating fatal leukoencephalopathy as the only manifestation of human immunodeficiency virus infection. Ann Neurol 23:519-522.

Jung S, Aliberti J, Graemmel P, Sunshine MJ, Kreutzberg GW, Sher A, Littman DR (2000a) Analysis of Fractalkine Receptor CX3CR1 Function by Targeted Deletion and Green Fluorescent Protein Reporter Gene Insertion. In: Mol Cell Biol, pp 4106-4114.

Jung S, Aliberti J, Graemmel P, Sunshine MJ, Kreutzberg GW, Sher A, Littman DR (2000b) Analysis of fractalkine receptor CX(3)CR1 function by targeted deletion and green fluorescent protein reporter gene insertion. Mol Cell Biol 20:4106-4114.

Kanzer MD (1990) Neuropathology of AIDS. Crit Rev Neurobiol 5:313-362.

Kaul M, Lipton SA (1999) Chemokines and activated macrophages in HIV gp120-induced neuronal apoptosis. Proc Natl Acad Sci U S A 96:8212-8216.

Kaul M, Garden GA, Lipton SA (2001) Pathways to neuronal injury and apoptosis in HIV-associated dementia. Nature 410:988-994.

Kaul M, Zheng J, Okamoto S, Gendelman HE, Lipton SA (2005) HIV-1 infection and AIDS: consequences for the central nervous system. Cell Death Differ 12 Suppl 1:878-892.

Kelder W, McArthur JC, Nance-Sproson T, McClernon D, Griffin DE (1998) Beta-chemokines MCP-1 and RANTES are selectively increased in cerebrospinal fluid of patients with human immunodeficiency virus-associated dementia. Ann Neurol 44:831-835.

Kelschenbach JL, Saini M, Hadas E, Gu CJ, Chao W, Bentsman G, Hong JP, Hanke T, Sharer LR, Potash MJ, Volsky DJ (2012) Mice chronically infected with chimeric HIV resist peripheral and brain superinfection: a model of protective immunity to HIV. J Neuroimmune Pharmacol 7:380-387.

Kettenmann H, Kirchhoff F, Verkhratsky A (2013) Microglia: new roles for the synaptic stripper. Neuron 77:10-18.

Ketzler S, Weis S, Haug H, Budka H (1990) Loss of neurons in the frontal cortex in AIDS brains. Acta Neuropathol 80:92-94.

Khairova RA, Machado-Vieira R, Du J, Manji HK (2009) A potential role for pro-inflammatory cytokines in regulating synaptic plasticity in major depressive disorder. Int J Neuropsychopharmacol 12:561-578.

Khan MZ, Brandimarti R, Shimizu S, Nicolai J, Crowe E, Meucci O (2008) The chemokine CXCL12 promotes survival of postmitotic neurons by regulating Rb protein. Cell Death Differ 15:1663-1672.

Kim BO, Liu Y, Ruan Y, Xu ZC, Schantz L, He JJ (2003) Neuropathologies in transgenic mice expressing human immunodeficiency virus type 1 Tat protein under the regulation of the astrocyte-specific glial fibrillary acidic protein promoter and doxycycline. Am J Pathol 162:1693-1707.

Kim HJ, Martemyanov KA, Thayer SA (2008) Human immunodeficiency virus protein Tat induces synapse loss via a reversible process that is distinct from cell death. J Neurosci 28:12604-12613.

Kim HJ, Shin AH, Thayer SA (2011) Activation of Cannabinoid Type 2 Receptors Inhibits HIV-1 Envelope Glycoprotein gp120-Induced Synapse Loss. In: Mol Pharmacol, pp 357-366.

Kim SK, Eto K, Nabekura J (2012) Synaptic structure and function in the mouse somatosensory cortex during chronic pain: in vivo two-photon imaging. Neural Plast 2012:640259.

Kobayashi K, Imagama S, Ohgomori T, Hirano K, Uchimura K, Sakamoto K, Hirakawa A, Takeuchi H, Suzumura A, Ishiguro N, Kadomatsu K (2013) Minocycline selectively inhibits M1 polarization of microglia. Cell Death Dis 4:e525.

Kovalevich J, Langford D (2012) Neuronal toxicity in HIV CNS disease. Future Virol 7:687-698.

Kucukdereli H, Allen NJ, Lee AT, Feng A, Ozlu MI, Conatser LM, Chakraborty C, Workman G, Weaver M, Sage EH, Barres BA, Eroglu C (2011) Control of excitatory CNS synaptogenesis by astrocyte-secreted proteins Hevin and SPARC. Proc Natl Acad Sci U S A 108:E440-449.

Langford D, Sanders VJ, Mallory M, Kaul M, Masliah E (2002) Expression of stromal cell-derived factor 1alpha protein in HIV encephalitis. J Neuroimmunol 127:115-126.

Langford TD, Letendre SL, Larrea GJ, Masliah E (2003) Changing patterns in the neuropathogenesis of HIV during the HAART era. Brain Pathol 13:195-210.

Lashomb AL, Vigorito M, Chang SL (2009) Further characterization of the spatial learning deficit in the human immunodeficiency virus-1 transgenic rat. J Neurovirol 15:14-24.

Latremoliere A, Woolf CJ (2009) Central sensitization: a generator of pain hypersensitivity by central neural plasticity. J Pain 10:895-926.

Lavi E, Strizki JM, Ulrich AM, Zhang W, Fu L, Wang Q, O'Connor M, Hoxie JA, González-Scarano F (1997) CXCR-4 (Fusin), a co-receptor for the type 1 human immunodeficiency virus (HIV-1), is expressed in the human brain in a variety of cell types, including microglia and neurons. Am J Pathol 151:1035-1042.

Lazarini F, Casanova P, Tham TN, De Clercq E, Arenzana-Seisdedos F, Baleux F, Dubois-Dalcq M (2000) Differential signalling of the chemokine receptor CXCR4 by stromal cell-derived factor 1 and the HIV glycoprotein in rat neurons and astrocytes. Eur J Neurosci 12:117-125.

Lee MH, Wang T, Jang MH, Steiner J, Haughey N, Ming GL, Song H, Nath A, Venkatesan A (2011) Rescue of adult hippocampal neurogenesis in a mouse model of HIV neurologic disease. Neurobiol Dis 41:678-687.

Lee S, Varvel NH, Konerth ME, Xu G, Cardona AE, Ransohoff RM, Lamb BT (2010) CX3CR1 deficiency alters microglial activation and reduces beta-amyloid deposition in two Alzheimer's disease mouse models. Am J Pathol 177:2549-2562.

Lee SC, Hatch WC, Liu W, Kress Y, Lyman WD, Dickson DW (1993) Productive infection of human fetal microglia by HIV-1. Am J Pathol 143:1032-1039.

Lehre KP, Rusakov DA (2002) Asymmetry of glia near central synapses favors presynaptically directed glutamate escape. Biophys J 83:125-134.

Letendre SL, Zheng JC, Kaul M, Yiannoutsos CT, Ellis RJ, Taylor MJ, Marquie-Beck J, Navia B, Consortium HN (2011) Chemokines in cerebrospinal fluid correlate with cerebral metabolite patterns in HIV-infected individuals. J Neurovirol 17:63-69.

Li JL, Zhuang K, Wu GY, Ho WZ (2015) Magnetic resonance imaging study of a simian/human immunodeficiency virus-infected Chinese rhesus macaque with HIV-associated dementia. AIDS Res Hum Retroviruses 31:272-273.

Li W, Huang Y, Reid R, Steiner J, Malpica-Llanos T, Darden TA, Shankar SK, Mahadevan A, Satishchandra P, Nath A (2008) NMDA receptor activation by HIV-Tat protein is clade dependent. J Neurosci 28:12190-12198.

Li Z, Wei H, Piirainen S, Chen Z, Kalso E, Pertovaara A, Tian L (2016) Spinal versus brain microglial and macrophage activation traits determine the differential neuroinflammatory responses and analgesic effect of minocycline in chronic neuropathic pain. Brain Behav Immun 58:107-117.

Lian H, Yang L, Cole A, Sun L, Chiang AC, Fowler SW, Shim DJ, Rodriguez-Rivera J, Taglialatela G, Jankowsky JL, Lu HC, Zheng H (2015) NFκB-activated astroglial release of complement C3 compromises neuronal morphology and function associated with Alzheimer's disease. Neuron 85:101-115.

Liang SL, Carlson GC, Coulter DA (2006) Dynamic regulation of synaptic GABA release by the glutamate-glutamine cycle in hippocampal area CA1. J Neurosci 26:8537-8548.

Liddelow SA, Barres BA (2017) Reactive Astrocytes: Production, Function, and Therapeutic Potential. Immunity 46:957-967.

Liddelow SA et al. (2017) Neurotoxic reactive astrocytes are induced by activated microglia. Nature 541:481-487.

Limatola C, Lauro C, Catalano M, Ciotti MT, Bertollini C, Di Angelantonio S, Ragozzino D, Eusebi F (2005) Chemokine CX3CL1 protects rat hippocampal neurons against glutamate-mediated excitotoxicity. J Neuroimmunol 166:19-28.

Liu CC, Hu J, Zhao N, Wang J, Wang N, Cirrito JR, Kanekiyo T, Holtzman DM, Bu G (2017) Astrocytic LRP1 Mediates Brain Aβ Clearance and Impacts Amyloid Deposition. J Neurosci 37:4023-4031.

Liu F, Dai S, Gordon J, Qin X (2014) Complement and HIV-I infection/HIV-associated neurocognitive disorders. J Neurovirol 20:184-198.

Liu NQ, Lossinsky AS, Popik W, Li X, Gujuluva C, Kriederman B, Roberts J, Pushkarsky T, Bukrinsky M, Witte M, Weinand M, Fiala M (2002) Human immunodeficiency virus type 1 enters brain microvascular endothelia by macropinocytosis dependent on lipid rafts and the mitogen-activated protein kinase signaling pathway. J Virol 76:6689-6700.

Liu Y, Jones M, Hingtgen CM, Bu G, Laribee N, Tanzi RE, Moir RD, Nath A, He JJ (2000) Uptake of HIV-1 tat protein mediated by low-density lipoprotein receptor-

related protein disrupts the neuronal metabolic balance of the receptor ligands. Nat Med 6:1380-1387.

Liu Z, Condello C, Schain A, Harb R, Grutzendler J (2010) CX3CR1 in microglia regulates brain amyloid deposition through selective protofibrillar amyloid-beta phagocytosis. J Neurosci 30:17091-17101.

Lööv C, Hillered L, Ebendal T, Erlandsson A (2012) Engulfing astrocytes protect neurons from contact-induced apoptosis following injury. PLoS One 7:e33090.

Macosko EZ, Basu A, Satija R, Nemesh J, Shekhar K, Goldman M, Tirosh I, Bialas AR, Kamitaki N, Martersteck EM, Trombetta JJ, Weitz DA, Sanes JR, Shalek AK, Regev A, McCarroll SA (2015) Highly Parallel Genome-wide Expression Profiling of Individual Cells Using Nanoliter Droplets. Cell 161:1202-1214.

Mankowski JL, Spelman JP, Ressetar HG, Strandberg JD, Laterra J, Carter DL, Clements JE, Zink MC (1994) Neurovirulent simian immunodeficiency virus replicates productively in endothelial cells of the central nervous system in vivo and in vitro. J Virol 68:8202-8208.

Marcario JK, Pendyala G, Riazi M, Fleming K, Marquis J, Callen S, Lisco SJ, Fowler SC, Cheney PD, Buch SJ (2016) Effects of Morphine on Behavioral Task Performance in SIV-Infected Rhesus Macaques. J Neuroimmune Pharmacol 11:348-357.

Marchionni I, Beaumont M, Maccaferri G (2012) The chemokine CXCL12 and the HIV-1 envelope protein gp120 regulate spontaneous activity of Cajal-Retzius cells in opposite directions. J Physiol 590:3185-3202.

Marcondes MC, Flynn C, Watry DD, Zandonatti M, Fox HS (2010) Methamphetamine increases brain viral load and activates natural killer cells in simian immunodeficiency virus-infected monkeys. Am J Pathol 177:355-361.

Marcondes MC, Flynn C, Huitron-Rezendiz S, Watry DD, Zandonatti M, Fox HS (2009) Early antiretroviral treatment prevents the development of central nervous system abnormalities in simian immunodeficiency virus-infected rhesus monkeys. AIDS 23:1187-1195.

Marcondes MC, Burdo TH, Sopper S, Huitron-Resendiz S, Lanigan C, Watry D, Flynn C, Zandonatti M, Fox HS (2007) Enrichment and persistence of virus-specific

CTL in the brain of simian immunodeficiency virus-infected monkeys is associated with a unique cytokine environment. J Immunol 178:5812-5819.

Marsden MD, Zack JA (2015) Studies of retroviral infection in humanized mice. Virology 479-480:297-309.

Martiskainen H, Haapasalo A, Kurkinen KM, Pihlajamäki J, Soininen H, Hiltunen M (2013) Targeting ApoE4/ApoE receptor LRP1 in Alzheimer's disease. Expert Opin Ther Targets 17:781-794.

Maschke M, Kastrup O, Esser S, Ross B, Hengge U, Hufnagel A (2000) Incidence and prevalence of neurological disorders associated with HIV since the introduction of highly active antiretroviral therapy (HAART). J Neurol Neurosurg Psychiatry 69:376-380.

Masliah E, Heaton RK, Marcotte TD, Ellis RJ, Wiley CA, Mallory M, Achim CL, McCutchan JA, Nelson JA, Atkinson JH, Grant I (1997) Dendritic injury is a pathological substrate for human immunodeficiency virus-related cognitive disorders. HNRC Group. The HIV Neurobehavioral Research Center. Ann Neurol 42:963-972.

Mathys H, Adaikkan C, Gao F, Young JZ, Manet E, Hemberg M, De Jager PL, Ransohoff RM, Regev A, Tsai LH (2017) Temporal Tracking of Microglia Activation in Neurodegeneration at Single-Cell Resolution. Cell Rep 21:366-380.

Maung R, Hoefer MM, Sanchez AB, Sejbuk NE, Medders KE, Desai MK, Catalan IC, Dowling CC, de Rozieres CM, Garden GA, Russo R, Roberts AJ, Williams R, Kaul M (2014) CCR5 knockout prevents neuronal injury and behavioral impairment induced in a transgenic mouse model by a CXCR4-using HIV-1 glycoprotein 120. J Immunol 193:1895-1910.

McGuire JL, Gill AJ, Douglas SD, Kolson DL, Group CHATERC (2016) The complement system, neuronal injury, and cognitive function in horizontally-acquired HIV-infected youth. J Neurovirol 22:823-830.

Medders KE, Sejbuk NE, Maung R, Desai MK, Kaul M (2010) Activation of p38 MAPK is required in monocytic and neuronal cells for HIV glycoprotein 120-induced neurotoxicity. J Immunol 185:4883-4895.

Melendez RI, Roman C, Capo-Velez CM, Lasalde-Dominicci JA (2015) Decreased glial and synaptic glutamate uptake in the striatum of HIV-1 gp120 transgenic mice. J Neurovirol.

Melkus MW, Estes JD, Padgett-Thomas A, Gatlin J, Denton PW, Othieno FA, Wege AK, Haase AT, Garcia JV (2006) Humanized mice mount specific adaptive and innate immune responses to EBV and TSST-1. Nat Med 12:1316-1322.

Meucci O, Fatatis A, Simen AA, Miller RJ (2000) Expression of CX3CR1 chemokine receptors on neurons and their role in neuronal survival. Proc Natl Acad Sci U S A 97:8075-8080.

Micheva KD, Busse B, Weiler NC, O'Rourke N, Smith SJ (2010) Single-synapse analysis of a diverse synapse population: proteomic imaging methods and markers. Neuron 68:639-653.

Milligan ED, Mehmert KK, Hinde JL, Harvey LO, Martin D, Tracey KJ, Maier SF, Watkins LR (2000) Thermal hyperalgesia and mechanical allodynia produced by intrathecal administration of the human immunodeficiency virus-1 (HIV-1) envelope glycoprotein, gp120. Brain Res 861:105-116.

Milligan ED, O'Connor KA, Nguyen KT, Armstrong CB, Twining C, Gaykema RP, Holguin A, Martin D, Maier SF, Watkins LR (2001) Intrathecal HIV-1 envelope glycoprotein gp120 induces enhanced pain states mediated by spinal cord proinflammatory cytokines. J Neurosci 21:2808-2819.

Mocchetti I, Nosheny RL, Tanda G, Ren K, Meyer EM (2007) Brain-derived neurotrophic factor prevents human immunodeficiency virus type 1 protein gp120 neurotoxicity in the rat nigrostriatal system. Ann N Y Acad Sci 1122:144-154.

Morizawa YM, Hirayama Y, Ohno N, Shibata S, Shigetomi E, Sui Y, Nabekura J, Sato K, Okajima F, Takebayashi H, Okano H, Koizumi S (2017) Author Correction: Reactive astrocytes function as phagocytes after brain ischemia via ABCA1-mediated pathway. Nat Commun 8:1598.

Mosier DE, Gulizia RJ, Baird SM, Wilson DB (1988) Transfer of a functional human immune system to mice with severe combined immunodeficiency. Nature 335:256-259.

Mukherjee S, Rodriguez-Canales J, Hanson J, Emmert-Buck MR, Tangrea MA, Prieto DA, Blonder J, Johann DJ (2013) Proteomic analysis of frozen tissue samples using laser capture microdissection. Methods Mol Biol 1002:71-83.

Nakasujja N, Miyahara S, Evans S, Lee A, Musisi S, Katabira E, Robertson K, Ronald A, Clifford DB, Sacktor N (2013) Randomized trial of minocycline in the treatment of HIV-associated cognitive impairment. Neurology 80:196-202.

Nath A (2002) Human immunodeficiency virus (HIV) proteins in neuropathogenesis of HIV dementia. J Infect Dis 186 Suppl 2:S193-198.

Nath A, Conant K, Chen P, Scott C, Major EO (1999) Transient exposure to HIV-1 Tat protein results in cytokine production in macrophages and astrocytes. A hit and run phenomenon. J Biol Chem 274:17098-17102.

Navia BA, Cho ES, Petito CK, Price RW (1986) The AIDS dementia complex: II. Neuropathology. Ann Neurol 19:525-535.

Neher JJ, Emmrich JV, Fricker M, Mander PK, Théry C, Brown GC (2013) Phagocytosis executes delayed neuronal death after focal brain ischemia. Proc Natl Acad Sci U S A 110:E4098-4107.

Neniskyte U, Brown GC (2013) Lactadherin/MFG-E8 is essential for microglia-mediated neuronal loss and phagoptosis induced by amyloid β. J Neurochem 126:312-317.

Neniskyte U, Gross CT (2017) Errant gardeners: glial-cell-dependent synaptic pruning and neurodevelopmental disorders. Nat Rev Neurosci 18:658-670.

Neumann H, Kotter MR, Franklin RJ (2009) Debris clearance by microglia: an essential link between degeneration and regeneration. Brain 132:288-295.

Nguyen JV, Soto I, Kim KY, Bushong EA, Oglesby E, Valiente-Soriano FJ, Yang Z, Davis CH, Bedont JL, Son JL, Wei JO, Buchman VL, Zack DJ, Vidal-Sanz M, Ellisman MH, Marsh-Armstrong N (2011) Myelination transition zone astrocytes are constitutively phagocytic and have synuclein dependent reactivity in glaucoma. Proc Natl Acad Sci U S A 108:1176-1181.

Nicolai J, Burbassi S, Rubin J, Meucci O (2010) CXCL12 inhibits expression of the NMDA receptor's NR2B subunit through a histone deacetylase-dependent pathway contributing to neuronal survival. Cell Death Dis 1:e33.

Noda M, Doi Y, Liang J, Kawanokuchi J, Sonobe Y, Takeuchi H, Mizuno T, Suzumura A (2011) Fractalkine attenuates excito-neurotoxicity via microglial clearance of damaged neurons and antioxidant enzyme heme oxygenase-1 expression. J Biol Chem 286:2308-2319.

Nomura K, Vilalta A, Allendorf DH, Hornik TC, Brown GC (2017) Activated Microglia Desialylate and Phagocytose Cells via Neuraminidase, Galectin-3, and Mer Tyrosine Kinase. J Immunol 198:4792-4801.

Norgren N, Rosengren L, Stigbrand T (2003) Elevated neurofilament levels in neurological diseases. Brain Res 987:25-31.

Nosheny RL, Bachis A, Acquas E, Mocchetti I (2004) Human immunodeficiency virus type 1 glycoprotein gp120 reduces the levels of brain-derived neurotrophic factor in vivo: potential implication for neuronal cell death. Eur J Neurosci 20:2857-2864.

Nottet HS, Jett M, Flanagan CR, Zhai QH, Persidsky Y, Rizzino A, Bernton EW, Genis P, Baldwin T, Schwartz J (1995) A regulatory role for astrocytes in HIV-1 encephalitis. An overexpression of eicosanoids, platelet-activating factor, and tumor necrosis factor-alpha by activated HIV-1-infected monocytes is attenuated by primary human astrocytes. J Immunol 154:3567-3581.

Nzwalo H, Añón RP, Àguas MJ (2012) Acute encephalitis as initial presentation of primary HIV infection. BMJ Case Rep 2012.

Okamoto S, Kang YJ, Brechtel CW, Siviglia E, Russo R, Clemente A, Harrop A, McKercher S, Kaul M, Lipton SA (2007) HIV/gp120 decreases adult neural progenitor cell proliferation via checkpoint kinase-mediated cell-cycle withdrawal and G1 arrest. Cell Stem Cell 1:230-236.

Okerlund ND, Kivimäe S, Tong CK, Peng IF, Ullian EM, Cheyette BN (2010) Dact1 is a postsynaptic protein required for dendrite, spine, and excitatory synapse development in the mouse forebrain. J Neurosci 30:4362-4368.

Olmos G, Lladó J (2014) Tumor necrosis factor alpha: a link between neuroinflammation and excitotoxicity. Mediators Inflamm 2014:861231.

Orandle MS, MacLean AG, Sasseville VG, Alvarez X, Lackner AA (2002) Enhanced expression of proinflammatory cytokines in the central nervous system is

associated with neuroinvasion by simian immunodeficiency virus and the development of encephalitis. J Virol 76:5797-5802.

Pagani F, Paolicelli RC, Murana E, Cortese B, Di Angelantonio S, Zurolo E, Guiducci E, Ferreira TA, Garofalo S, Catalano M, D'Alessandro G, Porzia A, Peruzzi G, Mainiero F, Limatola C, Gross CT, Ragozzino D (2015) Defective microglial development in the hippocampus of Cx3cr1 deficient mice. Front Cell Neurosci 9:111.

Paolicelli RC, Bisht K, Tremblay M (2014) Fractalkine regulation of microglial physiology and consequences on the brain and behavior. Front Cell Neurosci 8:129.

Paolicelli RC, Bolasco G, Pagani F, Maggi L, Scianni M, Panzanelli P, Giustetto M, Ferreira TA, Guiducci E, Dumas L, Ragozzino D, Gross CT (2011) Synaptic pruning by microglia is necessary for normal brain development. Science 333:1456-1458.

Pattarini R, Pittaluga A, Raiteri M (1998) The human immunodeficiency virus-1 envelope protein gp120 binds through its V3 sequence to the glycine site of N-methyl-D-aspartate receptors mediating noradrenaline release in the hippocampus. Neuroscience 87:147-157.

Patton HK, Zhou ZH, Bubien JK, Benveniste EN, Benos DJ (2000) gp120-induced alterations of human astrocyte function: Na(+)/H(+) exchange, K(+) conductance, and glutamate flux. Am J Physiol Cell Physiol 279:C700-708.

Peng H, Erdmann N, Whitney N, Dou H, Gorantla S, Gendelman HE, Ghorpade A, Zheng J (2006) HIV-1-infected and/or immune activated macrophages regulate astrocyte SDF-1 production through IL-1beta. Glia 54:619-629.

Peng J, Vigorito M, Liu X, Zhou D, Wu X, Chang SL (2010) The HIV-1 transgenic rat as a model for HIV-1 infected individuals on HAART. J Neuroimmunol 218:94-101.

Pereira CF, Middel J, Jansen G, Verhoef J, Nottet HS (2001) Enhanced expression of fractalkine in HIV-1 associated dementia. J Neuroimmunol 115:168-175.

Perry SW, Norman JP, Litzburg A, Zhang D, Dewhurst S, Gelbard HA (2005) HIV-1 transactivator of transcription protein induces mitochondrial hyperpolarization and synaptic stress leading to apoptosis. J Immunol 174:4333-4344.

Perry SW, Hamilton JA, Tjoelker LW, Dbaibo G, Dzenko KA, Epstein LG, Hannun Y, Whittaker JS, Dewhurst S, Gelbard HA (1998) Platelet-activating factor receptor activation. An initiator step in HIV-1 neuropathogenesis. J Biol Chem 273:17660-17664.

Persidsky Y, Buttini M, Limoges J, Bock P, Gendelman HE (1997) An analysis of HIV-1-associated inflammatory products in brain tissue of humans and SCID mice with HIV-1 encephalitis. J Neurovirol 3:401-416.

Persidsky Y, Limoges J, McComb R, Bock P, Baldwin T, Tyor W, Patil A, Nottet HS, Epstein L, Gelbard H, Flanagan E, Reinhard J, Pirruccello SJ, Gendelman HE (1996) Human immunodeficiency virus encephalitis in SCID mice. Am J Pathol 149:1027-1053.

Poluektova L, Gorantla S, Faraci J, Birusingh K, Dou H, Gendelman HE (2004) Neuroregulatory events follow adaptive immune-mediated elimination of HIV-1-infected macrophages: studies in a murine model of viral encephalitis. J Immunol 172:7610-7617.

Poluektova LY, Munn DH, Persidsky Y, Gendelman HE (2002) Generation of cytotoxic T cells against virus-infected human brain macrophages in a murine model of HIV-1 encephalitis. J Immunol 168:3941-3949.

Ponath G, Ramanan S, Mubarak M, Housley W, Lee S, Sahinkaya FR, Vortmeyer A, Raine CS, Pitt D (2017) Myelin phagocytosis by astrocytes after myelin damage promotes lesion pathology. Brain 140:399-413.

Potash MJ, Chao W, Bentsman G, Paris N, Saini M, Nitkiewicz J, Belem P, Sharer L, Brooks AI, Volsky DJ (2005) A mouse model for study of systemic HIV-1 infection, antiviral immune responses, and neuroinvasiveness. Proc Natl Acad Sci U S A 102:3760-3765.

Potter MC, Figuera-Losada M, Rojas C, Slusher BS (2013) Targeting the glutamatergic system for the treatment of HIV-associated neurocognitive disorders. J Neuroimmune Pharmacol 8:594-607.

Potter SS (2018) Single-cell RNA sequencing for the study of development, physiology and disease. Nat Rev Nephrol 14:479-492.

Raghavan R, Stephens EB, Joag SV, Adany I, Pinson DM, Li Z, Jia F, Sahni M, Wang C, Leung K, Foresman L, Narayan O (1997) Neuropathogenesis of chimeric simian/human immunodeficiency virus infection in pig-tailed and rhesus macaques. Brain Pathol 7:851-861.

Ragin AB, Wu Y, Storey P, Cohen BA, Edelman RR, Epstein LG (2006) Monocyte chemoattractant protein-1 correlates with subcortical brain injury in HIV infection. Neurology 66:1255-1257.

Ranki A, Nyberg M, Ovod V, Haltia M, Elovaara I, Raininko R, Haapasalo H, Krohn K (1995) Abundant expression of HIV Nef and Rev proteins in brain astrocytes in vivo is associated with dementia. AIDS 9:1001-1008.

Ransohoff RM (2009) Chemokines and chemokine receptors: standing at the crossroads of immunobiology and neurobiology. Immunity 31:711-721.

Rao JS, Kim HW, Kellom M, Greenstein D, Chen M, Kraft AD, Harry GJ, Rapoport SI, Basselin M (2011) Increased neuroinflammatory and arachidonic acid cascade markers, and reduced synaptic proteins, in brain of HIV-1 transgenic rats. J Neuroinflammation 8:101.

Rao VR, Sas AR, Eugenin EA, Siddappa NB, Bimonte-Nelson H, Berman JW, Ranga U, Tyor WR, Prasad VR (2008) HIV-1 clade-specific differences in the induction of neuropathogenesis. J Neurosci 28:10010-10016.

Rappaport J, Joseph J, Croul S, Alexander G, Del Valle L, Amini S, Khalili K (1999) Molecular pathway involved in HIV-1-induced CNS pathology: role of viral regulatory protein, Tat. J Leukoc Biol 65:458-465.

Reddy PV, Gandhi N, Samikkannu T, Saiyed Z, Agudelo M, Yndart A, Khatavkar P, Nair MP (2012) HIV-1 gp120 induces antioxidant response element-mediated expression in primary astrocytes: role in HIV associated neurocognitive disorder. Neurochem Int 61:807-814.

Reid W et al. (2001) An HIV-1 transgenic rat that develops HIV-related pathology and immunologic dysfunction. Proc Natl Acad Sci U S A 98:9271-9276.

Reid WC, Casas R, Papadakis GZ, Muthusamy S, Lee DE, Ibrahim WG, Nair A, Koziol D, Maric D, Hammoud DA (2016) Neurobehavioral Abnormalities in the HIV-1

Transgenic Rat Do Not Correspond to Neuronal Hypometabolism on 18F-FDG-PET. PLoS One 11:e0152265.

Reshef R, Kreisel T, Beroukhim Kay D, Yirmiya R (2014) Microglia and their CX3CR1 signaling are involved in hippocampal- but not olfactory bulb-related memory and neurogenesis. Brain Behav Immun 41:239-250.

Reshef R, Kudryavitskaya E, Shani-Narkiss H, Isaacson B, Rimmerman N, Mizrahi A, Yirmiya R (2017) The role of microglia and their CX3CR1 signaling in adult neurogenesis in the olfactory bulb. eLife 6:e30809.

Resnick L, Berger JR, Shapshak P, Tourtellotte WW (1988) Early penetration of the blood-brain-barrier by HIV. Neurology 38:9-14.

Ricci G, Volpi L, Pasquali L, Petrozzi L, Siciliano G (2009) Astrocyte-neuron interactions in neurological disorders. J Biol Phys 35:317-336.

Riddick NE, Hermann EA, Loftin LM, Elliott ST, Wey WC, Cervasi B, Taaffe J, Engram JC, Li B, Else JG, Li Y, Hahn BH, Derdeyn CA, Sodora DL, Apetrei C, Paiardini M, Silvestri G, Collman RG (2010) A novel CCR5 mutation common in sooty mangabeys reveals SIVsmm infection of CCR5-null natural hosts and efficient alternative coreceptor use in vivo. PLoS Pathog 6:e1001064.

Roberts ES, Masliah E, Fox HS (2004) CD163 identifies a unique population of ramified microglia in HIV encephalitis (HIVE). J Neuropathol Exp Neurol 63:1255-1264.

Roberts ES, Zandonatti MA, Watry DD, Madden LJ, Henriksen SJ, Taffe MA, Fox HS (2003) Induction of pathogenic sets of genes in macrophages and neurons in NeuroAIDS. Am J Pathol 162:2041-2057.

Roberts ES, Huitron-Resendiz S, Taffe MA, Marcondes MC, Flynn CT, Lanigan CM, Hammond JA, Head SR, Henriksen SJ, Fox HS (2006) Host response and dysfunction in the CNS during chronic simian immunodeficiency virus infection. J Neurosci 26:4577-4585.

Rogers JT, Morganti JM, Bachstetter AD, Hudson CE, Peters MM, Grimmig BA, Weeber EJ, Bickford PC, Gemma C (2011) CX3CR1 deficiency leads to impairment of hippocampal cognitive function and synaptic plasticity. J Neurosci 31:16241-16250.

Rostasy K, Egles C, Chauhan A, Kneissl M, Bahrani P, Yiannoutsos C, Hunter DD, Nath A, Hedreen JC, Navia BA (2003) SDF-1alpha is expressed in astrocytes and neurons in the AIDS dementia complex: an in vivo and in vitro study. J Neuropathol Exp Neurol 62:617-626.

Rothstein JD, Dykes-Hoberg M, Pardo CA, Bristol LA, Jin L, Kuncl RW, Kanai Y, Hediger MA, Wang Y, Schielke JP, Welty DF (1996) Knockout of glutamate transporters reveals a major role for astroglial transport in excitotoxicity and clearance of glutamate. Neuron 16:675-686.

Rottman JB, Ganley KP, Williams K, Wu L, Mackay CR, Ringler DJ (1997) Cellular localization of the chemokine receptor CCR5. Correlation to cellular targets of HIV-1 infection. Am J Pathol 151:1341-1351.

Ru W, Tang SJ (2016) HIV-1 gp120Bal down-Regulates Phosphorylated NMDA Receptor Subunit 1 in Cortical Neurons via Activation of Glutamate and Chemokine Receptors. J Neuroimmune Pharmacol 11:182-191.

Ru W, Tang SJ (2017) HIV-associated synaptic degeneration. Mol Brain 10:40.

Sacktor N (2002) The epidemiology of human immunodeficiency virus-associated neurological disease in the era of highly active antiretroviral therapy. J Neurovirol 8 Suppl 2:115-121.

Sacktor N, Haughey N, Cutler R, Tamara A, Turchan J, Pardo C, Vargas D, Nath A (2004) Novel markers of oxidative stress in actively progressive HIV dementia. J Neuroimmunol 157:176-184.

Saha RN, Pahan K (2003) Tumor necrosis factor-alpha at the crossroads of neuronal life and death during HIV-associated dementia. J Neurochem 86:1057-1071.

Sano H, Hsu DK, Apgar JR, Yu L, Sharma BB, Kuwabara I, Izui S, Liu FT (2003) Critical role of galectin-3 in phagocytosis by macrophages. J Clin Invest 112:389-397.

Santoro TJ, Bryant JL, Pellicoro J, Klotman ME, Kopp JB, Bruggeman LA, Franks RR, Notkins AL, Klotman PE (1994) Growth failure and AIDS-like cachexia syndrome in HIV-1 transgenic mice. Virology 201:147-151.

Saylor D, Dickens AM, Sacktor N, Haughey N, Slusher B, Pletnikov M, Mankowski JL, Brown A, Volsky DJ, McArthur JC (2016) HIV-associated neurocognitive disorder - pathogenesis and prospects for treatment. Nat Rev Neurol 12:309.

Schafer DP, Lehrman EK, Kautzman AG, Koyama R, Mardinly AR, Yamasaki R, Ransohoff RM, Greenberg ME, Barres BA, Stevens B (2012) Microglia sculpt postnatal neural circuits in an activity and complement-dependent manner. Neuron 74:691-705.

Scott RS, McMahon EJ, Pop SM, Reap EA, Caricchio R, Cohen PL, Earp HS, Matsushima GK (2001) Phagocytosis and clearance of apoptotic cells is mediated by MER. Nature 411:207-211.

Seay K, Qi X, Zheng JH, Zhang C, Chen K, Dutta M, Deneroff K, Ochsenbauer C, Kappes JC, Littman DR, Goldstein H (2013) Mice transgenic for CD4-specific human CD4, CCR5 and cyclin T1 expression: a new model for investigating HIV-1 transmission and treatment efficacy. PLoS One 8:e63537.

Self RL, Mulholland PJ, Nath A, Harris BR, Prendergast MA (2004) The human immunodeficiency virus type-1 transcription factor Tat produces elevations in intracellular Ca2+ that require function of an N-methyl-D-aspartate receptor polyamine-sensitive site. Brain Res 995:39-45.

Sevigny JJ, Albert SM, McDermott MP, McArthur JC, Sacktor N, Conant K, Schifitto G, Selnes OA, Stern Y, McClernon DR, Palumbo D, Kieburtz K, Riggs G, Cohen B, Epstein LG, Marder K (2004) Evaluation of HIV RNA and markers of immune activation as predictors of HIV-associated dementia. Neurology 63:2084-2090.

Sevigny JJ, Albert SM, McDermott MP, Schifitto G, McArthur JC, Sacktor N, Conant K, Selnes OA, Stern Y, McClernon DR, Palumbo D, Kieburtz K, Riggs G, Cohen B, Marder K, Epstein LG (2007) An evaluation of neurocognitive status and markers of immune activation as predictors of time to death in advanced HIV infection. Arch Neurol 64:97-102.

Shah A, Singh DP, Buch S, Kumar A (2011a) HIV-1 envelope protein gp120 up regulates CCL5 production in astrocytes which can be circumvented by inhibitors of NF-κB pathway. Biochem Biophys Res Commun 414:112-117.

Shah A, Verma AS, Patel KH, Noel R, Rivera-Amill V, Silverstein PS, Chaudhary S, Bhat HK, Stamatatos L, Singh DP, Buch S, Kumar A (2011b) HIV-1 gp120 induces expression of IL-6 through a nuclear factor-kappa B-dependent mechanism: suppression by gp120 specific small interfering RNA. PLoS One 6:e21261.

Sharer LR, Baskin GB, Cho ES, Murphey-Corb M, Blumberg BM, Epstein LG (1988) Comparison of simian immunodeficiency virus and human immunodeficiency virus encephalitides in the immature host. Ann Neurol 23 Suppl:S108-112.

Sheridan GK, Murphy KJ (2013) Neuron-glia crosstalk in health and disease: fractalkine and CX3CR1 take centre stage. Open Biol 3:130181.

Shi B, De Girolami U, He J, Wang S, Lorenzo A, Busciglio J, Gabuzda D (1996) Apoptosis induced by HIV-1 infection of the central nervous system. J Clin Invest 98:1979-1990.

Shin AH, Thayer SA (2013) Human immunodeficiency virus-1 protein Tat induces excitotoxic loss of presynaptic terminals in hippocampal cultures. Mol Cell Neurosci 54:22-29.

Shin AH, Kim HJ, Thayer SA (2012) Subtype selective NMDA receptor antagonists induce recovery of synapses lost following exposure to HIV-1 Tat. Br J Pharmacol 166:1002-1017.

Shinozaki Y, Shibata K, Yoshida K, Shigetomi E, Gachet C, Ikenaka K, Tanaka KF, Koizumi S (2017) Transformation of Astrocytes to a Neuroprotective Phenotype by Microglia via P2Y. Cell Rep 19:1151-1164.

Shultz LD, Lyons BL, Burzenski LM, Gott B, Chen X, Chaleff S, Kotb M, Gillies SD, King M, Mangada J, Greiner DL, Handgretinger R (2005) Human lymphoid and myeloid cell development in NOD/LtSz-scid IL2R gamma null mice engrafted with mobilized human hemopoietic stem cells. J Immunol 174:6477-6489.

Sierra A, Abiega O, Shahraz A, Neumann H (2013) Janus-faced microglia: beneficial and detrimental consequences of microglial phagocytosis. Front Cell Neurosci 7:6.

Sinclair E, Gray F, Ciardi A, Scaravilli F (1994) Immunohistochemical changes and PCR detection of HIV provirus DNA in brains of asymptomatic HIV-positive patients. J Neuropathol Exp Neurol 53:43-50.

Smyth K, Affandi JS, McArthur JC, Bowtell-Harris C, Mijch AM, Watson K, Costello K, Woolley IJ, Price P, Wesselingh SL, Cherry CL (2007) Prevalence of and risk factors for HIV-associated neuropathy in Melbourne, Australia 1993-2006. HIV Med 8:367-373.

Sokolowski JD, Chabanon-Hicks CN, Han CZ, Heffron DS, Mandell JW (2014) Fractalkine is a "find-me" signal released by neurons undergoing ethanol-induced apoptosis. Front Cell Neurosci 8:360.

Sporer B, Kastenbauer S, Koedel U, Arendt G, Pfister HW (2003) Increased intrathecal release of soluble fractalkine in HIV-infected patients. AIDS Res Hum Retroviruses 19:111-116.

Stellwagen D, Malenka RC (2006) Synaptic scaling mediated by glial TNF-alpha. Nature 440:1054-1059.

Stevens B, Allen NJ, Vazquez LE, Howell GR, Christopherson KS, Nouri N, Micheva KD, Mehalow AK, Huberman AD, Stafford B, Sher A, Litke Alan M, Lambris JD, Smith SJ, John SWM, Barres BA (2007a) The Classical Complement Cascade Mediates CNS Synapse Elimination. Cell 131:1164-1178.

Stevens B, Allen NJ, Vazquez LE, Howell GR, Christopherson KS, Nouri N, Micheva KD, Mehalow AK, Huberman AD, Stafford B, Sher A, Litke AM, Lambris JD, Smith SJ, John SW, Barres BA (2007b) The classical complement cascade mediates CNS synapse elimination. Cell 131:1164-1178.

Strazza M, Pirrone V, Wigdahl B, Nonnemacher MR (2011) Breaking down the barrier: the effects of HIV-1 on the blood-brain barrier. Brain Res 1399:96-115.

Sui Y, Li S, Pinson D, Adany I, Li Z, Villinger F, Narayan O, Buch S (2005) Simian human immunodeficiency virus-associated pneumonia correlates with increased expression of MCP-1, CXCL10, and viral RNA in the lungs of rhesus macaques. Am J Pathol 166:355-365.

Sui Y, Stehno-Bittel L, Li S, Loganathan R, Dhillon NK, Pinson D, Nath A, Kolson D, Narayan O, Buch S (2006) CXCL10-induced cell death in neurons: role of calcium dysregulation. Eur J Neurosci 23:957-964.

Sui Y, Potula R, Dhillon N, Pinson D, Li S, Nath A, Anderson C, Turchan J, Kolson D, Narayan O, Buch S (2004) Neuronal apoptosis is mediated by CXCL10

overexpression in simian human immunodeficiency virus encephalitis. Am J Pathol 164:1557-1566.

Sun J, Zheng JH, Zhao M, Lee S, Goldstein H (2008) Increased in vivo activation of microglia and astrocytes in the brains of mice transgenic for an infectious R5 human immunodeficiency virus type 1 provirus and for CD4-specific expression of human cyclin T1 in response to stimulation by lipopolysaccharides. J Virol 82:5562-5572.

Suzuki M, El-Hage N, Zou S, Hahn YK, Sorrell ME, Sturgill JL, Conrad DH, Knapp PE, Hauser KF (2011) Fractalkine/CX3CL1 protects striatal neurons from synergistic morphine and HIV-1 Tat-induced dendritic losses and death. Mol Neurodegener 6:78.

Sá MJ, Madeira MD, Ruela C, Volk B, Mota-Miranda A, Paula-Barbosa MM (2004) Dendritic changes in the hippocampal formation of AIDS patients: a quantitative Golgi study. Acta Neuropathol 107:97-110.

Tang SJ (2014) Synaptic activity-regulated Wnt signaling in synaptic plasticity, glial function and chronic pain. CNS Neurol Disord Drug Targets 13:737-744.

Tang Y, Le W (2016) Differential Roles of M1 and M2 Microglia in Neurodegenerative Diseases. Mol Neurobiol 53:1181-1194.

Tang Z, Gan Y, Liu Q, Yin JX, Shi J, Shi FD (2014) CX3CR1 deficiency suppresses activation and neurotoxicity of microglia/macrophage in experimental ischemic stroke. J Neuroinflammation 11:26.

Tauber SC, Staszewski O, Prinz M, Weis J, Nolte K, Bunkowski S, Brück W, Nau R (2016) HIV encephalopathy: glial activation and hippocampal neuronal apoptosis, but limited neural repair. HIV Med 17:143-151.

Tervo HM, Goffinet C, Keppler OT (2008) Mouse T-cells restrict replication of human immunodeficiency virus at the level of integration. Retrovirology 5:58.

Thomas FP, Chalk C, Lalonde R, Robitaille Y, Jolicoeur P (1994) Expression of human immunodeficiency virus type 1 in the nervous system of transgenic mice leads to neurological disease. J Virol 68:7099-7107.

Tian C, Sun L, Jia B, Ma K, Curthoys N, Ding J, Zheng J (2012) Mitochondrial glutaminase release contributes to glutamate-mediated neurotoxicity during

human immunodeficiency virus-1 infection. J Neuroimmune Pharmacol 7:619-628.

Toggas SM, Masliah E, Rockenstein EM, Rall GF, Abraham CR, Mucke L (1994) Central nervous system damage produced by expression of the HIV-1 coat protein gp120 in transgenic mice. Nature 367:188-193.

Ton H, Xiong H (2013) Astrocyte Dysfunctions and HIV-1 Neurotoxicity. J AIDS Clin Res 4:255.

Tong N, Perry SW, Zhang Q, James HJ, Guo H, Brooks A, Bal H, Kinnear SA, Fine S, Epstein LG, Dairaghi D, Schall TJ, Gendelman HE, Dewhurst S, Sharer LR, Gelbard HA (2000) Neuronal fractalkine expression in HIV-1 encephalitis: roles for macrophage recruitment and neuroprotection in the central nervous system. J Immunol 164:1333-1339.

Tornatore C, Chandra R, Berger JR, Major EO (1994) HIV-1 infection of subcortical astrocytes in the pediatric central nervous system. Neurology 44:481-487.

Traggiai E, Chicha L, Mazzucchelli L, Bronz L, Piffaretti JC, Lanzavecchia A, Manz MG (2004) Development of a human adaptive immune system in cord blood cell-transplanted mice. Science 304:104-107.

Tronche F, Kellendonk C, Kretz O, Gass P, Anlag K, Orban PC, Bock R, Klein R, Schütz G (1999) Disruption of the glucocorticoid receptor gene in the nervous system results in reduced anxiety. Nat Genet 23:99-103.

Tung TT, Nagaosa K, Fujita Y, Kita A, Mori H, Okada R, Nonaka S, Nakanishi Y (2013) Phosphatidylserine recognition and induction of apoptotic cell clearance by Drosophila engulfment receptor Draper. J Biochem 153:483-491.

Turchan J, Pocernich CB, Gairola C, Chauhan A, Schifitto G, Butterfield DA, Buch S, Narayan O, Sinai A, Geiger J, Berger JR, Elford H, Nath A (2003) Oxidative stress in HIV demented patients and protection ex vivo with novel antioxidants. Neurology 60:307-314.

Tyor WR, Glass JD, Griffin JW, Becker PS, McArthur JC, Bezman L, Griffin DE (1992) Cytokine expression in the brain during the acquired immunodeficiency syndrome. Ann Neurol 31:349-360.

Ullian EM, Sapperstein SK, Christopherson KS, Barres BA (2001) Control of synapse number by glia. Science 291:657-661.

Valero J, Paris I, Sierra A (2016) Lifestyle Shapes the Dialogue between Environment, Microglia, and Adult Neurogenesis. ACS Chem Neurosci 7:442-453.

Vasek MJ et al. (2016a) A complement-microglial axis drives synapse loss during virus-induced memory impairment. Nature 534:538-543.

Vasek MJ et al. (2016b) A complement–microglial axis drives synapse loss during virus-induced memory impairment. Nature 534:538.

Ventura R, Harris KM (1999) Three-dimensional relationships between hippocampal synapses and astrocytes. J Neurosci 19:6897-6906.

Vergote D, Butler GS, Ooms M, Cox JH, Silva C, Hollenberg MD, Jhamandas JH, Overall CM, Power C (2006) Proteolytic processing of SDF-1alpha reveals a change in receptor specificity mediating HIV-associated neurodegeneration. Proc Natl Acad Sci U S A 103:19182-19187.

Vigorito M, LaShomb AL, Chang SL (2007) Spatial learning and memory in HIV-1 transgenic rats. J Neuroimmune Pharmacol 2:319-328.

Vilalta A, Brown GC (2017) Neurophagy, the phagocytosis of live neurons and synapses by glia, contributes to brain development and disease. FEBS J.

Viviani B, Corsini E, Binaglia M, Galli CL, Marinovich M (2001) Reactive oxygen species generated by glia are responsible for neuron death induced by human immunodeficiency virus-glycoprotein 120 in vitro. Neuroscience 107:51-58.

Viviani B, Gardoni F, Bartesaghi S, Corsini E, Facchi A, Galli CL, Di Luca M, Marinovich M (2006) Interleukin-1 beta released by gp120 drives neural death through tyrosine phosphorylation and trafficking of NMDA receptors. J Biol Chem 281:30212-30222.

Vázquez-Santiago FJ, Noel RJ, Porter JT, Rivera-Amill V (2014) Glutamate metabolism and HIV-associated neurocognitive disorders. J Neurovirol 20:315-331.

Walz W (2000) Role of astrocytes in the clearance of excess extracellular potassium. Neurochem Int 36:291-300.

Wang EJ, Sun J, Pettoello-Mantovani M, Anderson CM, Osiecki K, Zhao ML, Lopez L, Lee SC, Berman JW, Goldstein H (2003a) Microglia from mice transgenic for a

provirus encoding a monocyte-tropic HIV type 1 isolate produce infectious virus and display in vitro and in vivo upregulation of lipopolysaccharide-induced chemokine gene expression. AIDS Res Hum Retroviruses 19:755-765.

Wang Z, Pekarskaya O, Bencheikh M, Chao W, Gelbard HA, Ghorpade A, Rothstein JD, Volsky DJ (2003b) Reduced expression of glutamate transporter EAAT2 and impaired glutamate transport in human primary astrocytes exposed to HIV-1 or gp120. Virology 312:60-73.

Weed MR, Gold LH, Polis I, Koob GF, Fox HS, Taffe MA (2004) Impaired performance on a rhesus monkey neuropsychological testing battery following simian immunodeficiency virus infection. AIDS Res Hum Retroviruses 20:77-89.

Weed MR, Hienz RD, Brady JV, Adams RJ, Mankowski JL, Clements JE, Zink MC (2003) Central nervous system correlates of behavioral deficits following simian immunodeficiency virus infection. J Neurovirol 9:452-464.

Weis S, Haug H, Budka H (1993) Neuronal damage in the cerebral cortex of AIDS brains: a morphometric study. Acta Neuropathol 85:185-189.

Wiley CA, Achim CL (1995) Human immunodeficiency virus encephalitis and dementia. Ann Neurol 38:559-560.

Witcher MR, Park YD, Lee MR, Sharma S, Harris KM, Kirov SA (2010) Three-dimensional relationships between perisynaptic astroglia and human hippocampal synapses. Glia 58:572-587.

Wu J, Bie B, Yang H, Xu JJ, Brown DL, Naguib M (2013) Suppression of central chemokine fractalkine receptor signaling alleviates amyloid-induced memory deficiency. Neurobiol Aging 34:2843-2852.

Xavier AL, Menezes JR, Goldman SA, Nedergaard M (2014) Fine-tuning the central nervous system: microglial modelling of cells and synapses. Philos Trans R Soc Lond B Biol Sci 369:20130593.

Xu H, Bae M, Tovar-y-Romo LB, Patel N, Bandaru VV, Pomerantz D, Steiner JP, Haughey NJ (2011) The human immunodeficiency virus coat protein gp120 promotes forward trafficking and surface clustering of NMDA receptors in membrane microdomains. J Neurosci 31:17074-17090.

Xu J, Xiao N, Xia J (2010) Thrombospondin 1 accelerates synaptogenesis in hippocampal neurons through neuroligin 1. Nat Neurosci 13:22-24.

Yang Y, Ge W, Chen Y, Zhang Z, Shen W, Wu C, Poo M, Duan S (2003) Contribution of astrocytes to hippocampal long-term potentiation through release of D-serine. Proc Natl Acad Sci U S A 100:15194-15199.

Yeh MW, Kaul M, Zheng J, Nottet HS, Thylin M, Gendelman HE, Lipton SA (2000) Cytokine-stimulated, but not HIV-infected, human monocyte-derived macrophages produce neurotoxic levels of l -cysteine. J Immunol 164:4265-4270.

Yowtak J, Lee KY, Kim HY, Wang J, Kim HK, Chung K, Chung JM (2011) Reactive oxygen species contribute to neuropathic pain by reducing spinal GABA release. Pain 152:844-852.

Yu Q, Yu R, Qin X (2010) The good and evil of complement activation in HIV-1 infection. Cell Mol Immunol 7:334-340.

Yuan L, Qiao L, Wei F, Yin J, Liu L, Ji Y, Smith D, Li N, Chen D (2013) Cytokines in CSF correlate with HIV-associated neurocognitive disorders in the post-HAART era in China. J Neurovirol 19:144-149.

Yuan SB, Shi Y, Chen J, Zhou X, Li G, Gelman BB, Lisinicchia JG, Carlton SM, Ferguson MR, Tan A, Sarna SK, Tang SJ (2014) Gp120 in the pathogenesis of human immunodeficiency virus-associated pain. Ann Neurol 75:837-850.

Zabel MK, Zhao L, Zhang Y, Gonzalez SR, Ma W, Wang X, Fariss RN, Wong WT (2016) Microglial phagocytosis and activation underlying photoreceptor degeneration is regulated by CX3CL1-CX3CR1 signaling in a mouse model of retinitis pigmentosa. Glia 64:1479-1491.

Zhan Y, Paolicelli RC, Sforazzini F, Weinhard L, Bolasco G, Pagani F, Vyssotski AL, Bifone A, Gozzi A, Ragozzino D, Gross CT (2014) Deficient neuron-microglia signaling results in impaired functional brain connectivity and social behavior. Nat Neurosci 17:400-406.

Zheng J, Thylin MR, Ghorpade A, Xiong H, Persidsky Y, Cotter R, Niemann D, Che M, Zeng YC, Gelbard HA, Shepard RB, Swartz JM, Gendelman HE (1999) Intracellular CXCR4 signaling, neuronal apoptosis and neuropathogenic mechanisms of HIV-1-associated dementia. J Neuroimmunol 98:185-200.

Zhou BY, Liu Y, Kim B, Xiao Y, He JJ (2004) Astrocyte activation and dysfunction and neuron death by HIV-1 Tat expression in astrocytes. Mol Cell Neurosci 27:296-305.

Zink MC, Brice AK, Kelly KM, Queen SE, Gama L, Li M, Adams RJ, Bartizal C, Varrone J, Rabi SA, Graham DR, Tarwater PM, Mankowski JL, Clements JE (2010) Simian immunodeficiency virus-infected macaques treated with highly active antiretroviral therapy have reduced central nervous system viral replication and inflammation but persistence of viral DNA. J Infect Dis 202:161-170.

VITA

Wenjuan Ru was born in Yunnan, China on February 4, 1985 to Kui Ru and Lianfen Li. She acquired her Bachelor's degree in Biology from Yunnan University in 2007. During her study at Yunnan University, she participated in undergraduate research programs in her third-year of study and joined a lab researching microbiologic studies led by Dr. Ying Zeng in Kunming Institute of Botany of the Chinese Academy of Science. There, she obtained various experimental skills such as microorganism culture, product extraction and strain classification. Most importantly, she discovered that fermentation products from some microorganism could inhibit growth of Mycobacterium tuberculosis (MTB). Then she pursued her Master's degree in the Department of Pharmacology at Guangdong Medical University. She completed her thesis research in Sun Yet-Sen University as a visiting scientist, where she focused on investigating the regulation of mTOR by glutamate-induced synaptic activity under the co-supervision of Dr. Shao-Jun Tang and Dr. Ling Zhong.

On July 2011, Wenjuan started to work at the University of Texas Medical Branch (UTMB) as a research fellow in Dr. Shao-Jun Tang's lab. Since then she mainly focused on understanding the cellular and molecular mechanism of HIV-1-associated neurological disorders. On September 2013, she enrolled at Graduate School of Biomedical Science and joined the Neuroscience Graduate Program at the same year. Her research involved determining the contribution of microglia-neuron interaction to HIV-infection- induced synaptic degeneration. During her PhD training, she received McLaughlin Pre-doctoral Fellow, a prestigious recognition for graduate students in UTMB and her abstract for the 2016 Society for Neuroscience annual meeting was selected for an oral presentation in San

Diego. She was awarded a number of prestigious scholarships in UTMB including James E. Beall II Memorial Award in Anatomy and Neurosciences in 2016, Oral presentation award in Neuroscience and Cell Biology Departmental Retreat in 2016, Robert Shope Endowed Scholarship in 2017.

Education

B.S., June 2007, Yunnan University, Kunming, Yunnan Province, China.

M.S., June 2010, Guangdong Medical University, Zhanjiang, Guangdong Province, China.

Publications

ARTICLES IN PEER-REVIEWED JOURNALS:

1. Ru, W. J.; Tang, S. J.; Zhong, L.; The mTOR pathway and its relationship with Alzheimer's disease. Chinese Journal of Comparative Medicine. 2010, 20, (8), 73-76.
2. Ru, W. J.; Peng, Y. X., Zhong, L., Tang, S. J.; A role of the mammalian target of rapamycin (mTOR) in glutamate-induced down-regulation of tuberous sclerosis complex proteins 2 (TSC2). Journal of Molecular Neuroscience. 47(2):340 (2012). PMID: 22492229.
3. Ru, W. J.; Tang, S. J.; HIV-1 gp120Bal down-Regulates Phosphorylated NMDA Receptor Subunit 1 in Cortical Neurons via Activation of Glutamate and Chemokine Receptors. Journal of Neuroimmune Pharmacology. 11(1):182-9 (2015). PMID: 26582091.
4. Ru, W., Tang, S.J. HIV-Associated Synapse Degeneration. Molecular Brain. 10(1):40 (2017). PMID: 28851400
5. Luo, H., Winkelmann, E., Zhu, S., Ru, W., Mays E., Silvas J.,[4] Vollmer, L., Gao, J., Peng, B-H., Bopp, N., Cromer, C., Shan, C., Xie, G., Li, G., Tesh, R., Popov, V., Shi, P-Y., Sun, S-C., Wu, P., Klein, R., Tang, S-J., Zhang, W., Aguilar, P., and Wang, T.

Peli1 facilitates virus replication and promotes neuroinflammation during West Nile virus infection. The Journal of Clinical Investigation. 2018. 10.1172/JCI99902.

ABSTRACTS:

1. Ru, W. J.; Tang, S. J.; Zhong, L.; Regulation of Wnt/β-catenin and mTOR/p70S6K pathways by synaptic activity in mouse cortical neurons (poster). The 8th Biennial Conference of the Chinese Society for Neuroscience. November 7-10, 2009, Guangzhou, China.
2. Ru, W. J. ; Tang, S. J. Glutamate Receptors, CXCR4 and Wnt signaling are involved in HIV-1 gp120 Bal-induced Synapse Loss. Fourth Biennial Translational Pain Research Symposium (poster). April 5, 2013, Houston, USA.
3. Ru, W. J. ; Tang, S. J. NMDA Receptors, CXCR4 and Wnt signaling in HIV-1 gp120-induced Synapse Loss (poster). 43rd Society for Neuroscience meeting. November 9-13, 2013, San Diego, USA.
4. Ru, W. J. ; Tang, S. J. NMDA Receptors, Microglia Contribute to HIV1-gp120Bal- induced synapse loss (poster). 44th Society for Neuroscience meeting. November 15-19, 2014, Washington DC, USA
5. Ru, W. J. ; Tang, S. J. NMDA Receptors, Microglia Contribute to HIV1-gp120Bal- induced synapse loss (poster). 2015 Neuroscience Research Conference: Advancing pain neuroscience discovery toward therapeutics. August 5-6, 2015, Dallas, USA.
6. Ru, W. J. ; Tang, S. J. Microglia Activation Contributes to HIV1-gp120- induced synapse degeneration. 46rd Society for Neuroscience meeting (oral presentation). November 12-17, 2016, San Diego, USA.
7. Ru, W. J. ; Tang, S. J. The Activation of Glial Cells Contributes to HIV1-gp120-induced Synapse Degeneration (poster). 2017 IHII / McLaughlin Colloquium, March, 31, 2017, Galveston, USA

8. Ru, W. J. ; Tang, S. J. Neuron-microglial interaction in HIV-1 gp120-induced synapse degeneration. (poster). 46rd Society for Neuroscience meeting (poster). November 12-17, 2016, Washington D.C., USA.
9. Ru, W., Bae, C., Liu, X., Tang, S.J. Neuron-microglial interaction in HIV-1 gp120-induced synapse degeneration in the spine pain circuit (poster). April 10-14, 2018, Chicago, USA. The Joint Conference of 24th Scientific Conference of the Society on NeuroImmune Pharmacology and 15th International Symposium on NeuroVirology.

HONORS/ AWARDS:

2017: Robert Shope Endowed Scholarship from the University of Texas Medical Branch in Galveston.

2016: Oral presentation award in Neuroscience and Cell Biology Departmental Retreat.

2016: James E. Beall II Memorial Award in Anatomy and Neurosciences

2016/2018: American Association for the Advancement of Science (AAAS) membership and subscription prize for 3 years, Washington, D.C.

2016/2018: Jmaes W. Mclaughlin Predoctoral Fellowship, UTMB, Galveston, TX.

2010: Excellent M. Med graduate student honor, Guangdong Medical University, Guangdong, China.

2005: “Donglu” scholarship Award, Yunnan University, Kunming, Yunnan, China.